

INTERFACIAL DESIGN FOR A BIOACTIVE COMPOSITE

By

JEANNE MARIE MACDONALD

A DISSERTATION PRESENTED TO THE GRADUATE SCHOOL
OF THE UNIVERSITY OF FLORIDA IN PARTIAL FULFILLMENT
OF THE REQUIREMENTS FOR THE DEGREE OF
DOCTOR OF PHILOSOPHY

UNIVERSITY OF FLORIDA

2001

[This dissertation is dedicated to all of those who gave their love and support during the writing of the dissertation, especially my husband Glenn.]

ACKNOWLEDGMENTS

I would first like to thank my advisor and doctoral committee chairman, Dr. Anthony Brennan, whose guidance and knowledge were instrumental during the completion of this work. I would also like to thank the members of the supervisory committee for their valuable input: Dr. Ronald Baney, Dr. Christopher Batich, Dr. Elliot Douglas, and Dr. Kenneth Wagener.

I cannot thank enough all of my colleagues, both past and present, who gave the support and collaboration necessary to make it through this arduous process: Jeremy Mehlem, Jennifer Russo, Clay Bohn, Wade Wilkerson, Adam Feinberg, Amy Gibson, Nikhil Kothurkar, Brian Hatcher, Leslie Wilson, Charles Seegert, Dr. Luxsamee Plangsangmas, Xiaomei Qian, Jamie Rhodes, Lee Zhao, Dr. Brent Gila, Dr. Drew Amery, Dr. Bob Hadba, Dr. Chris Widenhouse, Dr. Rodrigo Orifice, Dr. James Marrotta, and Paul Martin and all the other students, faculty, and staff that made my experience at the University of Florida memorable.

Special thanks goes out to Dr. W. Greg Sawyer and his students in the Mechanical Engineering Department for his help with friction and wear testing. Dr. Sawyer provided both equipment and guidance.

I also wish to acknowledge the Center for the Development of Alternatives to Dental Amalgam at the University of Florida, especially Mr. Ben Lee in the dental biomaterials laboratory. I also thank the NIH-NIDR (grant no. 2-P50-DE 09307) for helping to fund my research.

Finally, I would like to thank my parents and family for supporting my continued education including my new family the Macdonalds. Last, but not least, I would like to thank my husband, Glenn, for his love and support through the years of my education.

TABLE OF CONTENTS

	<u>page</u>
ACKNOWLEDGMENTS.....	iii
LIST OF TABLES	viii
LIST OF FIGURES.....	ix
ABSTRACT	xiii
INTRODUCTION.....	1
BACKGROUND.....	7
Dental Restorative Materials.....	7
Dental Composites	8
The Matrix.....	8
The Filler.....	11
Anhydrides in Dental Materials	12
Bioactivity of Bioglass®.....	14
Uses for Bioactive Glasses.....	15
Mechanical Properties.....	17
Composite Interfaces.....	20
Hydrolytic Degradation of Composites.....	22
Degree of Cure	24
Wear of Composites	26
Summary	28
 SURFACE MODIFICATION OF PARTICULATE BIOGLASS® IN DENTAL RESINS THROUGH A METHACRYLATE BASED COUPLING SYSTEM.....	 29
Introduction	29
Experimental Procedure	35
Silanation of Substrates.....	35
Analysis of Glass.....	36
Composite Production.....	36
Analysis of Composites.....	37
Thermoanalysis testing.....	37

Physical testing.....	38
Mechanical testing.....	39
Confirmation of Silanation.....	39
Evaluation of Composite Manufacturing Procedure.....	42
Physical Characteristics of Bioactive Composites.....	45
Mechanical Properties of Methacryloxypropyl triethoxysilane: Methyl triethoxysilane Modified Bioglass Composites	60
Conclusions	73
 DESIGNED INTERFACE FOR BIOACTIVE POLYMER COMPOSITES UTILIZING SULFONATED POLYSULFONE	75
Introduction	75
Experimental	77
Preparation of sulfonated polysulfone.....	77
Methods of Polysulfone Analysis	78
Spectroscopic techniques	78
Thermal techniques	78
Grafting Sulfonated Polysulfone.....	79
Preparation of Composites	79
Materials.....	79
Mechanical testing of composites	81
Characterization of Sulfonated Polysulfone.....	81
Assignments	92
Thermal Analysis of Sulfonated Polysulfone.....	93
Determination of Processing Procedure for Grafting SPSF to Bioglass.....	95
Mechanical Properties of Sulfonated Polysulfone Modified Bioglass Composites.....	99
Conclusions	113
 CHARACTERIZATION OF THE COMPOSITE INTERFACE BY DYNAMIC MECHANICAL AND WEAR ANALYSIS.....	115
Introduction	115
Roughness	116
Wear	116
Dynamic Mechanical Analysis and Three Phase Modeling of Composites	117
Experimental Procedure	119
Dynamic Mechanical Spectroscopy	122
Three-Phase Model	127
Wear of Dental Samples.....	140
Conclusions	154
 CONCLUSIONS.....	156

LIST OF REFERENCES	164
BIOGRAPHICAL SKETCH.....	175

LIST OF TABLES

<u>Table</u>	<u>Page</u>
2.1. Proposed Reaction stages of Bioglass® as it bonds to tissue	16
3.1. Composition of salt-soak for 1 L of solution	37
3.2. Results from XPS on silica surfaces modified with a methacrylate based silane-coupling agent	43
3.3. Coefficients from the curve fitting of the Vickers Hardness results.	45
3.4. Coefficients from the curve fitting of the water sorption results.	51
3.5. Deconvoluted carbon peak areas comparing different MAMTES:MTES systems.....	65
4.1. Composition of salt-soak for a 1 L of solution.....	81
4.2. Proton NMR data and degree of sulfonation for unmodified and modified polysulfone. Lightly, moderately and highly sulfonated polysulfones refer to samples made with 1:1, 6:5, and 2:1 molar ratios, respectively, of ClSO ₃ H to PSF repeat unit	86
4.3. Infrared assignments of polysulfone and its sulfonated derivative	92
4.4. Design of experiment to determine the effect of SPSF concentration during grafting procedure.....	96
5.1. Fitting parameters for modeling and quantifying the filler adhesion in composites with 30 v% Bioglass® with various surface treatments.....	137
5.2. Roughness data before and after 10 hour wear runs for the resin and composites comparing different filler surface treatments	150

LIST OF FIGURES

<u>Figure</u>	<u>Page</u>
1.1. 2,2'-bis-(4-methacryloylethoxyphenyl) propane (Bis-MEPP).....	4
1.2. Tri-ethylene glycol dimethacrylate (TEGDMA).....	4
1.3. Nadic methyl anhydride (Methyl-5-norbornene-2,3-dicarboxylic anhydride)	4
2.1. The structure of 2,2-bis(4-(2-hydroxy-3-methacryloyloxyprop-1-oxy)phenol)propane (Bis-GMA).....	9
2.2. Tri-ethylene glycol dimethacrylate (TEGDMA).....	10
3.1. XPS spectra of silica and silica modified with a methacrylate based silane-coupling agent	43
3.2. Thermogravimetric analysis of composite with 30 v% Bioglass® filler.	44
3.3. Vickers hardness number verses time after light-cure of three different resin systems.	46
3.4. Vickers hardness number verses time after light-cure of three different resin and composite systems.....	48
3.5. Percent weight gain of two cured resin systems resulting from time in water bath..	52
3.6. Percent weight gain of two cured resin systems verses the square root of time spent.	53
3.7a. Composites soaked in nanopure water at 37°C.....	55
3.7b. Composites soaked in salt solution at 37°C	58
3.8. Percent weight gain verses $t^{1/2}$ comparing composites and resins soaked in either water or a salt solution.	59
3.9. Schematic of the silanation by methacryloxypropyl triethoxysilane (MAMTES) coupling agent mixed with methyl triethoxysilane (MTES) coupling agent	61

3.10.	Tensile strength of composites varying the post-cure treatment and the ratio of MAMTES to MTES used to modify the filler	63
3.11.	XPS spectra comparing the carbon region of silica and silica modified with 1:1 and 3:1 ratios of MAMTES to MTES.....	65
3.12.	Flexural strengths of composites varying the post-cure treatment and the ratio of MAMTES to MTES used to modify the filler	69
3.13.	Flexural modulus of composites varying the post-cure treatment and the ratio of MAMTES to MTES used to modify the filler	70
4.1.	Polysulfone repeat unit.....	76
4.2.	(a) unreacted polysulfone, (b) sulfonated polysulfone.....	83
4.3.	Proton NMR of unreacted polysulfone	84
4.4.	Predicted scheme for the sulfonation of polysulfone via chlorosulfonic acid	85
4.5.	Proton NMR scan of lightly sulfonated polysulfone.....	88
4.6.	Proton NMR scan of moderately sulfonated polysulfone	88
4.7.	Proton NMR scan of highly sulfonated polysulfone.....	90
4.8.	FTIR spectra of sulfonated and unmodified polysulfones	91
4.9.	Differential scanning calorimetry scans for unmodified and sulfonated polysulfones	94
4.10.	Tensile strength of dry composites varying the amount of nadic methyl anhydride in the resin and the grafting procedure of the filler.....	97
4.11.	Tensile strength of composites varying the post-cure treatment and the degree of sulfonation used to modify the filler	100
4.12.	SEM fracture surface of a soaked composite containing 30 v% unmodified Bioglass®	105
4.13.	SEM fracture surface of a dry composite containing 30 v% Bioglass® modified with SPSF (DS=0.6).....	106
4.14.	SEM fracture surface of a soaked composite containing 30 v% Bioglass® modified with SPSF (DS=0.6)	107
4.15.	SEM fracture surface of a soaked composite containing 30 v% Bioglass® modified with SPSF (DS=1.4) showing evidence of HCA growth.....	108

4.16.	Flexural strength of composites varying the post-cure treatment and the degree of sulfonation used to modify the filler.....	110
4.17.	Flexural modulus of composites varying the post-cure treatment and the degree of sulfonation used to modify the filler.....	111
5.1.	316 steel pin prior to wear test	121
5.2.	Tan δ response of neat resin and Bioglass® composites at 1 hertz.....	124
5.3.	Storage modulus of neat resin and Bioglass® composites at 1 hertz.....	126
5.4.	The three-phase block model: f and m refer to filler and matrix attributes, respectively, Φ refers to the volume fraction, K and λ describe the reinforcement efficiency and the amount of matrix material, respectively, and E refers to the modulus.....	128
5.5.	Comparison between the neat resin system, a composite made with 30 v% unmodified Bioglass®, and the simulated tan δ response of the composite.	131
5.6.	Comparison between the neat resin system, a composite made with 30 v% Bioglass® modified with SPSF (DS = 0.6), and the simulated tan δ response of the composite.....	132
5.7.	Comparison between the neat resin system, a composite made with 30 v% Bioglass® modified with the 5:1 MAMTES to MTES coupling system, and the simulated tan δ response of the composite.	133
5.8.	Comparison between the neat resin system, a composite made with 30 v% Bioglass® modified with the 3:1 MAMTES to MTES coupling system, and the simulated tan δ response of the composite.	134
5.9.	Diagram of a Cole-Cole plot.	138
5.10.	Cole-Cole plot for resin and composites with 30 v% Bioglass®	139
5.11.	Wear track of unlubricated resin sample (a) at the end of wear track, (b) in the middle of wear track.	142
5.12.	Surface of steel pin after wear test without lubrication.....	144
5.13.	End of wear track of lubricated resin sample.....	145
5.14.	Wear weight and volume of resin and composites comparing different filler surface treatments after 10 hour wear runs.....	149
5.15.	Profile of the end of the wear track for a neat resin sample.....	151

5.16.	Profile of the end of the wear track for 30 v% Bioglass® filled composite.	151
5.17.	Example wear track of neat resin	152
5.18.	Example wear track of composite filled with 30 v% Bioglass®	153
6.1.	Schematic showing the incorporation and hydrolysis of nadic methyl anhydride and the interaction with a calcium ion	163

Abstract of Dissertation Presented to the Graduate School
of the University of Florida in Partial Fulfillment of the
Requirements for the Degree of Doctor of Philosophy

INTERFACIAL DESIGN FOR A BIOACTIVE COMPOSITE

By

Jeanne Marie Macdonald

December 2001

Chairman: Anthony B. Brennan

Major Department: Materials Science and Engineering

The objective for this project is to develop a bioactive dental composite showing enhanced mechanical properties through the development of a designed interface and to experimentally evaluate and model these interfaces. The efficiency of the surface modifications is analyzed as it relates to the bioactivity of the filler, a sol-gel derived bioglass (60 mol% SiO₂, 36 mol% CaO, 4 mol% P₂O₅), and to the enhancement of mechanical properties. Among the filler surfaces studied are a methacryloxypropyl triethoxysilane (MAMTES) coupling agent combined with a methyl triethoxysilane (MTES) coupling agent, and a grafted sulfonated polysulfone (SPSF) with different degrees of sulfonation.

The resin system chosen is based on 2,2'-bis-(4-methacryloylethoxyphenyl) propane using triethylene glycol dimethacrylate as a diluent to improve processability. To help offset the polymerization shrinkage, nadic methyl anhydride is added. Hydrolysis of this anhydride provides a mechanism for offsetting shrinkage.

A dependence on the ratio of methacrylate functionalized coupling agent on the reinforcing capabilities of the filler was discovered. This dependence also translates into the stabilization of the interface after a solution soak. Enhanced properties at mid-level ratios of MAMTES to MTES show the importance of the coupling system and not just the presence of a coupling agent to the enhancement of a composite. Evidence of the bioactivity of the composites is seen in a comparison of composite samples after submersion in either pure water or a salt solution. Additional weight gain could be the result of the sorption of HCA forming ions (calcium and phosphate) from the salt solution. The lower weight gain rate for the silanated composite supports a shielding effect of the coupling agent to the bioactivity of the filler.

Sulfonated polysulfones were successfully prepared and grafted onto the Bioglass® filler. A dependence on the level of sulfonation on the reinforcing capabilities of the filler was discovered. At higher degrees of sulfonation there is an increased water attraction at the interface that leads to a higher propensity for hydrolytic degradation and lowered mechanical properties. Along with the lowered mechanical properties, however, there is evidence of HCA growth that is necessary for the condition of bioactivity.

CHAPTER 1

INTRODUCTION

The development of new dental materials is driven by the patient's desire for the natural appearance of teeth, easier preparation, and for properties that mimic biological materials. The ideal dental material must adhere tenaciously to the surrounding tissue and be resistant to degradation in the oral environment. These needs have led to the study of polymer-based composites as a restorative material using inorganic fillers for reinforcement. Polymer based composites, however, have shown numerous areas that need to be improved. Important physical and mechanical considerations for dental composites include polymerization shrinkage, thermal conductivity, linear coefficient of thermal expansion, water sorption, radiopacity, strength, modulus, hardness, penetration resistance, abrasive wear and bond strength to natural tissues [1].

Polymerization shrinkage is cited as one of the major reasons for dental restoration failure in the oral environment [2], [3], [4], [5]. Stresses from polymerization shrinkage can exceed the bond strength of the composites to the tooth structure or from the composite filler to the matrix, resulting in marginal leakage possibly leading to recurrent decay and compromised mechanical properties. The shrinkage is a direct function of the amount of organic matrix in the composite material. Traditionally, this problem has been overcome through the tedious method of polymerizing the composite in layers to reduce the effects of shrinkage [1].

Along with polymerization shrinkage, another major factor in dental composite failure is water sorption. The influx of water can result in the leaching of restorative material and in stress concentrations that lead to cracking and/or reduced mechanical properties. In addition, the influx of water can lead to discoloration of the restoration by water-soluble stains. Water sorption has been mainly associated with the organic matrix. Two ways to combat this effect are to either design a material which will not absorb water, design a material that will take advantage of any water that is absorbed. Water sorption is accompanied by a swelling of the composite, but not only is it an ineffective way to counteract polymerization shrinkage it can also lead to stresses that cause material failure.

The amount of biting force varies from 130 to 40 pounds force depending on both the patient and the tooth location [1]. In areas of the mouth, where contact areas as small as 0.001 in^2 are achieved, this applied force translates into stresses as high as 130,000 psi. The compressive and tensile strengths of a material may also be significantly different. Brittle materials such as human enamel, amalgam, and polymeric composites have large differences between their mechanical strengths but are all typically stronger in compression than in tension. The modulus, or stiffness, of the composites is dominated by the amount of filler, which is important in applications where high biting forces are involved.

Wear of posterior restorations can cause deterioration of the occlusion, shifting of teeth, decreased masticatory function, recurrent caries, and compromised aesthetics. Common fillers used in dental composites include quartz, glasses composed of barium,

strontium or zinc, and pyrogenic silica. The formation and maintenance of the filler-polymer bond are important to the wear resistance of composites [6].

Dental composites are typically composed of high-molar-mass dimethacrylate monomers containing inorganic reinforcing agents that are cured by exposure to a visible-light source. In light-cured dental systems the polymerization is initiated by radicals that are formed upon exposure to light in the blue-wavelength region. The actual polymerization process is similar to a chemically initiated polymerization. The most common organic matrices are based on bisphenol-A bis(2-hydroxypropyl) methacrylate (Bis-GMA) [7]. Bis-GMA is a highly viscous liquid so that curing is inhibited due to early gelation. To aid the degree of cure, diluents are often added such as ethylene glycol dimethacrylate [8], [9].

In this study the base resin chosen is an ethoxylated Bis-GMA otherwise known as 2,2'-bis-(4-methacryloyloxyphenyl) propane (Bis-MEPP) (Figure 1.1). By removing the hydroxy groups from the backbone of the Bis-GMA monomer, the structural advantages of Bis-GMA are preserved while eliminating the polar groups, thus reducing a water-sorbing species. Triethylene glycol dimethacrylate (TEGDMA) (Figure 1.2) is added as a diluent to improve processability and the degree of cure.

To help offset the polymerization shrinkage in dental resins, nadic methyl anhydride (NMA) (Figure 1.3), a cyclic anhydride with an unsaturated vinyl group, has been added to the base resin system of Bis-MEPP and TEGDMA. The large density difference between the cyclic anhydride and its corresponding dicarboxylic acid implies that the hydrolysis of the anhydride could provide a mechanism of offsetting polymerization shrinkage [10]. In addition, the ionic interactions provided by the

anhydride functionality may also lead to an increase in the wetting and bonding of the resin to composite fillers and to bone tissue. The unsaturated vinyl group from NMA provides a mechanism for the free radical polymerization of NMA with Bis-MEPP, TEGDMA, or other monomers containing vinyl groups.

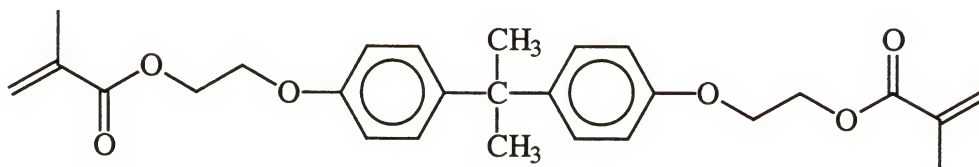


Figure 1.1. 2,2'-bis-(4-methacryloyloxyphenyl) propane (Bis-MEPP)

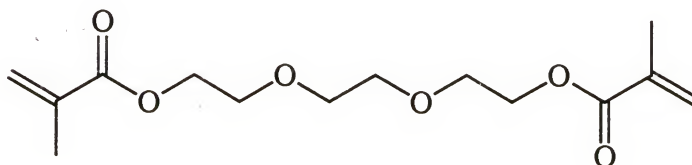


Figure 1.2. Tri-ethylene glycol dimethacrylate (TEGDMA)

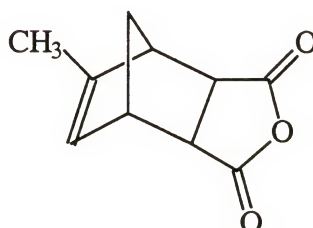


Figure 1.3. Nadic methyl anhydride (Methyl-5-norbornene-2,3-dicarboxylic anhydride)

To further reduce the effect of polymerization shrinkage, a non-shrinking filler of glass is added to the resin. To deal with the issue of water sorption, the type of glass chosen is bioactive. Bioglass® is an inorganic glass that has been shown to effectively bond to tissue through the simultaneous formation of calcium phosphate and a SiO₂-rich film layer. A melt-processed bioglass (46.1 SiO₂: 26.9 CaO: 2.6 P₂O₅: 24.4 Na₂O) has been demonstrated by Lin et al. [11] in a Bis-GMA system, and by M. P. Zamora et al. [12] in a Bis-GMA:TEGDMA resin system to significantly enhance the mechanical properties of the resin system.

This study uses a sol-gel derived Bioglass® (60 SiO₂: 36 CaO: 4 P₂O₅) rather than a melt derived Bioglass®. Sol-gel glasses are more porous and have a higher surface area. Monomers can penetrate the more porous sol-gel particles, leading to higher interfacial strengths between particles and polymerized resin impregnated within the pores. Bioglass® has also been shown by West and Wallace [13] to undergo a ring opening expansion reaction at their surface. A higher concentration of three and four silica member rings for sol gel particles leads to a larger potential of shrinkage offset due to the hydrolysis of these rings [14].

The higher silica content for the sol-gel glasses over melt derived glass reduces the rate of glass dissolution. The presence of a higher surface area, however, reduces the mean path of ion diffusion for the gel-derived materials allowing a rapid release of calcium and phosphate ions [14]. The formation of a hydroxy-carbonate-apatite layer on the surface of these composites will depend on their ability to diffuse the ions from the bulk or surface of the resin or the concentration of ions already present in solution. It may be possible that ions without a clear diffusion path to the surface of the composite could

further offset polymerization shrinkage by associating with the –COOH groups from the hydrolyzed anhydride rings.

The mechanical properties of the composite system depend heavily on the interfacial bonding between the filler and the resin. To this end a designed interface using combinations of silane coupling agents and grafting polymers will be characterized. Improved bonding between the filler and the resin will reduce the degree of degradation of mechanical properties during in vitro testing.

The goal of this work is to test the reinforcing effect of a sol-gel derived glass, which typically has inferior mechanical properties to its melt derived counterparts, compared to an unfilled resin. The hypothesis is that the larger surface area and mesoporous structure of the sol-gel derived glass will allow better mechanical interlocking between the filler and the resin system. Another goal of this work is to show an ability to form a bioactive bond between the composite and the natural tooth structure. Since water sorption by a resin in the oral environment is expected, using a bioactive filler can take advantage of this phenomenon to facilitate the formation of a hydroxy-carbonate-apatite layer capable of bonding to natural tissues. In addition to examining the reinforcing effect of the porous filler, two surface modifying systems will be examined. One surface modifying system involves an examination of the ratio of a methacrylate functionalized coupling agent to a non-functionalized coupling agent and its effect on the hydrolytic degradation of the Bioglass®/resin interface. The second surface modifying system examines the degree of sulfonation of polysulfone grafted to the Bioglass® particles on the reinforcing effects and bioactivity of the filler particles.

CHAPTER 2 BACKGROUND

Dental Restorative Materials

Dentists obtaining impressions of the mouth in wax and constructing casts with plaster have been recorded as early as 1756 [15]. Material choice, unfortunately, occurred mostly through trial and error resulting in patient pain and discomfort. The goal of every implant material is to satisfy the biological and mechanical requirements of the original material being replaced. To meet the requirements of hardness and strength, metal alloys are commonly used. Dental amalgams are among the most commonly used restorative materials, primarily due to their ease of manipulation and relatively low cost. In recent years, however, amalgam use has been in decline in part due to the potential hazards associated with the mercury contained in dental amalgams and their lack of aesthetics. Although there is no definitive proof that amalgams cause toxic responses in patients, the conclusion that amalgams are absolutely safe cannot be made. There are studies that show mercury is released from amalgam restorations during mastication [16]. In addition, metallic materials, such as amalgam and gold alloy, have the ability to induce electrochemical reactions that can result in pain and corrosion. Metals also have high coefficients of thermal conductivity, which can transmit thermal changes, causing temperature sensitivity for the patients. Hence, other materials are constantly being examined for dental restorations.

Dental Composites

The Matrix

In order to obtain a composite with overall good mechanical properties a polymer with acceptable mechanical properties is essential. The structure of the polymer must be considered to minimize the agglomeration of the inorganic component and provide effective stress transfer to the filler. Molecular weight, chemical functionality, chemical activity, solubility, and thermal characteristics are some of the features that have to be studied during the choice of the organic precursor.

Ever since the introduction of the first resin-based dental composites in the early 1960's their use in dentistry has continuously increased [17]. The superior aesthetics of organic materials and their ability to bond with enamel explains the increased usage. One of the first polymers used as fillings was acrylics in the mid 1940's. Large volumetric shrinkage during polymerization, large coefficients of thermal expansion, and high creep rates excluded further use of the acrylics. Bis-GMA, diluted in triethylene glycol dimethacrylate (Figures 2.1 and 2.2), has been the most commonly used resin system for dental composite materials. Bis-GMA was introduced by Bowen in 1965 and with the addition of a glass filler led to the first commercial glass filled, dental composite [18]. The bulky nature of the bisphenol-A group leads to a rigid polymer with lower polymerization shrinkage. Bis-GMA-based materials, however, show a relatively higher water sorption due to the two hydroxy groups in the Bis-GMA molecule [19]. Since the development of Bis-GMA, frequent structural modifications have been made using the hydroxyl group. Esterification of the hydroxyl groups with varying molar mass aliphatic and aromatic acids decreases the viscosity and volume shrinkage with increasing aliphatic chain length [20]. The increasing aliphatic chain length, however, also leads to a

decrease in modulus. Aromatic acids enhance the mechanical properties of the resin when an oxy-spacer is present but the viscosity of the monomer increases. Other studies have shown similar trends in viscosity and cure shrinkage by modifying the hydroxyl group of Bis-GMA with dimethyl siloxy and dimethyl isopropyl siloxy side groups [21]. Reactive diluents such as TEGDMA are effective at lower levels, but large amounts can negatively affect matrix properties by increasing polymerization shrinkage and water sorption [22]. Reduced matrix viscosity simplifies filler addition and allows for higher filler loads. A matrix material showing improved compressive, diametral tensile properties, and increased modulus, as measured by micro-indentation when compared to a 60/40 Bis-GMA/TEGDMA system, was found in binary mixtures of urethane-based monomers with three and four methacryl groups [23].

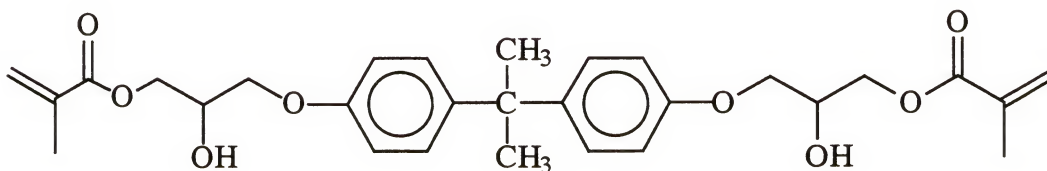


Figure 2.1. The structure of 2,2-bis(4-(2-hydroxy-3-methacryloyloxyprop-1-oxy)phenol)propane (Bis-GMA)

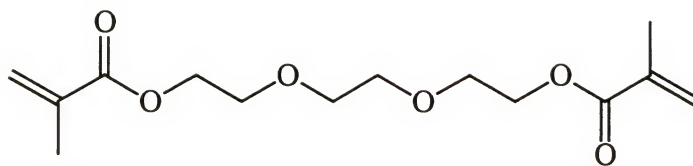


Figure 2.2. Tri-ethylene glycol dimethacrylate (TEGDMA)

Some of the advantages of using thermosets over thermoplastics are lower initial viscosity that allows a fast and homogeneous dispersion of fillers and enhanced wettability, high resistance to moisture and solvents, high resistance to creep, higher thermal stability, and higher elastic modulus.

Chemically cured resins consist of a base paste containing initiators (e.g., benzoyl peroxide) and a catalyst paste usually containing an amine. Some of the drawbacks of chemically cured systems are their increased risk for discoloration due to the amine content, their tendency to incorporate air bubbles during the mixing of the two pastes, and their fixed reaction time. During the last 20 years the use of chemically cured resins has declined in favor of light-cured composites [17]. These materials consist of a single paste and have controlled finishing times. A visible light cure is preferable to a UV-light cured material for several reasons. UV-light sources provide a shallower polymerization depth [24], a reduced light intensity over time, and cost more than a visible-light source. In addition, there are potential hazards of exposing the oral mucosa to UV light since this tissue lacks protective pigmentation [25].

Visible light-cured systems usually contain camphoroquinone as the initiator and an aromatic amine as an accelerator. The amine simplifies electron withdrawal from the

camphoroquinone when exposed to visible light with a wavelength of 468 nm. This reaction generates free radicals for the polymerization of the resin.

The Filler

The filler phase of resin composites varies considerably between different materials. The decision to use fillers in composites is determined by the level of benefits certain fillers can provide. For many commercial composites that do not require a high level of mechanical strength, filler is a way to use low-cost materials to make up for the bulk of the polymer resin. Fillers are also a way to add particular properties that the base resin is unable to provide. This can include colorants and UV protectors such as carbon black. In this study the use of filler is three-fold. Primarily the filler acts as a non-shrinking component that takes up a significant volume in the dental composite. In this role, the filler reduces the effects of the resin as it shrinks upon curing. Secondly, the filler can reinforce the resin. Through a strong interfacial bond the resin component in composites transfers stress to the filler component. In high strength composites, the filler can also help deter crack propagation. Thirdly, through the use of a bioactive material the filler can also reinforce the bond between the composite and the tooth structure.

Considerations for a composite material include the following: i) filler composition, ii) filler shape, iii) filler dimensions, and iv) filler volume fraction. As long as bonding between the filler and the matrix material is maintained, the filler acts as the reinforcing phase of the composite, improving mechanical properties as the filler content increases [26].

The average diameter of the filler particles in traditional dental composites is about 8-30 μm , while some modern composites contain filler with an average particle

size in the 0.7 to 3.6 μm range [27]. The large surface area of smaller filler particles can increase the viscosity of the resin system leading to a limited volume fraction of filler [28]. Since increasing amounts of filler material are usually desired for the required mechanical properties, there is a limit to the minimum particle diameter. Blends of various particle sizes are one method used to increase the packing efficiency of the inorganic filler.

Common fillers used in dental materials are silica and silicate-based glasses such as zirconium glass, ytterbium trifluoride, lithium aluminosilicate, and barium borosilicate [29], [30]. Silica is chemically stable, increases the hardness of the composite, decreases the polymerization shrinkage, and reduces the thermal expansion of the composites. Silica also has a favorable refractory index resulting in aesthetically acceptable materials. Adding different metal oxides can add radiopacity for simpler x-ray diagnosis, improve color matching to natural teeth and reduce hardness for easier polishing. Durability of these glasses varies with composition and glass-modifying elements such as Ba, Sr, and Zn, which can leach out in an aqueous environment [31]. Leaching of the ions reduces the strength of the filler and increases the risk of rupturing the filler-matrix.

Anhydrides in Dental Materials

Anhydrides have been used for both structural and adhesive purposes in dental materials [32]. Anhydrides have been studied as crosslinking agents for monomers containing hydroxy or amide groups as well as resin composites systems based on UDMA, HEMA, Bis-GMA, and TEGDMA [33]. A cyclic anhydride can react with either of these functionalities to form an ester or amide linkage, leaving a reactive hydroxy group at the end of the carboxylic acid. An anhydride containing an unsaturated double

bond makes it possible to copolymerize with other monomers. A 20% increase in mechanical properties was seen for the combination of maleic anhydride and methacrylamide [33].

Zamora et al. have shown the ability of a cyclic anhydride to incorporate with propoxylated Bis-GMA/TEGDMA [34]. The ability of the cyclic anhydride to offset polymerization shrinkage by as much as 2% was confirmed by post-polymerization volume expansions observed after swelling in water. The hydrolysis was confirmed by a residual weight gain in dehydrated samples as well as FTIR observations. An offset to polymerization shrinkage was also revealed when a cyclic anhydride was added to a Bis-MEPP/TEGDMA system [10].

Another important aspect for dental restorative materials is their ability to adhere to substrates. It has been suggested by Hotz et al. [35] that the prerequisite for adhesion is the presence of free pendent -COOH groups. These groups are assumed to establish hydrogen bonding with chemically reactive surfaces. The glass ionomer cement adheres only to reactive polar substrates like enamel and dentine. Therefore it may be important to know the extent to which the -COOH group in our investigation will be associated with the ions in the system or if there is an effect on the number of free pendent groups on the surface. Since adhesion is a surface property and there is likely to be a sufficient amount of unreacted -COOH groups at the surface this may not be a significant issue. A larger concern for this study is the offsetting of polymer shrinkage that the -COOH groups associating with cations may provide.

Bioactivity of Bioglass®

Fixation of an implant in place is required for dental applications. In the late sixties fixation was demonstrated by integrating the tissue and implant material through the formation of a dynamic high-strength interphase that mimics natural tissue [36]. Bioactive glass was the first material proven to bond to living tissue by the formation of a HCA (hydroxy-carbonate-apatite) interphase [37]. A series of bioactive glasses and ceramics, including hydroxyapatite (HA), Bioglass®, and A-W glass-ceramic, have emerged as new biomaterials with an advantage of encouraging bone ongrowth.

Bioglass® is an inorganic glass that has been shown to effectively bond to tissue through the controlled crystallization of glasses. When Bioglass® is inserted into living tissue a silica-gel forms on its surface by an ion-exchange reaction between the glass and the surrounding body fluids. Next to the silica-gel is a layer high in calcium and phosphorous that is initially amorphous but eventually crystallizes to form HCA. The HCA deposit resembles living bone and is the layer on which new bone can grow. The new bone forms strong chemical bonds to the calcium phosphate layer. Mechanical strength measurements show that the strength of the bone/calcium phosphate interface exceeds the strength of the bone itself [5]. In the oral environment, enamel and dentine are made up of approximately 92 vol% and 48 vol% of hydroxyapatite, respectively [38].

The HCA layer begins to form within a few hours. Stem cells, the forerunners of bone growth, attach to the calcium phosphate layer in about 24 hours. Hench et al. [39] [37], [36] have proposed twelve stages of reactions to occur at the Bioglass® tissue interface. These stages are summarized in Table 2.1. Reaction stages 1-5 occur on the material side while reaction stages 6-12 on the tissue side while stages 6 and 7 probably overlap with stages 3-5.

The bonding rate of melt processed Bioglass® to bone depends on the glass composition. Bioglass® with 42-53% SiO₂ forms a bond to bone or soft tissue, within days. Bioglass® with 54-60% SiO₂ requires 2-4 weeks to bond to bone but does not bond with soft tissue. Melt processed Bioglass® with more than 60% SiO₂ does not have the ability to bond to any living tissue [36]. While the rate of bonding of melt processed Bioglass® implants to bone depends on the glass composition, sol-gel processed Bioglass has a compositional range of bioactivity that extends to 100% SiO₂ [40].

Uses for Bioactive Glasses

The first application of bioactive glasses was to make pieces to replace damaged bones in the middle ear [39]. Benefits for the use of bioactive glasses were then found in the oral environment to fill the cavity in the jawbone caused from the removal of teeth due to disease or injury. Further dental applications of bioactive glass involve the repair of teeth with periodontal disease. In this application, crushed bioactive glass particles are mixed with saline and placed around a tooth to stimulate bone growth to save the tooth [5]. Bioactive glasses have also been used in bone cements [41], [42], [43]. A bioactive bone cement consisting of bioactive glass ceramic powder with silica glass powder and Bis-GMA based resin shows a higher bonding strength than traditional PMMA bone cement for up to 6 months after surgery when used for canine total hip arthroplasty [44]. Bioactive bone cements using Bis-GMA have also shown greater intrusion volume in 5 mm holes than PMMA bone cement when used for acetabular cup fixation in a stimulated acetabular activity [45].

Table 2.1 Proposed Reaction stages of Bioglass® as it bonds to tissue [35], [46], [38]

STAGE	REACTIONS
1	Rapid exchange of Na^+ with H^+ or H_3O^+ from solution: $\text{Si-O-Na}^+ + \text{H}^+ + \text{OH}^- \rightarrow \text{Si-OH} + \text{Na}^+ + \text{OH}^-$
2	Loss of soluble silica in the form of $\text{Si}(\text{OH})_4$ to the solution resulting from breakage of Si-O-Si bonds and formation of Si-OH at the glass/solution interface: $2(\text{Si-O-Si}) + 2(\text{H}_2\text{O}) \rightarrow \text{Si-OH} + \text{OH-Si}$
3	Condensation and repolymerization of a SiO_2 –rich layer on the surface depleted in alkalis and alkaline-earth cations: $\text{RO}_3 - \text{Si} - \text{OH} + \text{HO} - \text{Si} - \text{O}_3 \rightarrow (\text{Si-O})_3 - \text{Si} - \text{O} - (\text{Si} - \text{O})_3 + \text{H}_2\text{O}$
4	Migration of Ca^{2+} and PO_4^{3-} groups to the surface through the SiO_2 -rich layer forming a $\text{CaO-P}_2\text{O}_5$ –rich film on top of the SiO_2 –rich layer, followed by growth of the amorphous $\text{CaO-P}_2\text{O}_5$ –rich film by incorporation of soluble calcium and phosphates from solution.
5	Crystallization of the amorphous $\text{CaO-P}_2\text{O}_5$ film by incorporation of OH^- , or CO_3^{2-} anions from solution to form a mixed hydroxyl-carbonate apatite layer.
6	Agglomeration and chemical bonding of biological moieties in the HCA layer
7	Action of macrophages
8	Attachment of osteoblast stem cells
9	Differentiation of stem cells
10	Generation of matrix
11	Crystallization of matrix
12	Proliferation of bone

Newer glass-ceramics and glass/polymer composites are being studied as possibilities for replacing metal amalgams used for fillings [5]. M. P. Zamora et al. [12] demonstrated improved mechanical properties by increasing the amount of a melt

processed Bioglass® added to 2,2-Bis[4-(2-methacryloxypropoxy)phenyl]propane and triethyleneglycol dimethacrylate. Measurements taken at room temperature for dynamic mechanical analysis at 1 Hz of composites samples showed that as the Bioglass® concentration increased from 0, 20, to 40 v% filler, the storage modulus increased from 6.3, 9.0, to 16.1 GPa, respectively. Lin et al. studied the effects of the melt derived Bioglass® concentration on the mechanical strength of Bis-GMA composite resin and an acrylate-based composite resin [11]. Their results indicated that the compressive strength, modulus of rupture and wear thickness of the Bis-GMA-based composite resin is superior to the acrylate-based composite resin. The difference in mechanical strength between these two composite resins is attributed to the 3-D cross-linking network of the Bis-GMA polymer, which provides a stiffer matrix for the material. The mechanical strength of these composites initially increases with the filler content, but begins to decrease after 40% addition. A theoretical study by West and Wallace [13] calculated that Bioglass® will undergo a ring opening expansion reaction at the surface that may partially offset polymerization shrinkage in the resin system.

Bioglass's positive influence on mechanical properties and the possibility of further polymerization shrinkage offset suggest that it would be beneficial to further investigate the possibility of incorporating Bioglass® into the system studied here.

Mechanical Properties

The average biting force of a person with natural dentin is approximately 77 kg (170 lbs) when distributed over a number of teeth in the posterior part of the mouth [15]. This load can translate to stresses as high as 1970 kg/cm^2 for an individual tooth.

When composite materials are placed into function, ideally the stresses produced are absorbed by the resin matrix and transferred via good bonding to the stronger inorganic filler. Since the improvement to the physiochemical properties in the composite is primarily due to the filler particles and the bond formed with the matrix, it is essential to the longevity of the material to focus on this bond. Should bond failure occur between the filler and the matrix, as may occur in an aqueous environment, the strength of the composite decreases. One way to improve this bond is through the use of silane coupling agents, however; this bond is in a non-equilibrium state when subject to an aqueous environment and therefore can become suspect during the function of the composite. Improved filler bond reliability could be achieved by the use of porous filler particles. With such a filler, the monomer may penetrate the porous surface and enhance a mechanical retention of the resin to the filler particles. In addition, the monomer reacts with the coupling agent that is chemically bonded to the filler surface, thus forming a chemical bond between the matrix and filler.

A high modulus of elasticity is necessary for a restoration to withstand the high stress levels. High stiffness of the composite will reduce the deformation of the composite at the tooth-restoration interface. Since enamel has a high modulus of elasticity (~48 GPa), the modulus of a composite should ideally be close to that of the enamel because a lower modulus composite will cause higher stresses to be transferred to the tooth structure near the restoration-tooth interface.

Tensile strength is determined by the bond properties between the filler and the matrix. Optimized bonding results in tensile strength properties slightly higher than that of the pure resin. Thus, an increase in filler content should not have a dramatic effect on

improving the tensile strength. On the other hand, incomplete filler-matrix bonding weakens the material and a reduction in tensile strength of the composite may occur with time. As with the tensile properties, increased filler fraction increases the compressive strength, at least as long as good bonding exists between the filler and the matrix.

The use of composites in posterior restorations has increased the concern for microleakage (bacterial penetration) and recurrent caries around the restorative materials. This concern relates to the polymerization shrinkage, the water sorption ability, and dimensional fluctuations caused by thermal changes in the oral environment. Each of these factors contributes to marginal instability, and since organic/inorganic composites generally do not possess the same ability to corrode and seal marginal gaps as amalgams, there is a risk for permanent gap formation around these restorations [17]. In the same vein as the corroding amalgam, a bioactive composite that can take advantage of a filler that has the ability to leach or absorb ions in a continuous bond formation to the natural tissues is desired.

One problem is how to establish a true chemical bond to hydroxyapatite and/or dentinal collagen. The functional carboxyl groups can form complexes with calcium and other metals and thus have the ability to form good seals with the tooth structure. These polycarboxylate cements form strong bonds to enamel and weaker bonds to dentin (due to the dentin's lower calcium content, higher organic content, and unbondable areas consisting of tubules).

One of the main criticisms of current resin-based composite materials is that they are susceptible to dimensional changes. In dental materials this poses a serious problem, especially when the dimensional change involves shrinkage. Polymerization shrinkage

can be enough to disrupt the seal between the resin and the material it is bonded to. It can also result in stresses and strains that lead to cracks in the resin. These cracks or gaps can lead to leakage pathways and the potential for the formation of caries.

Composite Interfaces

It is often necessary to use a binder between the filler particles and the resin matrix to transfer stresses between the more ductile resin and the stiffer filler. The strength of this bond is extremely important. If debonding occurs, large changes in wear resistance and tensile strength will result. Currently available composites use mechanical and/or chemical mechanisms of filler-matrix bonding. In composites containing inorganic filler the filler is treated with a silane-coupling agent. The silane molecules have the ability to bond to the filler surfaces by forming covalent Si-O-Si bonds while providing additional functional groups that can participate in the polymerization of the matrix.

To improve mechanical properties a rigid interface can lead to high levels of stress transfer from the matrix to the fillers so that more stress is supported by the high-elastic modulus, high strength fillers. Another concern is environmental stability. The interface between the matrix and the fillers can act as a pathway for corrosion leading to filler debonding and composite failure.

In polymer composites, three types of interactions can be defined as they relate to the interface: mechanical, physical, and chemical. Mechanical interlocking can occur between the filler and the matrix when rough surfaces of the filler are combined with filler/matrix wettability to form high levels of interfacial strength. An example of a physical interaction can occur through differences in the coefficients of thermal

expansion, relaxation temperatures or surface energies of the involved phases. Chemical interactions are bonds produced between the constituents.

Silanes such as methacryloxy propyltriethoxysilane and glycidoxypropyl trimethoxysilane and copolymers such as poly(styrene-co-methacryloxy propyltriethoxysilane) have been shown to improve strengths up to a specific concentration [47]. After this concentration is reached, the silanes are only physically adsorbed on the bonded layers and a decrease in mechanical properties is measured. The physically adsorbed silanes can act as a source for crack formation.

Producing more rigid interfaces in composites through the use of silane treatments can also enhance the lifetime of composites [48], [49]. The effect of hydrolytic degradation is particularly strong at weak interfaces resulting in filler debonding. More rigid interfaces imply larger degrees of physical and chemical interactions that will restrict attack by water.

Silane coupling agents are a common method used to improve adhesion between phases of glass reinforced composites. Other methods, however, have also been employed to enhance polymer/filler interactions including methods such as plasma treatments, ozone treatments, and polymer coatings or grafts [50].

Polymer grafts can contain special chemical groups that have a high affinity towards groups present on the filler surface, for example, silanol groups on silica. Factors that affect the grafting procedure are the surface density of silanol groups, the polymer molecular weight, and the number of reactive groups on each chain.

Poly(methyl methacrylate) was grafted onto glass beads and used in poly(vinyl chloride) composites [51]. The ability for PMMA to dissolve in PVC allows the grafted

chains to entangle more readily with the matrix chains leading to higher levels of stress transfer. Improvements in yield stress were observed, however, no improvement in elastic modulus was seen and the strain to failure decreases.

Co-reaction of the organofunctional groups of a coupling agent in a thermosetting resin can be achieved during cure bridging a glass filler to the resin leading to a stronger interfacial bond. A theoretical approach by Bergeret and Alberola [52] to quantify the molecular mobility of a styrene-methacrylic acid copolymer glass bead composite was developed by studying the dynamic mechanical behavior and thermal properties of the composite. They concluded that higher filler content and smaller particle size leads to a greater number of anchored bonds. This effect is enhanced for beads coated by a silane.

The adhesion of silane agents to the matrix is still under investigation. Two mechanisms have been identified in promoting matrix adhesion in thermosetting resins. The first type describes a crosslinked siloxane formed on the filler surface that restricts the diffusion of the matrix. A sharp interface is formed so that adhesion depends primarily on the formation of primary bonds. The second mechanism describes a silane and a cross-linkable resin, which interdiffuse and react with each other giving rise to an interpenetrating network.

Hydrolytic Degradation of Composites

Resin-based restoratives, once polymerized, will still be constantly interacting with their surrounding environment. Mainly, this involves the resin's response to the presence of water. Water, which diffuses into the matrix, can cause free unreacted monomers and ions to leach out – further contributing to shrinkage and weight loss. Conversely, water can absorb into the matrix and lead to swelling. The chemistry of

contemporary restorative materials that incorporate hydrophilic resin molecules may lead to significant volumetric changes for several months after placement.¹

The water sorption capacity and the degree of swelling produced in composites are related to the volume fraction of polymer. Accordingly, water sorption capacity is highest for materials with the lowest inorganic filler fractions. Soderholm, et al., investigated the leakage of filler elements from four composites after storage in water using atomic absorption spectrophotometry [53]. Taking into account the total filler surface areas of the fillers, the quartz and pyrolytic silica containing composites leach less silicon than composites containing strontium and/or barium glasses.

Some studies related to water storage show a decrease in bond strength with time while others show the opposite effect. These findings can be interpreted as 1) occurrence of hydrolytic degradation at the resin-dentin interface, 2) swelling of composite causing a decrease in stress level at the interface, and 3) water plasticization of the polymer thereby improving the stress distribution at the interface.

Martin and Jedynekiewicz [54] studied the net dimensional changes in three light-cured dental composites after storage in water (37°C) for 24 months, using an automatic laser radial micrometer. The three composites included: 1. a urethane modified bis-GMA and EBPADMA, 2. a bis-GMA-TEGDMA, and 3. a UDMA-TCB composite. The three composite samples made from each resin system contained 77, 70, and 75 wt% glass, respectively. The measured polymerization shrinkage of each composite is 3.5, 4.0, and 3.23 vol%, respectively.

The shrinking of dental resins due to cure can cause defects around filler particles and increase the difficulties in obtaining adhesive bonding to both the tooth and filler. In

addition the restorative material can expand due to the adsorption of water or other oral contents. Expansion can cause internal stresses from heterogeneous swelling leading to material failure from cyclic sorption and desorption of fluids. It was questioned by Bowen, Rapson, and Dickson [55] whether it is possible to have hygroscopic expansion equal to or compensate for the polymerization shrinkage. In their work, only one commercially available restorative composite and two experimental composites based on Bis-GMA were able to offset polymerization shrinkage through the absorption of water. The resulting residual shrinkage, however, reportedly occurs after at least 225 days of immersion. Within this time frame, however, the composite could have already debonded from the filler or tooth structure and the subsequent absorption of water become either a non-issue because of sample failure or an additional mechanism for sample failure. What is more important is the kinetics of water absorption and shrinkage after initial cure. Since the restoration to the tooth is performed in as dry a condition as possible, water uptake primarily occurs after the initial polymerization shrinkage of the composite. It is therefore of great concern to determine whether there is any further shrinkage after the initial cure of the sample.

Degree of Cure

There have been several reports of incomplete conversion after the initial light cure [56], [57], [58]. As a polymer network forms, the onset of vitrification limits monomer diffusion so that the mobility of reactive chain ends is reduced limiting the extent of reaction. Most commercial dental composites have an extent of polymerization of between 52 and 75% [59]. A limitation on the degree of cure results in a more heterogeneous structure. The unreacted chain ends and monomers can then act as

defects. Unreacted species along with a limited amount of active chains in a network restricts the mechanical and physical properties of these materials.

Most of the studies cited above focus on an additional heat treatment to improve the mechanical or physical properties of the resin composites. A heat treatment, however, can have adverse affects on the tissues surrounding the tooth. For composites, a post-cure heat treatment can produce additional internal stresses especially at temperatures near the glass transition temperatures of the materials. As the samples cool, significant tensile stresses within the composite occur, particularly at the filler/matrix interface; here the difference in thermal expansion coefficient between the filler and matrix is important. Internal stresses could contribute to lower fracture toughness values for post-cured composites. The addition of a post-cure heat treatment has not been shown to ultimately improve physical properties. After sufficient time, light-cured materials have similar properties to the post-cure heat-treated materials [56],[57]. Therefore, the important issue is the speed at which the highest conversion can be achieved.

The reduction of unreacted monomer components remaining in the composite is critical to enhancing color stability, lowering leachable materials into a patient's mouth and enhancing biocompatibility of the restoration. In addition, given the applications for these materials, the mechanical and physical properties of the composites in water are critical. Water sorption on less cured samples could cause a greater reduction in the mechanical properties because a more fully cured sample would have a polymer network more resistant to degradation. Increasing the degree of conversion in composites results in lower solubility [60]. Solubility has been linked to the degradation of composites in vivo due to the softening on the materials [61].

The ability of the resin to reach a significant degree of conversion becomes even more important in applications where filler will be used. It is possible for a filler to impede to degree of cure as indicated by the work of Ferracane and Marker [60] where the extent of cure was found to be dependent upon the barium glass filler volume.

According to work done by Ferracane and Condon [62] there is a rapid elution of uncured monomer or oligomers with the simultaneous absorption of water by the composite. This will lead to a lower density for materials less fully cured prior to emersion in water than for composites with a higher degree of cure. The lower crosslink density could contribute to lower mechanical properties of light-cured only materials compared to post-cure heat-treated materials after emersion in water. The final properties of heat cured materials often remain higher than those that were light-cured only when emersed in water, but both materials experience similar reductions as a result of aging in water [57].

Wear of Composites

Laboratory studies have shown that an increase in volume of bonded filler increases the wear resistance of dental composites pointing to the resin as the weak-link [1], [6] [63]. However if the filler becomes un-bonded and poorly retained, an increase in filler fraction could accelerate the wear rate. Almost all currently employed inorganic fillers are non-porous solid structures. However, inadequate wear resistance limits their use in posterior restorations [38]. Composites made from a porous silica gel powder (diameter averaging to 10.0 microns) in triethylglycol dimethacrylate were shown to have a low wear resistance comparable with a commercial product [38] as measured by the wear rate. An important factor in the wear resistance is the mechanical interlocking

between the filler and the matrix. Reducing the ability of the matrix to diffuse into the pores of the filler has the potential to significantly lower the wear resistance of the composites.

Besides using the filler to improve the wear properties of a composite, increasing the degree of cure, i.e. reducing the level of remaining double bonds, also acts to improve wear properties [64], [65]. Ferracane et al. [66] studied the degree of cure in composites containing equal amounts of Bis-GMA and TEGDMA with a strontium glass filler, as it relates to resistance to wear. Their study showed that the resistance to abrasive wear of a dental composite can be improved by enhancement of its degree of conversion. However, work done by de Gee et al. [65] concluded that any secondary cure, i.e. a heat treatment, may be used to improve the degree of conversion of a composite offers little advantage to increasing the wear resistance of the composites. Using commercial dental composites, de Gee et al. compared the wear rates of samples that were photo-cured to samples that were photo-cured and then heated to 125°C with a halogen lamp. They found that, within a few weeks, the composites that underwent only the initial cure attained a wear resistance comparable with the additionally light/heat-treated equivalents. The authors subscribed their finding to a gradual relaxation of polymerization contraction stresses in the matrix concentrated around the filler particles into a more homogenized distribution throughout the matrix. They suggest that the total stress within the samples during mechanical loading may be decreasing with time leading to an improved wear resistance that becomes comparable to the heat treated samples which have undergone an accelerated relaxation of local stresses due to the implementation of heat.

Summary

Many approaches have been taken to improve the mechanical properties of dental composites and improve their useful life span. Many obstacles have been identified in the pursuit of an ideal replacement for the natural tooth structure including toxicity, aesthetic appeal, polymerization shrinkage, hydrolytic stability, and wear resistance.

This work examines the feasibility of providing a bioactive composite capable of developing direct bonding to the natural tooth through the growth of a hydroxy-apatite layer by using a sol-gel derived Bioglass® filler. Growth of this bioactive layer needs time to develop and may be limited by the diffusion of activating elements, further surface adhesion techniques are needed to improve the bonding of the filler to the matrix.

This work explores the use of two filler surface modification systems based on (1) a methacryloxypropyl triethoxysilane coupling agent combined with a methyl triethoxysilane coupling agent system and (2) a grafted sulfonated polysulfone. The purpose is to design an interface capable of enhancing the interactions between the phases of a particulate filler and the matrix by promoting mechanical and chemical interlocking through the formation of an interpenetrating network between the matrix and a methacrylate functionalized polymer silanated to the filler.

CHAPTER 3

SURFACE MODIFICATION OF PARTICULATE BIOGLASS® IN DENTAL RESINS THROUGH A METHACRYLATE BASED COUPLING SYSTEM

Introduction

Considerable effort has been made during the past 40 years to understand, control, and modify the filler-matrix interface [67]. It is at the interface where stress concentrations develop because of differences between thermal expansion coefficients of the reinforcement and matrix phases, loads applied to the structures and polymerization shrinkage (for thermosetting materials) and/or crystallization (for thermoplastic materials). The interface can also serve as a nucleation site, a preferential adsorption site, and a locus of chemical reactions.

Silane coupling agents are considered to be adhesion promoters between the organic matrix and the inorganic filler of composites. Enhanced adhesion improves the mechanical strength and chemical resistance of the composite. Although adhesion is the central function of silanes, there are many factors involved in the silane modification of the organic-inorganic interface that alter the properties of the composite. One important function of the silane treatment of the filler in a thermosetting resin is a reduction of the inhibitory action of the filler on the cure of the resin [68]. The silane strengthens the boundary layer of resin and thus has a positive effect on the properties on the composite even if failure is not initially located at the interface. With the appropriate coupling agent,

fracture of the composite does not occur at the interface or through the resin, but rather is directed through the filler.

In minute proportions, coupling agents at the interface can have a profound effect on the performance of a composite. Coupling agents contain chemical functional groups that can react with silanol groups on the glass. Attachments to the glass can thus be made by covalent bonds. In addition, coupling agents contain at least one other, different functional group that can co-react with the laminating resin during cure leading to a chain of primary bonds between the glass and the resin. The effectiveness of the coupling agent is directly related to the reactivity of the functional group.

Optimum mechanical performance of a mineral-reinforced organic polymer composite can impose contradictory requirements on the interface between the polymer and the mineral [69]: (1) Optimum stress transfer between high modulus fillers and a lower modulus resin requires an interphase region of intermediate modulus. (2) Composite toughness and ability to withstand differential thermal shrinkage between polymer and filler require a flexible boundary region or a controlled fiber pull-out to relieve localized stresses.

A flexible, deformable phase is desirable to accommodate stresses set up at the interface due to differential shrinkage between the resin and the filler during polymerization. The amount of silane in a typical glass finish is not sufficient to provide a low modulus layer at the interface, but it may be possible that the silane treated surface allows preferential adsorption of one of the ingredients in the resin [70]. Unbalanced cure at the interphase region could also provide a flexible resin much thicker than the silane layer.

In the opposite extreme, the silane coupling agent could function by “tightening-up” the polymer structure at the interface layer [71]. In this way maximum bonding between the resin and the filler is obtained with strong resistance to hydrolytic cleavage. These morphology-changing theories seem more appropriate to thermoplastic resins that have more mobility in their bulk than their thermosetting counterparts, however, the filler can have varying degrees of catalytic effect on thermosetting resins [72] which can alter the morphology of the composite interface. In general, the silica surfaces inhibit cure [73] resulting in lower mechanical properties and chemical resistance. Thus silane treatments can be used to overcome this inhibition.

There are several theories of how bonding occurs through coupling agents so as to improve the mechanical properties of composites. The oldest and probably the most accepted of these is that coupling agents contain chemical functional groups through which primary bonding can occur between the filler and resin [74].

Another possible factor in a coupling agent’s ability to improve composite properties is that physical adsorption of the resin on the high-energy surfaces of the filler could provide adhesive strength in excess of the cohesive strength of organic resins, assuming that complete wetting can be obtained [72]. In order to obtain complete wetting of a surface, the resin must initially be of low viscosity and have a surface tension lower than that of the filler surface. Because Bioglass® has a hydrophilic surface, under atmospheric conditions it is likely to be covered by a thin layer of water. Thus the spreading of a non-polar resin is reduced resulting in poor wetting. A polar resin, however, may be able to either adsorb the water or displace it. In this way a coupling agent can alter the polarity and thus the surface energy of the filler to make it more

favorable to wetting by the resin. Polarity can be described through the solubility parameter of the constituents. The closer the solubility parameters of the coupling agent and the resin, the more likely they are to intermingle.

Mohsen and Craig studied the effect of silanation on the dispersion of quartz and zirconia-silica fillers by monomers used to formulate dental composites [68]. The authors concluded several generalizations including that the effectiveness of silanation on the dispersion of the filler particles was greater (i) when silanation from ethanol solution was used compared to direct addition; (ii) when three times the minimum uniform coverage was used; (iii) when the silane contained methoxy rather than ethoxy groups; (iv) when the silanes were trialkoxy rather than dialkoxo compounds; (v) when the length and bulkiness of the organic functional groups was smaller; and (vi) when the organic functional group was methacrylate rather than acrylic.

A review of several possible theories of how silane coupling agents can improve the mechanical properties of a composite was developed by Plueddemann [69]. The restrained layer theory [69] suggest that silane coupling agents act by “tightening-up” the polymer structure at the interface while also providing direct bonding through silanol groups. It has generally been observed that polymer molecules adsorbed on a rigid filler particle are more closely packed than in the bulk. The degree of ordering of these adsorbed molecules decreases with distance from the reinforcement, resulting in a boundary region that has a modulus that is intermediate between the resin and the reinforcement providing a uniform stress transfer. It is difficult, however, to reconcile this concept with the need for stress relaxation at an interface because of differential thermal shrinkage between polymer and filler.

To deal with stresses due to different coefficients of thermal expansion, the deformable layer theory was developed [69]. In the deformable layer theory there is a preferential adsorption of certain constituents in the uncured resin or a catalytic effect due to the mineral filler on the resin, which is dependent of the filler finish, that results in stress relaxation through mechanical flexibility.

The maximum toughness for a rigid resin is obtained through a deformable layer while maximum chemical resistance is obtained through a rigid layer. Tough water-resistant composites may be prepared from rigid resins by bonding a thin elastomeric interlayer to the glass surface through a cross-linkable silane. Elastomeric interlayers can be selected that bond to the matrix resin by interdiffusion or some related mechanism.

The reversible hydrolyzable bond theory [69], proposes the reversible breaking and remaking of stressed bonds between coupling agent and glass in the presence of water. In this theory, water allows for the relaxation of stresses without loss of adhesion. Water resistance is possible under conditions of hydrolytic equilibrium only if the resin at the interface is rigid. Since stress relaxation by reversible hydrolysis at the interface is limited to molecular dimensions, this mechanism is most effective in resin composites with fine fibers or particulate fillers in which strains in the resin between particles are limited to small distances approaching molecular dimensions.

Exotherms of three catalyzed resin systems cured in the presence of mineral fillers were measured by Plueddemann [69]. Flexural strengths of composites were found to be better with silane-treated minerals that allow resins to cure with higher exotherms. Thus a restrained layer rather than a deformable layer must be the better morphology of the

filler-resin interface for optimum mechanical properties and water resistance. However, it is also necessary to provide a direct chemical bond between the resin and the filler.

Organic polymers with polar functional groups can form oxane bonds with mineral hydroxide surfaces. These covalent bonds can provide adhesive strength greater than the cohesive strength of the materials involved, but tend to have poor resistance to water [75]. Such hydrolysis has some degree of reversibility.

The silanol groups of the silane molecules usually condense with the surface hydroxyl groups and the silane molecule becomes a part of the filler. The distribution and the nature of the surface-active sites therefore, restrict the silane molecule in this monolayer. Three regions can be identified in the silane interphase: a chemisorbed monolayer at the filler surface, another chemically bound layer above the monolayer, and a loosely bound physisorbed layer that can be rinsed off. Ishida reported that more than a monolayer is needed during the processing of the silanated fillers to yield the optimum strength of a composite material but that the presence of a physisorbed layer yields unfavorable mechanical properties [76]. Ishida attributes this conclusion to steric considerations that hinder the formation of the necessary interfacial chemical bonds or the improper orientation of the organofunctional groups for chemical bonding. In addition, multiple layers of chemisorbed silane can lead to interpenetrating network formations. Using a silane treating solution with varying concentrations created the thickness variation, the higher concentration solution may be said to yield more loosely bound silane layers.

For this project, three surface variations on particulate sol-gel Bioglass® are studied. Among these are: (1) dried, untreated Bioglass®, (2) grafted sulfonated

polysulfone (SPSF) with different degrees of sulfonation (Chapter 4), and (3) methacryloxypropyl triethoxysilane (MAMTES) coupling agent combined with methyl triethoxysilane (MTES) coupling agent. This chapter deals with the coupling system MAMTES:MTES. Concerns include the ability of the coupling system to improve the mechanical properties of the composites and to investigate the effect of both the amount of coupling agent used during processing and the ratio of MAMTES to MTES. Other points of interest studied are the effects of the post-cure environment of the composites and how the submersion of the samples in either a water or salt solution effects the physical properties of the samples.

Experimental Procedure

Silanation of Substrates

Silica glass pieces and Bioglass® particulate were silanated using a ratio of methacryloxypropyl triethoxysilane (MAMTES) coupling agent and methyl triethoxysilane (MTES) coupling agent. The coupling agent was first mixed into dry-toluene for 10 minutes at room temperature in a sealed polypropylene container. The substrates were then added and mixed using a stir plate for 75 minutes. Afterwards the silica pieces were rinsed three times with ethanol while the particle mixtures were centrifuged and rinsed with ethanol three times before either substrates were allowed to dry under vacuum at 100°C for 2 hours. The unsaturated bond of the methacrylate group on the coupling agent is sensitive to drying, therefore care must be taken to avoid severe drying conditions that could degrade the silane.

Prior to the silanation of the silica pieces they were sonicated for 15 minutes consecutively in dichloroethane, acetone, then methanol. They were then placed in a furnace at 420°C for 1 hour.

Analysis of Glass

Prior to any surface treatment, the Bioglass® particles are subjected to drying for no less than three hours at 120°C. The density of the particles was determined through helium pycnometry using a micropycnometer from Quantachrome Corporation. The surface area, used to determine the amount of coupling agent to be reacted, and the pore size, used to indicate the success of the surface treatment, for the particles are measured using the BET (Brunauer-Emmett-Taylor) method and the BJH (Barrett-Joyce-Halenda) method, respectively.

X-ray photoelectron spectroscopy was performed using a Kratos DS800 Mg radiation XPS using a 90° incident beam. Prior to the analysis the samples were dried at 90°C under vacuum before placing into the XPS sample chamber where the pressure is reduced for 12 hours.

Composite Production

The matrix material is comprised of 2,2'-bis-(4-methacryloyl ethoxyphenyl) propane (Bis-MEPP), tri-ethylene glycol dimethacrylate (TEGDMA), and nadic methyl anhydride (NMA). Bis-MEPP and TEGDMA were diluted with acetone and passed over inhibitor removal columns obtained from Aldrich. The acetone was then removed by roto-vaping. NMA was used as received. The initiator system used was 0.5 w% camphoroquinone (CQ) and 0.5 w% N,N-dimethyl-p-toluidine (DMPT). To initiate the

ring opening of NMA, 2.5 w% diaryl iodonium hexafluoroantimonate relative to NMA was added.

The resin was mixed on a Genie Vortex mixer in containers that exclude light. 30 v% Bioglass® ($d < 20 \mu\text{m}$) was then hand mixed into the resin. Composites were processed using vacuum to facilitate particle wetting and resin degassing.

The uncured composites were then molded between glass plates separated from the material by polyethylene terephthalate film. The mold was then illuminated using a UniXS twin Xenon strobe lamp light cure oven manufactured by Heraeus Kulzer on both sides for 180 seconds. If necessary the samples were then cut using a slow speed diamond saw. To produce tensile samples an aluminum mold made to ASTM type 5 dogbone specifications was used so that no post cure cutting was necessary.

Samples designated as 'dry' were placed in sample bags and stored in desiccators. Alternate post cure environments included a water soak in ultrapure ($17\text{-}18 \text{ M}\Omega\text{-cm}$) water and a salt-water soak, both held at 37°C for 5 weeks.

The composition of the salt-water soak (Table 3.1) is based on artificial saliva but lacking in proteins. The pH of the solution is adjusted to 6.7 with NaOH or HCl and the volume increased to 1L using ultrapure water.

Analysis of Composites

Thermoanalysis testing

Thermogravimetric analysis (TGA) on synthesized materials was performed using a TG/DTA 320 Seiko apparatus. The heating rate used was $10^\circ\text{C}/\text{min}$ in a nitrogen flow of $200 \text{ ml}/\text{min}$. The sample and an alumina reference were introduced into a platinum crucible to be heated from 30 to 1000°C .

Table 3.1. Composition of salt-soak for 1 L of solution

Salt	Concentration
Potassium phosphate	25 mM in 0.1 L
Sodium dibasic phosphate	24 mM in 0.1L
Potassium hydrogen carbonate	150 mM in 0.1 L
Sodium chloride	100 mM in 0.1 L
Magnesium chloride hexahydrate	1.5 mM in 0.1 L
Citric acid	25 mM in 0.006 L
Calcium chloride dihydrate	15 mM in 0.1 L

Dynamic scanning calorimetry (DSC) analysis was performed in a DSC 220 Seiko thermoanalysis system. The analysis was performed at a heating rate of 10°C/min with a continuous flow of nitrogen gas (80 ml/min). The sample and an alumina reference were sealed in aluminum pans for testing: A background, acquired by running the same program on an empty pan and alumina reference, was subtracted from each sample scan.

Physical testing

Both the composites and the Bioglass® particles were analyzed with scanning electron microscopy (SEM) equipped with an energy-dispersive x-ray analyzer (EDS). Samples were carbon coated and analyzed in a SEM JEOL 6400 EDS Tractor System II EDS system.

Hardness testing (ASTM E384-89) was performed on cured samples using a Micromet 3 microhardness tester from Buehler LTD. A Vickers indenter was used under a load of 50 gf with a 50s dwell time. The number obtained is calculated from dividing the applied load by the surface area of the indentation.

Water sorption tests were performed on samples cured into pellets 1.2 cm in diameter with a thickness of 0.2 cm. Samples were suspended in either water or a salt solution at 37°C. These samples were periodically removed from the solution, wiped off with a dry cloth and weighed. After changing the solution the samples were again submerged for further conditioning.

Mechanical testing

The ASTM D790-81 four-point bend procedure was used to measure flexure properties. An Instron 1122 fitted with a four-point fixture with a support span of 40 mm and a load span of 20 mm. The crosshead speed used was 1 mm/min. The sample size was 7 x 2 x 45 mm.

Tensile testing was performed according to ASTM D638-89 using the Type 5 sample geometry. An Instron 1122 was fitted with pneumatic grips with a clamping force of 80 psi. The crosshead speed was 0.05 inches/min (1.3 mm/min) corresponding with an elongation rate of 5% per minute.

Confirmation of Silanation

Helium pycnometry was used to determine the volume of the Bioglass® particles in order to be able to calculate the density of the particles and consequently to determine the concentration of filler needed to produce the composites. The technique employs Archimedes principle of fluid displacement to determine the volume. The displaced fluid is a gas (helium with a purity of 99.999%) that can penetrate the finest pores. Six samples were analyzed and a density of $2.6 \pm 0.1 \text{ g/cm}^3$ for the untreated Bioglass® was measured.

The surface area, pore volume, and pore volume distribution of the unmodified Bioglass® was determined by the Brunauer-Emmett-Teller (BET) and Barrett-Joyce-Halenda (BJH) methods using nitrogen as the adsorbed gas. The amount of nitrogen absorbed depends on the partial pressure of the sample chamber. Therefore, the amount of nitrogen adsorbed at different partial pressures can be isothermally measured during the adsorption and desorption of the sample at liquid nitrogen temperatures. An isothermal plot is created of the relative pressure against $[W(P_0/P-1)]^{-1}$, where W is the weight of gas absorbed at a relative pressure. The weight of a single monolayer of gas is obtained from the slope and the intercept of this plot. The surface area of a sample can then be calculated using the recorded cross-sectional area of a hexagonally-close-packed nitrogen monolayer at 77K (16.2 \AA^2). For the unmodified Bioglass® the specific surface area was measured to be $128 \text{ m}^2/\text{g}$, the average pore diameter was measured to be 122 \AA with the diameters of the pores ranging from $45\text{-}985 \text{ \AA}$ with a total pore volume of 0.443 cc/g , consistent with a mesoporous particle. After silanation there was no significant change in the pore characteristics.

X-ray photoelectron spectroscopy (XPS) was performed on modified and unmodified silica plates to verify the success of the silanation technique. The XPS spectra, from 0 to 350 eV, are reproduced in Figure 3.1 showing the results of an unmodified silica piece and a silica piece silanated in a solution of dry-toluene and a 1:1 ratio of MAMTES to MS coupling agent. The peaks are identified in the spectrum as the 1s carbon peak, at approximately 286 eV and the 1s and 2p silicon peaks at 156 and 105 eV, respectively. A semi-quantitative software routine that computes the area under specified peaks was used to verify the amount of each element on the surface of the

samples. These calculations are reported in Table 3.2 for the silica piece and two modified silica pieces modified with either a 1:1 or a 2:1 ratio of MAMTES to MS. Evidence of the successful modification of the surface is seen in the formation of a second peak, 283 eV, in the vicinity of the original carbon peak and an increase in the percent of carbon recorded from the spectra.

There will always be contamination from atmospheric carbon and oxygen. Since the spectra from the samples was recorded during a 4 sample run in the same chamber, the carbon contamination is the same in each spectra so that any additional carbon recorded from the modified sample is real and from the silanation. For the 1:1 molar ratio, approximately 41% carbon is added and for the 2:1 molar ratio, approximately 59% carbon is added. Assuming that the reactivities of the coupling agents with the glass are the same, then the additional carbon can be related to the 20% more carbon found in MAMTES verses MTES.

The measured increase in carbon from the 1:1 mole ratio to the 2:1 ratio is approximately 43.9%; this agrees well with the calculated increase, which is 45.5 %. The similarity between the measured and calculated amount of carbon increase suggests the deposition of the coupling agents as monolayers rather than the formation of multilayers. The addition of a second carbon peak indicates the addition of a second binding energy involving carbon. This peak can be identified as resulting from the vinyl group on the methacrylate functionalized coupling agent.

The amount of hydroxyl groups per square nanometer has been reported as five on a glass surface. Using this assumption and the surface area measured by BET/BJH, the number of hydroxyl groups is approximately 2.56×10^{19} per gram of Bioglass® particle.

Even assuming that every three hydroxyl groups is capable of reacting with a the coupling agent, the number of coupling agent molecules needed to form a uniform surface is only 8.5×10^{18} , which translates into approximately 1.3×10^{-7} ml per 100 grams of Bioglass®. The likelihood that every three-hydroxyl groups is capable of reacting with a silane molecule and that the diffusion of every silane molecule through the toluene solution to the glass surface occurs is small. This explains the observation by Mohsen et al.[68] that a 3x concentration of silanation was more effective than a 1x concentration. Since silanes can also condense with themselves via the alkoxy groups rather than with the hydroxyl groups on the surface of the fillers, several times the minimum amount is actually needed for optimum silanation.

Evaluation of Composite Manufacturing Procedure

Figure 3.2 shows the thermogravimetric analysis of a composite filled with 30 v% Bioglass®. With helium pycnometry the density of the resin and glass was determined to be 1.2 and 2.6 g/ml, respectively. Using this it is possible to calculate the weight fraction of the glass in the composite to be 50.3 w%. Throughout this work, the volume fraction of the composites were checked along with the degree of homogeneous mixing of the filler by taking samples from different locations in a sample and comparing them.

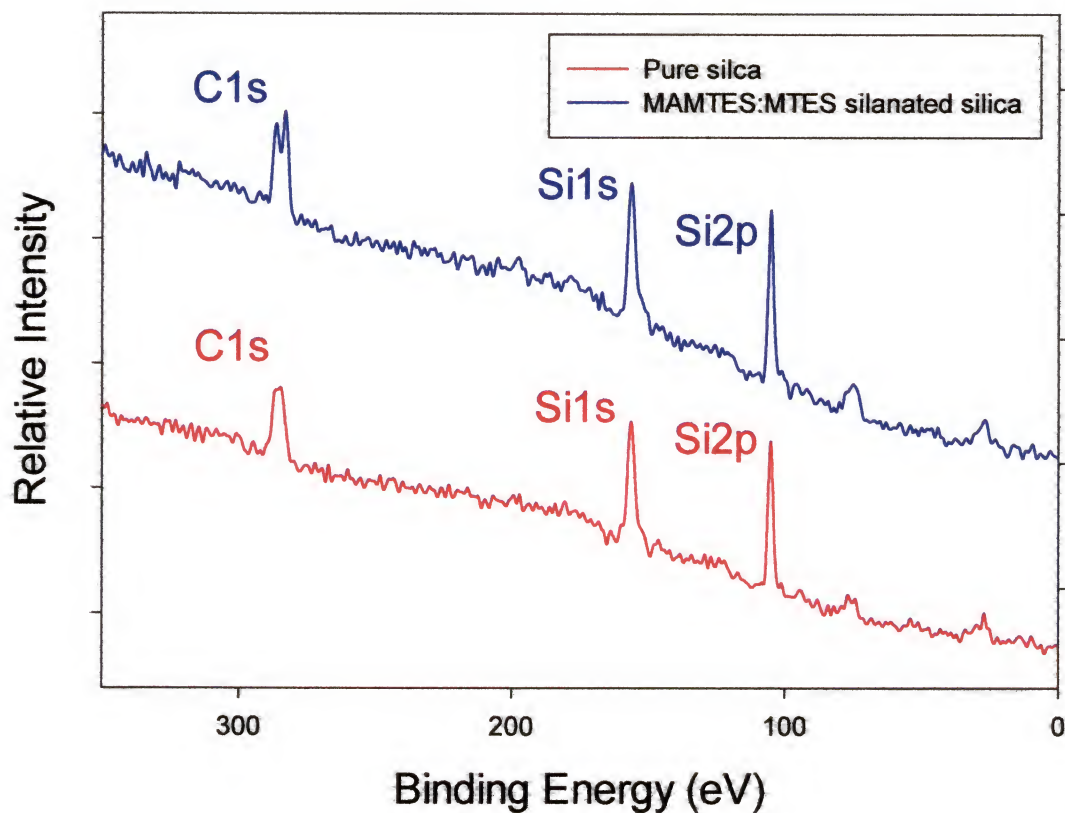


Figure 3.1. XPS spectra of silica and silica modified with a methacrylate based silane-coupling agent

Table 3.2. Results from XPS on silica surfaces modified with a methacrylate based silane-coupling agent

Elements	Position (eV)	Silica	MAMTES:MTES 1:1	MAMTES:MTES 2:1
		Atomic Concentration (%)		
Carbon, 1s	286	17 ± 0	24 ± 4	27 ± 2
Oxygen, 1s	534	66 ± 0	60 ± 3	58 ± 3
Silicon, 2p	105	17 ± 0	16 ± 1	15 ± 2

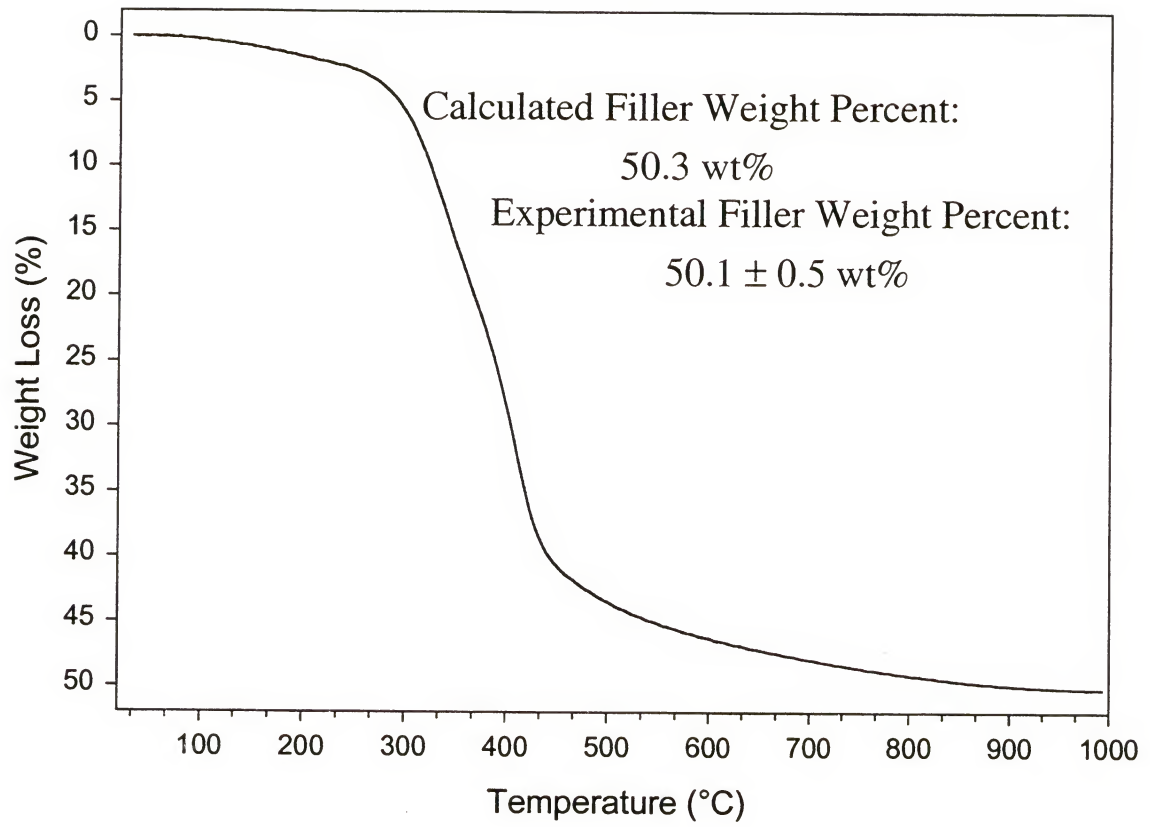


Figure 3.2. Thermogravimetric analysis of composite with 30 v% Bioglass® filler.

Physical Characteristics of Bioactive Composites

During the days after light cure, the hardening of three resin systems were found to have significant increases in the measured Vickers hardness number (Figure 3.3).

Using the equation for exponential growth (Eq 3.1), the trends of these increases were modeled, where y is the Vickers hardness number and x is the time after cure. The coefficients of the equation are recorded in Table 3.3.

$$y = y_0 + a(1 - e^{-bx}) \quad \text{Eq. 3.1}$$

Table 3.3. Coefficients from the curve fitting of the Vickers Hardness results.

Resin System	y_0	a	B
20/48/32 w/DMPT	11.5798	2.8419	0.0284
40/36/24 w/DMPT	3.0156	1.0656	0.0121
40/36/24 w/o DMPT	1.4121	0.7039	0.0119

The initial hardness of the 20/48/32 resin system is over 277% higher than the 40/36/24 resin system with the DMPT initiator and over 735% higher than the 40/36/24 resin system without the DMPT initiator. In addition, the rate of increase for the 20/48/32 resin system is significantly greater than the rates of the 40/36/24 resin systems. The leveling off of the hardness properties for all three resins systems appears to occur on roughly the same time-scale of 5 to 6 days.

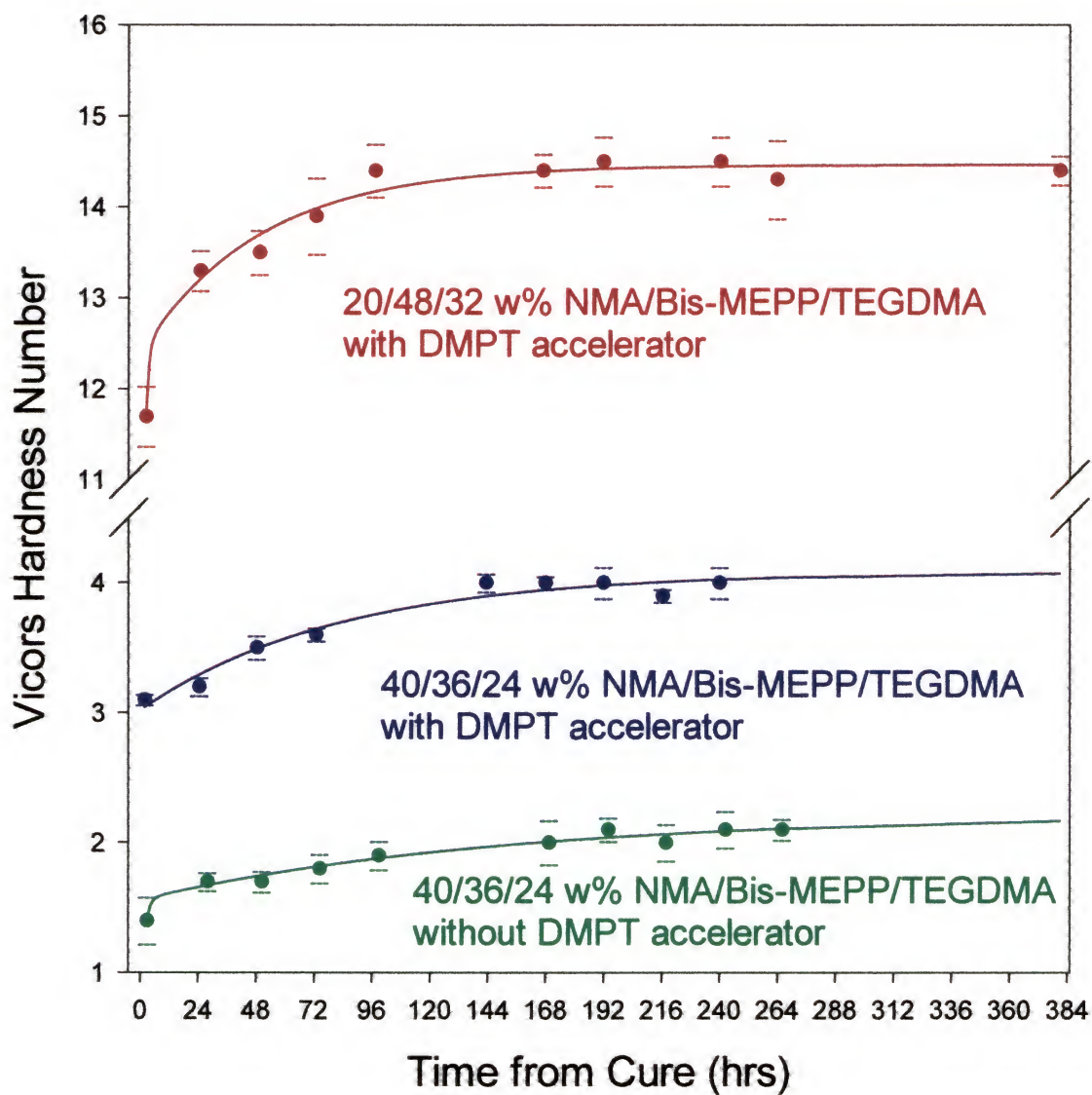


Figure 3.3. Vickers hardness number versus time after light-cure of three different resin systems.

Several studies have related the hardness of a material with its degree of cure [77], [63], [78], i.e. low degrees of cure in the resin is associated with low hardness. Therefore one explanation for the increase in hardness observed in the resin samples over time is that the samples are continuing to cure after the initial light curing. The stabilization of the hardness with time can be related to the reduced movement of any remaining reactive species that effectively inhibits further cure. Several processes can occur to affect the degree of cure for the samples here. First is the amount of initiators present, second is the amount of diluent and third is the reactivity of the components.

The relationship of increasing hardness over time due to additional curing is supported by the work done by Mehlem [10]. Mehlem's study showed that resins of 54/36/10 and 48/32/20 resin systems Bis-MEPP, TEGDMA and NMA averaged an additional enthalpy due to cure of 0.8 ± 0.3 and 0.9 ± 0.2 mJ/mg, respectively. Although the change in enthalpy between these two resin systems is not significant, it does illustrate the presence of uncured material, after the initial light cure, which still harbors the ability of further conversion.

It is expected that systems containing larger amounts of NMA will initially exhibit lower levels of conversion due to the slower kinetics of NMA when compared to Bis-MEPP or TEGDMA. Besides the low reactivity of NMA there is a limit to the degree of conversion for a sample due to early vitrification. NMA is denser than either Bis-MEPP or TEGDMA and has a lower functionality, both factors lower the amount of crosslinking capable of a material as NMA is increased.

In Figure 3.4 the hardness of composites filled with 30 v% Bioglass® both silanated with a 3:1 ratio of MAMTES to MTES and unsilanated is compared to the neat resin, each involving a matrix of 20 v% NMA.

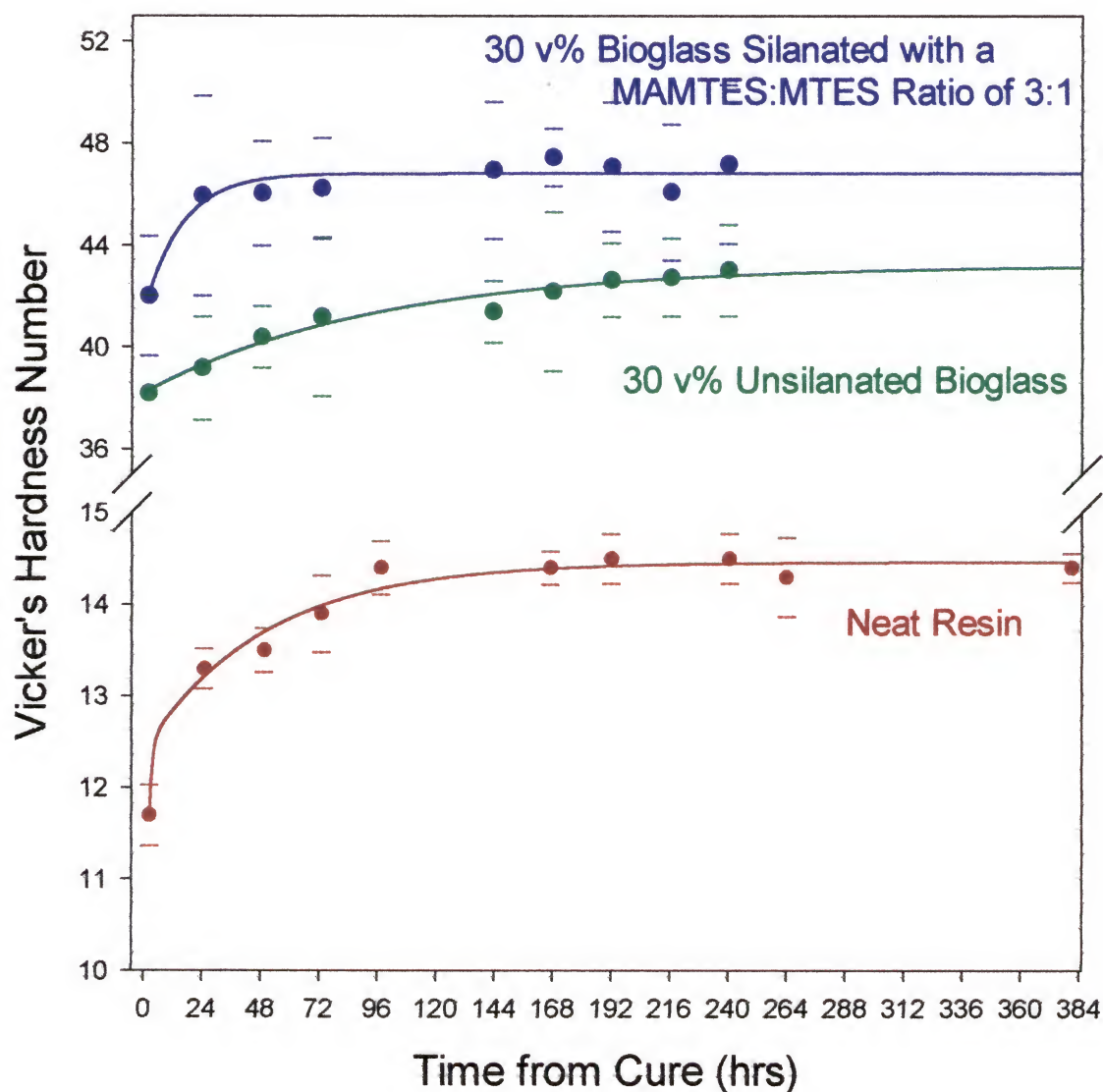


Figure 3.4. Vickers hardness number verses time after light-cure of three different resin and composite systems

As expected, the hardness increases dramatically with the addition of the inorganic filler. A monolithic 45S5 Bioglass® sample has a reported VHN of 458 ± 9.4 [79]. The VHN numbers for the composites in this study fall 68 and 71 % below that predicted by the rule of mixtures for the silanated and unsilanated composites, respectively. A possible reason for the lower hardness numbers is the effect of the “skin-layer” which is a layer resin that occurs during the processing of composites. Differences in the hardness values of the composites may also indicate the way in which the two phases (filler and resin) are arranged and bonded. The major resistance to the penetration of the indenter in these two composites comes from a frictional force as the particles are forced to move in the matrix and from resistance to deformation of the matrix [79]. Therefore, the obtained results indicate that microhardness testing can be used as an indication of particle matrix adhesion.

The much more gradual increase in hardness of the composite made from unsilanated glass when compared to either the neat resin sample or silanated composite may be related to a decrease in the degree of cure resulting from diffractive light scattering [77] that limits the penetration of the activating light. Generally, mineral surfaces inhibit free radical polymerization proportionally to their surface area [77], [69]. The treatment of the filler surfaces with silanes may partially restore the curing efficiency of the composites [69] as supported by the steep increase in hardness of the silanated composite not seen in the unsilanated composite, and the overall higher hardness of the silanated composite in Figure 3.4. Other works have cited a decrease in the degree of cure upon silanation. Ferracane et al. [80] measured no significant decrease in the degree of cure when a methacryloxypropyl trimethoxy silanated pyrogenic SiO₂ microfiller

(DC=65.4±1.7) was added to a 60:40 weight ratio of Bis-GMA and TEGDMA (DC=64.4±1.6), but an increase in the degree of cure when unsilanated microfiller (DC=68.4±1.1) was added. Work done by Labella et al. [81] measured an increase in the Vickers hardness number, from 42.6±1.6 to 48.4±1.9, when 34.9 v% silanated hydroxyapatite (HA) filler was added to a Bis-GMA/tetrahydrofurfuryl methacrylate (70/30 w/w) resin system compared to an unsilanated HA filler. These results are similar to those of this study, which finds a VHN of 47.2±2.7 for the resin filled with silanated Bioglass® and a VHN of 43.03±1.8 for the resin filled with untreated particulate. The increased hardness indicates that the composite is more resistant to adhesive failure when loaded to yield. The leveling off of the ultimate hardness occurs faster in the composite samples than in the neat resins (Figure 3.3). In the filled composites, the accelerated setting reaction could be a result of the heat capacities of the fillers, which insulate the exothermic heat of conversion.

Water uptake is given as one of the major contributing factors in the failure of most resin composite dental materials. In the TEGDMA:Bis-MEPP:NMA system, this is most likely due to the polar nature of NMA and its ability to hydrolyze. It is believed that the water swells and plasticizes the matrix causing a reduction in strength. Therefore, increasing the concentration of NMA in the resin system results in an increase in water sorption.

Two of the three resin systems, 20/48/32 and 40/36/24 with DMPT, were used for water sorption studies of the neat resins (Figure 3.5). During the time of water submersion there is a significant increase in the weight of the samples. The mechanisms of water diffusion for the two samples, however, are different as shown by the two

different equations needed to fit the data. The 20/48/32 samples were fitted using the exponential growth equation (Eq. 3.2) and the 40/36/24 samples were fitted using the sigmoidal equation (Eq. 3.3) where y is the percent weight gain and x is the soak time. The coefficients of the equations are recorded in Table 3.4.

$$y = y_0 + a(1 - e^{-bx}) + c(1 - e^{-dx}) \quad \text{Eq. 3.2}$$

$$y = y_0 + \frac{a}{\left(1 - e^{-(x-x_0)/b}\right)^c} \quad \text{Eq. 3.3}$$

Table 3.4. Coefficients from the curve fitting of the water sorption results.

Resin System	y_0	A	b	C	$d \text{ or } x_0$
20/48/32 w/DMPT	-0.0209	1.6121	0.0197	5.0157	0.0028
40/36/24 w/DMPT	64.6153	6.2459	12.4146	1.0064	-0.0330

Unlike the 20/48/32 sample, the 40/36/24 sample visibly cracked after 6 days of the water soak so that further measurements were unrepresentative. Prior to the failure of sample 40/36/24, this sample began with a slower weight-gain rate that then significantly increased until a possible leveling off.

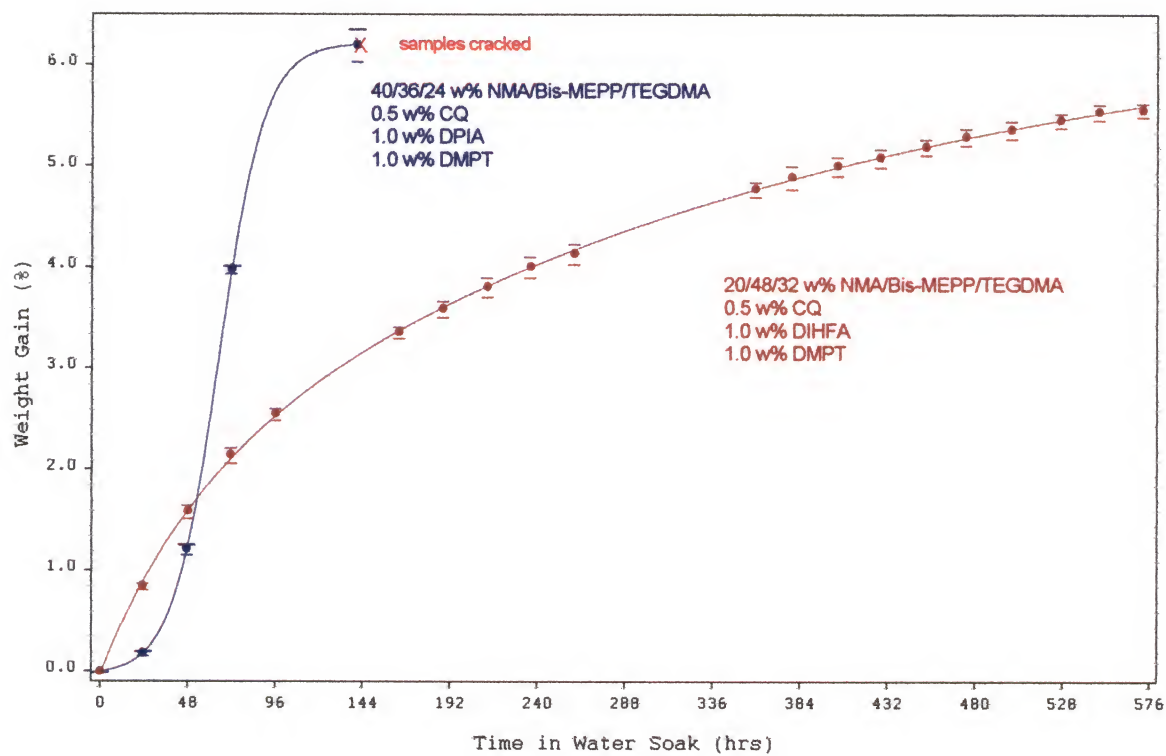


Figure 3.5. Percent weight gain of two cured resin systems resulting from time in water bath.

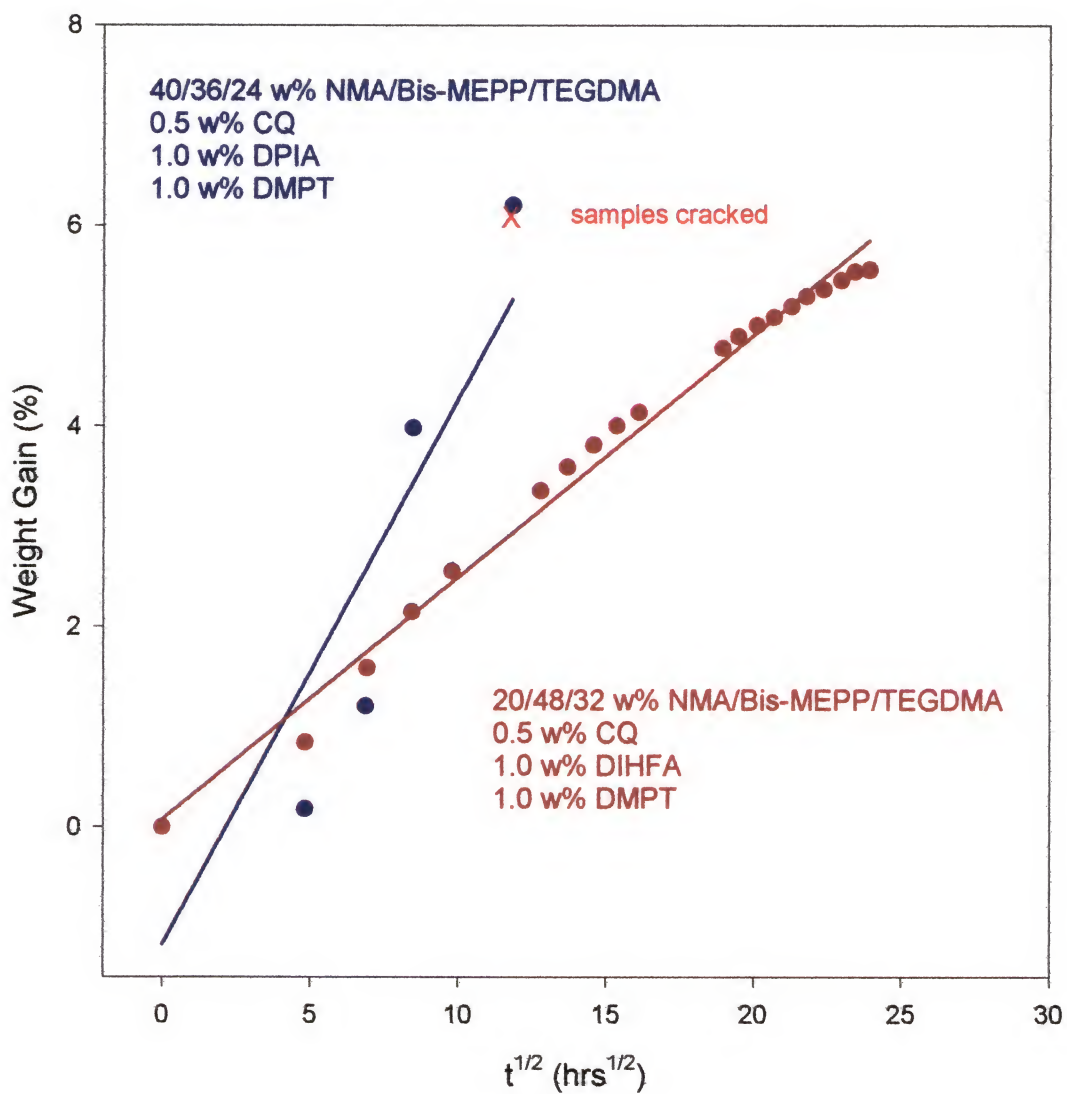


Figure 3.6. Percent weight gain of two cured resin systems verses the square root of time spent.

The relative diffusion coefficients can be determined by graphing the weight gain by the square root of the diffusion time (Figure 3.6). Increasing the NMA concentration leads to an increased diffusion coefficient. The plot for the 40/36/24 sample does not extrapolate through the origin in the graph. This deviation could be due to the leaching of monomer during the soaking procedure, which has been shown to occur in similar resin systems [10], [82], [83], [84], [62] containing TEGDMA and either Bis-MEPP, urethane dimethacrylate, or Bis-GMA.

Increasing the NMA concentration leads to an increased diffusion coefficient. The plot for the 40/36/24 sample does not extrapolate through the origin in the graph. This deviation could be the leaching of monomer during the soaking procedure or because of cracks through the sample resulting from strain on the network structure.

NMA is a polar molecule therefore compositions that contain anhydride take up more water. It is assumed that water swells and plasticizes the matrix causing a reduction in strength. It has been shown that water degrades the filler matrix bond, which accounts for the decrease in strength in the filler composites. The larger amount of water absorbed by the NMA magnifies these effects.

Figure 3.7a shows the effect of adding 30 v% filler to the diffusion properties of the resins submerged in nanopure water held at 37°C. In Figure 3.7a, an untreated filler composite is compared to a 3 to 1 silanated filler composite and a 10/54/36 NMA/Bis-MEPP/TEGDMA resin.

The addition of a filler significantly reduces the amount of water which is sorbed by the materials. The reduce water volume is expected since the polar resin is the primary

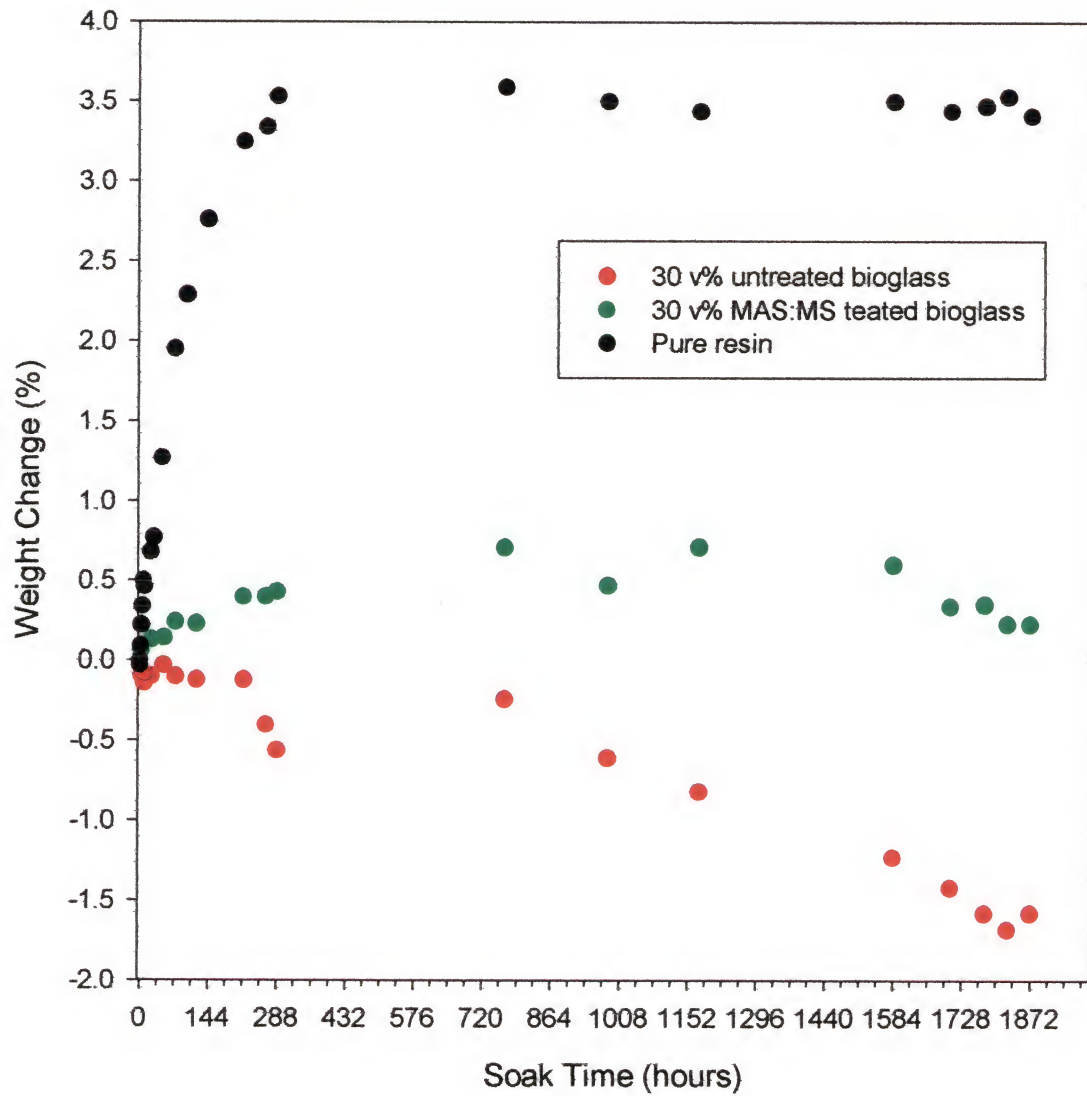


Figure 3.7a. Composites soaked in nanopure water at 37°C

reason for water uptake. The weight loss of the untreated filler verses the treated filler, however is more interesting. In the production of any composite, there is usually the formation of a “skin-layer” of pure resin so that the properties of the bulk material are different from the surface properties. It has been shown, through Soxlet extraction of cured materials, that weight loss of pure resin samples indicates a level of uncured material that has the ability to be leached from the bulk [10]. The loss of weight from the composite sample made with unsilanated glass could be identifying a tendency for the loss of this “skin-layer”. The lack of weight loss in the 3:1 silanated glass could be an indication of the effective binding of the skin-layer to the bulk material through the reinforcing effect of the filler. In addition to weight reduction through the leaching of the resin material, the bioactive filler may also be leaching ions to the nano-pure water. The silane-coupling system is then acting as a shield to the diffusion of water, protecting the filler/matrix interface.

As a comparison, the same samples were soaked in a salt-solution mimicking the ion concentrations and pH found in natural body solutions (Figure 3.7b). Somewhat surprisingly, is no significant change in the diffusion characteristics of the resin submerged nano-pure water and the one soaked in the salt solution. It was originally thought that different diffusion gradients would result from the addition of a salt concentration resulting in a difference in weight change. The weight change in the composite samples differs significantly in the salt solution compared to the pure water. Most obviously are the increased weight gains and the lack of an equilibrium weight for the salt solution soaked samples. A slightly lower weight gain rate is notice in the composite made in the silanated Bioglass®. If the diffusion of water is activating the

glass filler, then the additional weight gain could be the result of the sorption of HCA forming ions (calcium and phosphate) from the salt solution. The lower weight gain rate for the silanated composite is in support of a shielding effect of the coupling agent to the bioactivity of the filler. An alternative reason for the lower weight gain of the silanated composites is an increased degree of cure when compared to the composites made with unmodified Bioglass® as discussed above in relation the microhardness. A declining diffusion coefficient with increased cure times has been reported for commercial resin-modified glass-ionomer dental cements [85]. The increased extent of polymerization reduces the ease with which water molecules are able to diffuse through the structure. Using the rule of mixtures again, the amount of weight change for the composites soaked in the salt solution are only partially explained by the resin characteristics. Additional weight gain, therefore, is a result of the presence of the particles. This could mean that the composite samples are gaining weight through the sorption of HCA growing ions, or because of flaws at the particle/matrix interface, which ease the water diffusion. Figure 3.8 compares the weight change of the composites and resins soaked in either water or the salt-solution verses the square root of time spent in the soak. From Figure 3.8 it appears that, at short times, the resin samples and the composites soaked in the salt-solution follow Fick's law, as indicated by the initially linear weight change with time. Departures from Fick's law could be attributed to the changes in the concentration of the salt solution as it diffuses through the sample, and with the leaching of uncured material along with the dissolution of the particles which increases the heterogeneity of the samples.

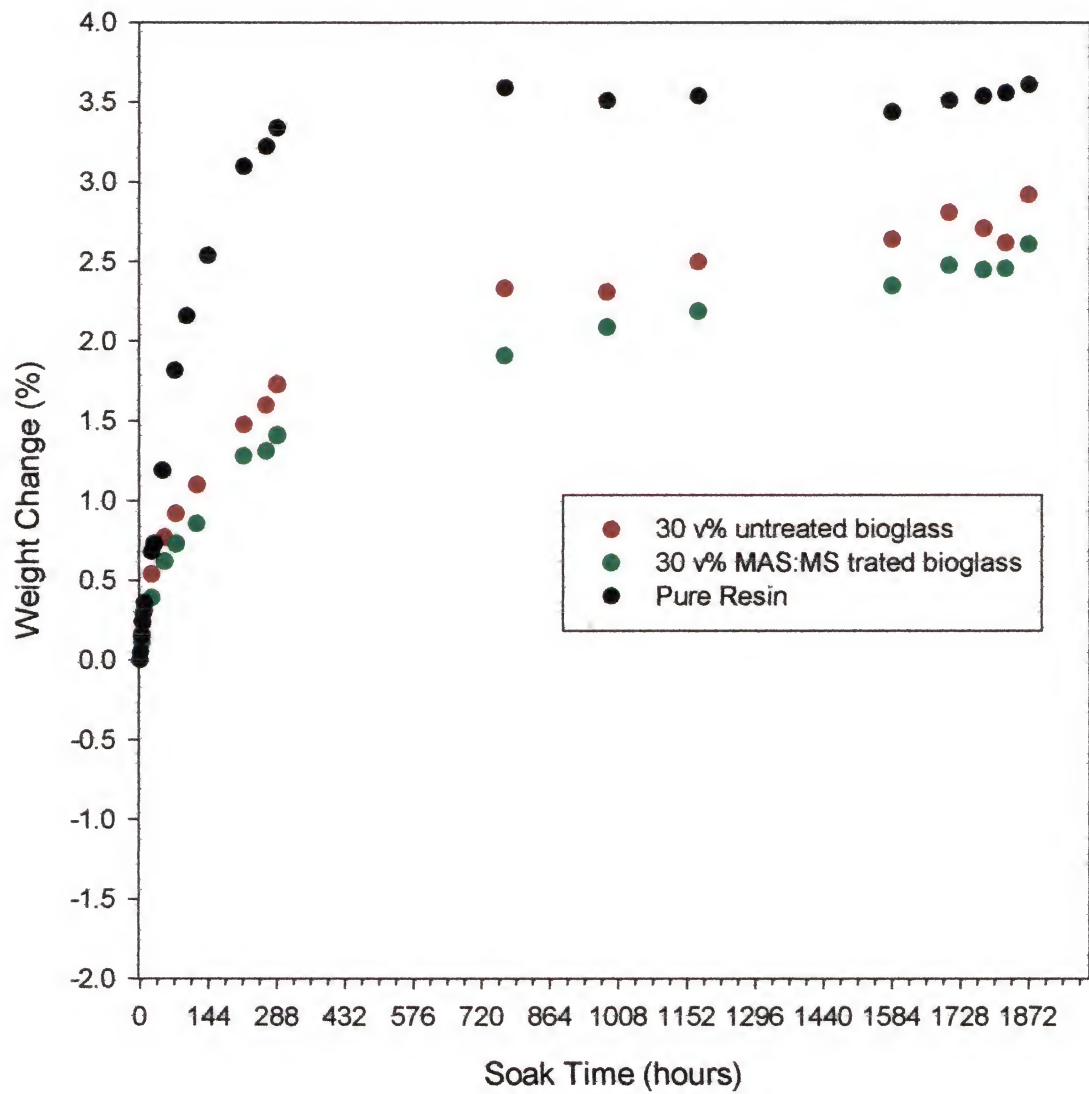


Figure 3.7b. Composites soaked in salt solution at 37°C

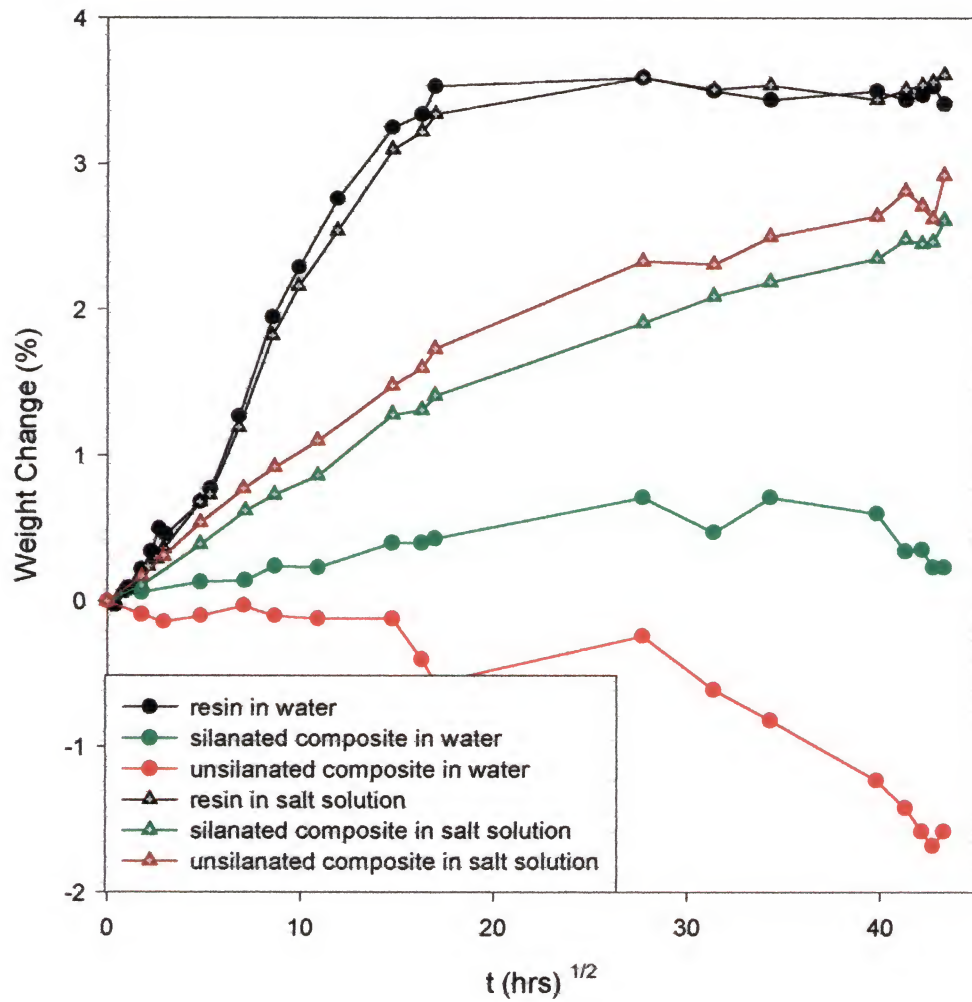


Figure 3.8. Percent weight gain versus $t^{1/2}$ comparing composites and resins soaked in either water or a salt solution.

Mechanical Properties of Methacryloxypropyl triethoxysilane: Methyl triethoxysilane Modified Bioglass Composites

The addition of a methacrylate-functionalized silane-coupling agent has the possibility of improving the energy dissipation between the particle and the resin in two ways. One is through the primary bonding of the methacrylate to the components in the dental resin. The other is through physical crosslinking from the diffusion of the resin and the linear methyl methacrylate polymer grafted to the particles (Figure 3.9). The reason for the addition of the MTES coupling agent is to limit the potential for significant amounts of crosslinking at the interface and increase the occurrence of linear growth of the methacrylate polymer from the glass surface.

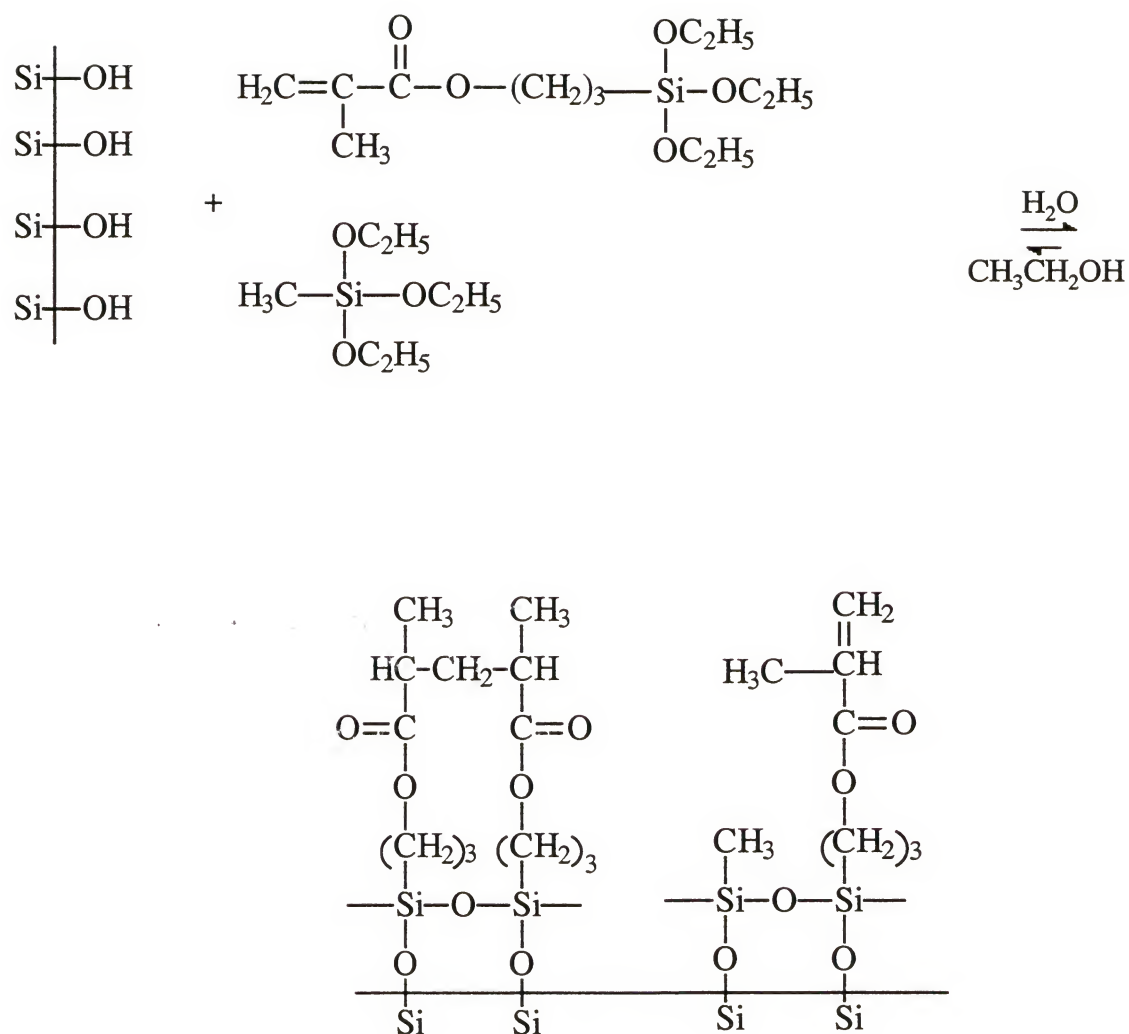


Figure 3.9. Schematic of the silanation by methacryloxypropyl triethoxysilane (MAMTES) coupling agent mixed with methyl triethoxysilane (MTES) coupling agent

Although simplified representations of coupling through organofunctional silanes often show a well-aligned monolayer of silane forming a covalent bridge between polymer and filler, the actual picture is much more complex. The hydrolyzed silane condenses to oligomeric siloxanols that initially are soluble and fusible, but ultimately can condense to rigid crosslinked structures. Contact of a treated surface with polymer matrix is made while the siloxanols still have some degree of solubility. Bonding with the matrix resin, then, can take several forms. For instance, the oligomeric siloxanol layer may be compatible in the liquid matrix resin and form a true copolymer during resin cure, or the oligomeric siloxanol may have partial solution compatibility with the matrix resin and form an interpenetrating polymer network as the siloxanols and matrix resin cure separately with a limited amount of copolymerization [75].

Results from XPS indicated the formation of a monolayer of coupling agent. XPS, however, is unable to determine the degree of crosslinking, which may have occurred and which has a significant impact on the density and stability of the interphase. Toluene, however, was specifically used as the solvent for silanation in order to form a monolayer of the coupling agent on the filler [86],[87].

In order to determine if there is a relationship between ratio of coupling agent used during processing and mechanical properties of the samples, three different ratios of MAMTES to MTES were examined. The tensile strengths of three, 20 w% NMA composites using fillers modified with the different coupling ratios are compared to an unmodified Bioglass® filled composite and an unfilled resin sample (Figure 3.10). In Figure 3.10 the affect of a 5-week soak in a salt solution is also recorded.

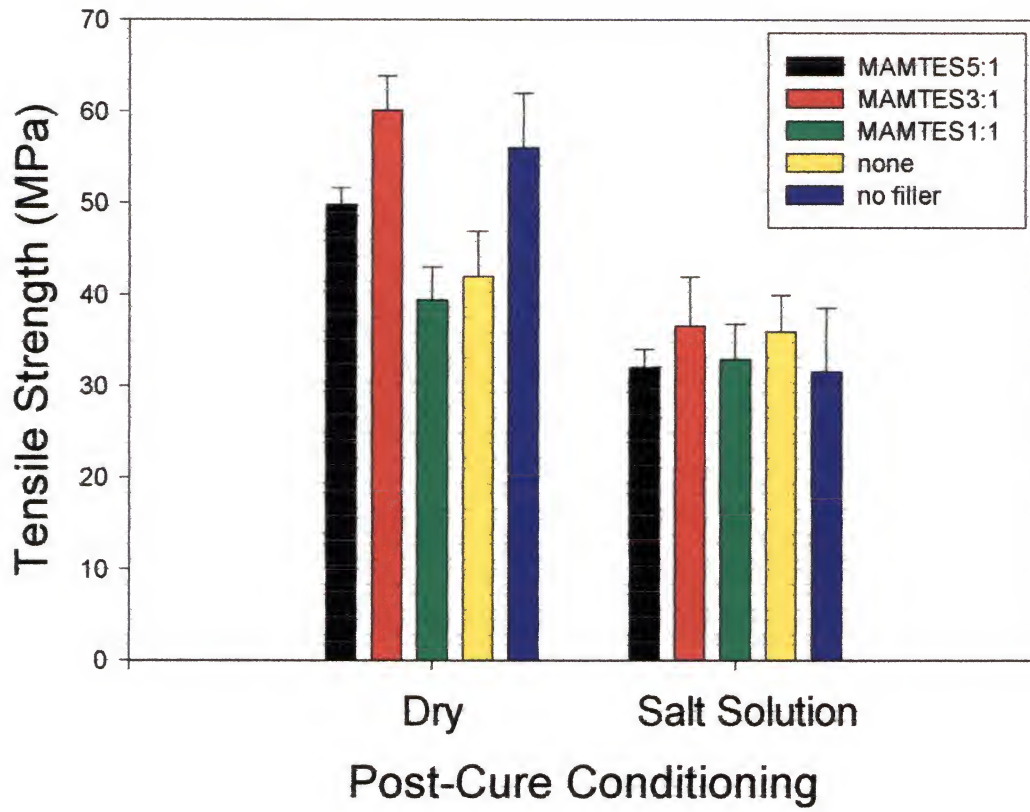


Figure 3.10. Tensile strength of composites varying the post-cure treatment and the ratio of MAMTES to MTES used to modify the filler

The differences between the soaked composites relative to the silane coupling ratios is not significant, however, there are significant differences in the tensile strengths of the dry composites. The functional group for bonding the coupling agent to the polymer matrix is the vinyl group on the methacryloxypropyl triethoxysilane coupling agent. Because this coupling agent can also crosslink with itself a second coupling agent has been added which can bond with the filler through its siloxane group, but has no functional group to bond with the resin. In this way the ability of MAMTES to crosslink with itself is sterically hindered by the addition of MTES to the filler. It then becomes important to balance the need for an adequate number of bonding sites for the resin with the need to avoid significant levels of methacrylate crosslinking in the coupling agent.

In Figure 3.10 the sample showing the highest tensile strength in the dry state is the one processed with a 3:1 ratio of MAMTES to MTES. All other composite samples decrease in strength from the neat resin, regardless of any surface modification. This indicates that the ability of the filler to act as a reinforcing agent depends on the amount of methacrylate functionalized coupling agent used during processing. Too much or too little and the fillers fail to reinforce the composite. XPS spectra of pure silica surfaces treated with either 3:1 or 1:1 ratios of MAMTES to MTES are compared in Figure 3.11. The change in the relative intensities of the two peaks representing the carbon peak could be an indication of the level of functionalization between the two MAMTES:MTES systems. Using a curve-fitting program, Peakfit from Jandel Scientific, the intensities of the two peaks were deconvoluted in order to compare the areas of the two peaks. The results of the deconvolution are depicted in Table 3.5.

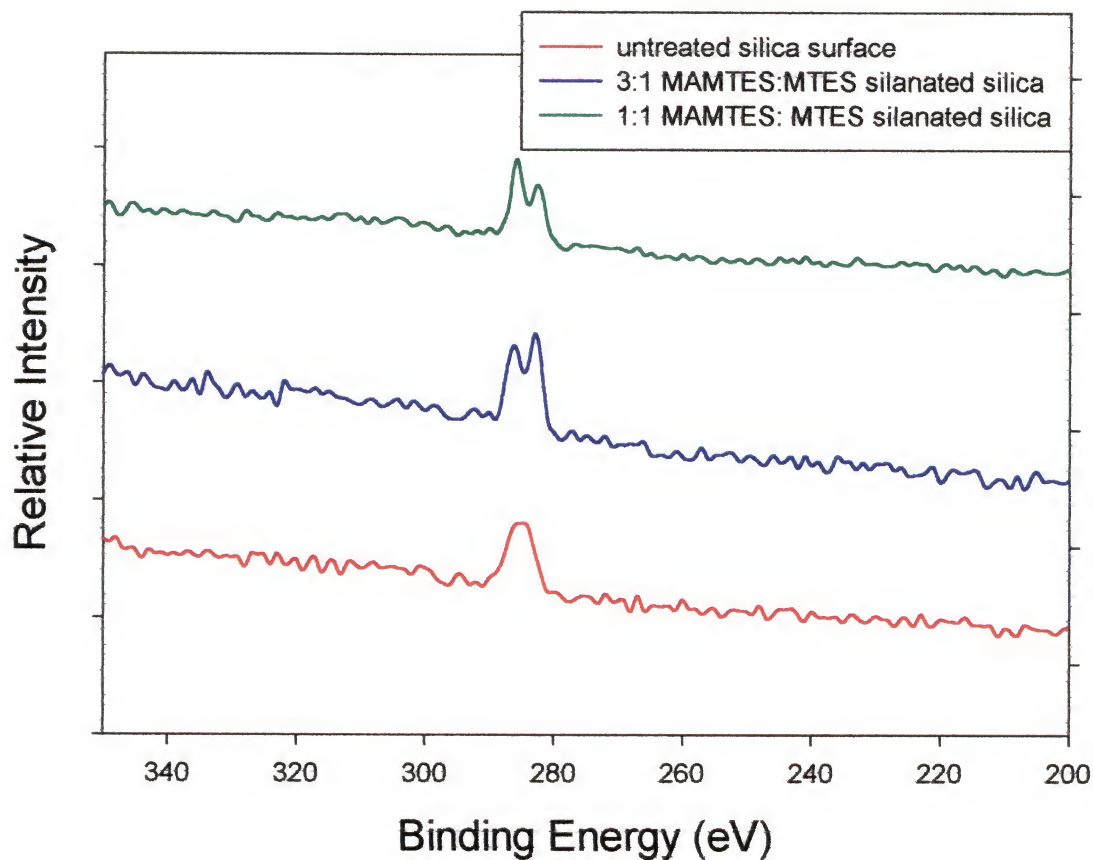


Figure 3.11. XPS spectra comparing the carbon region of silica and silica modified with 1:1 and 3:1 ratios of MAMTES to MTES.

Table 3.5. Deconvoluted carbon peak areas comparing different MAMTES:MTES systems

Coupling System MAMTES:MTES	Percent Intensity	
	286 eV Peak	283 eV Peak
3:1	51	48
1:1	57	42

The first comparison to note in Figure 3.10 is the decrease in tensile strength as a result of the salt solution soak. Using an experimental design program, Fusion Pro, developed by the S-Matrix Corp. a design was created comparing the post-cure environment and silane coupling agent ratio. From the design, the most important variable in determining the tensile strengths of the composite is the post-cure environment. The most likely explanation for the reduced tensile properties is the breakdown of the interface between the filler and matrix at the SiO_2 location and the reduction of tensile strength due to the resin.

In respects to the filler-resin interface, the polar nature of water causes the oxygen atom of water to orient toward the silicon atom attached to the filler [88], [89]. Stresses in the composite can cause the electron orbits of the silicon atoms to become disoriented, which can facilitate the attraction of the water molecule. The development of a polar bond between the negative end of the water molecule means that the remaining proton from the water molecule can orient to develop another polar bond with the bridging oxygen atom in the Si-O-Si bridge. At this point, a breakage of the Si-O-Si bridge would result in a proton transfer to the Si-O- group while the remaining Si- ion would associate with the remaining hydroxy group [88], [89]. The data illustrated in Figure 3.10 indicates a breakdown of the interface. The coupling agent that reinforces the composite in the dry state becomes less noticeable upon exposure to water. Soderholm, et al. [53] showed the hydrolytic degradation of a primarily SiO_2 filler in dental composites through leaching studies using atomic absorption spectrophotometry. Different sized silica particles leached roughly the same amount of silicon when the surface areas of the fillers were taken into effect. Filler-element leakage of four commercially available dental

composites [90] and silane treated quartz or barium filled composites using either a Bis-GMA/TEGDMA or UEDMA/TEGDMA resin system [91], were also investigated after water storage. Both investigations show that water causes leaking of Si from fillers in dental composites at a rate and amount based on structural differences, composition, and available filler surface area.

The tensile strengths of the soaked samples, however, show no significant differences regardless of surface treatment or the addition of Bioglass®. This lack of sensitivity to the filler surface modification indicates that there is a variable of greater influence affecting the composites. The variable consistent throughout the samples is the resin composition; therefore the likely limiting factor for the tensile strengths of the samples is the resin. There are a couple of factors that may be leading to the lower tensile strength in the neat resin sample with water exposure. In the dry condition the affect of NMA is to lower the tensile strength of the composites. It is thought that the reactivity of NMA is less than TEGDMA and Bis-MEPP [10]. As a result, composites containing NMA have higher levels of unreacted monomer or material that is not incorporated into the network structure. The unreacted material can act as a plasticizer for the system causing a reduction in the breaking strength of the composites. In addition, the addition of NMA increases the overall density of the resin prior to cure [10]. This increase in density can make it more difficult for the resin to form an interpenetrating network with the grafted polymer.

The reduction in tensile strength for the resin after exposure to the salt soak is approximately 43.75%. Since the composites contain 30v% filler and assuming there was no hydrolytic degradation stemming from the interface the predicted failure of the

composites upon exposure to the salt soak would be approximately 39.37%. The calculated 39.37% reduction in tensile strength is very close to the actual reduction of approximately 39.11% seen in the composite composed of the filler modified with the 3:1 ratio of MAMTES to MTES. This might suggest some level of interfacial protection from hydrolytic degradation due to the improved reinforcement from the 3:1 coupling agent. Since the other composite systems do not provide any reinforcing properties, this same calculation is not relevant.

The flexural strength of the neat resin and four composites are compared as a function of post-cure environment and coupling system (Figure 3.12). As with the tensile strengths, the highest flexural strengths occur prior to soaking. The magnitude of strength loss, however, is lower for the flexural tests compared to the tensile tests. In fact, for the 1:1 silane coupling system there is no significant flexural strength loss after a 5-week soak using Student's t-test at a 95% confidence level. The flexural strength of the pure resin sample is not recorded for the dry state because during testing these samples bottomed out on the fixtures before failing.

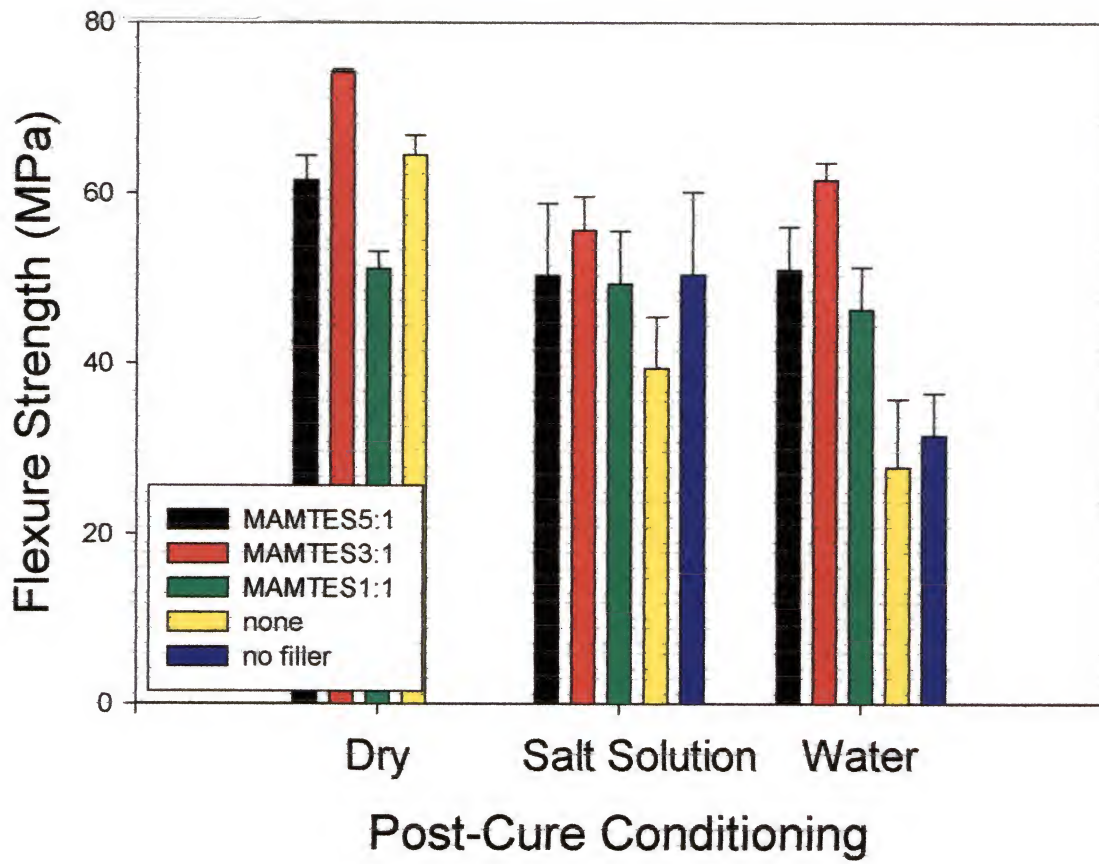


Figure 3.12. Flexural strengths of composites varying the post-cure treatment and the ratio of MAMTES to MTES used to modify the filler

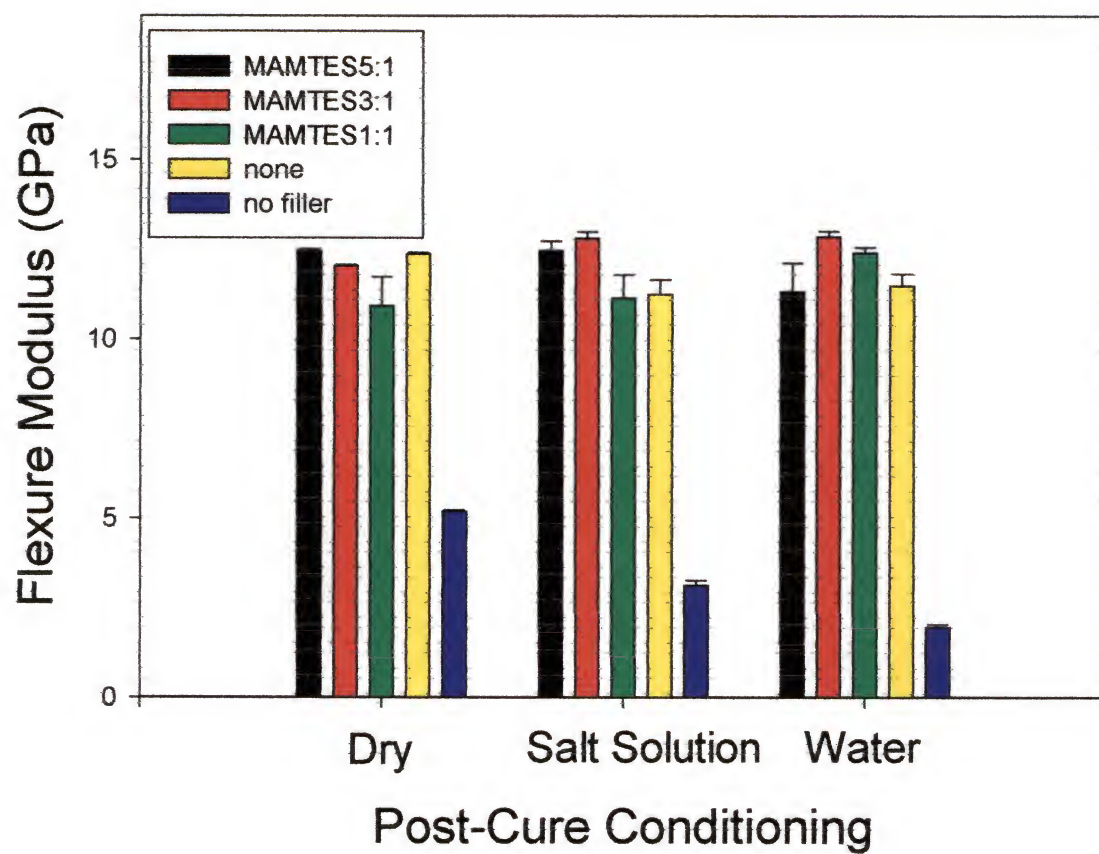


Figure 3.13. Flexural modulus of composites varying the post-cure treatment and the ratio of MAMTES to MTES used to modify the filler

As with the tensile strengths, the 3:1 MAMTES to MTES coupling system shows the highest flexural strength. Figure 3.13 depicts the flexural moduli of the different composite systems. The reinforcing effects of the filler are easily apparent from the increased modulus of the composites compared to the pure resin. Also, in agreement with both the tensile and flexural strengths reported earlier, the 3 to 1 coupling system results in the higher modulus, even after soaking, indicating a level of interfacial stability. Since the surface treatment is different for each composite and the resin has a significantly lower modulus, then the filler particle itself is the dominant variable. Indicating the importance of mechanical interlocking between the filler and the resin through resin filling of the filler's pores.

In a study comparing the filler leachability of composites stored in either distilled water or artificial saliva [91], a higher filler leaching was found in artificial saliva composites made using a silanated quartz. The mechanism hypothesized is that an ion exchange mechanism occurs at the filler surface assuming that during water interaction, the Si-O-Si structure becomes negatively charged. The negatively charged filler particles restrict the amount of cations that can leave the filler surface. Migrating positive ions diffusing through the matrix, however, interact with the negatively charged Si-O-Si surface. Interaction with the surface by the cations makes it easier for some of the original filler cations to leave the filler particles and diffuse into the storage medium [91]. With a bioactive filler, however, these migrating cations may facilitate the growth of a hydroxyapatite layer so that instead of hydrolytic degradation of the interface, the original filler cations remain in the composite.

Overall, however, there is very little difference between the flexural moduli of the composite materials. One common misconception is that excellent adhesion at the interface is necessary to provide the maximum realizable stiffness from a composite [67]. Since the elastic stiffness is defined as the strain approaches zero, matrix/filler adhesion has little bearing on this property. All that is required for maximum stiffness is that there be contact between the two phases so that load transfer can occur between the matrix and the filler. Therefore there any voids at the interface may effect the modulus of a composite so that matrix wetting of the filler plays a key role in increasing the modulus. The similar flexural modulus values for the composites indicate little change in the wetting properties of the matrix material in relation to surface modification.

Hydrogen bonding of carbonyl-containing molecules with mineral surfaces is well known [76]. As expected, the methacryloxy-functional silane also shows evidence of hydrogen bonding with glass particles. The Bioglass® produced by a sol-gel technique to form particles averaging 10 microns in diameter were silanated with a methacryloxypropyl trimethoxysilane coupling agent [38]. Wear rates for composites made with 34 wt% the gel powders and a crosslinked TEGDMA based resin increased as the degree of coupling increased. Showing that the samples with the highest wear resistance were made with powders having no surface modification. These findings oppose the general thought that the reinforcing effect of a silane coupling agent will increase the wear resistance of a composite [53] and show the importance of determining the proper processing method for applying the coupling agent. The use of a coupling agent was found to decrease the pore volume. The reduction in accessible pore volume likely led to a decrease in the pore penetration of the crosslinked resin system in the final

composite. The pore size, analyzed for this study using the BET, measures a specific surface area of $128 \text{ m}^2/\text{g}$ for the unmodified Bioglass®. The average pore diameter was measured to be 122 Å with the diameters of the pores ranging from $45\text{--}985 \text{ Å}$ and a total pore volume of 0.443 cc/g , consistent with a mesoporous particle. After silanation there was no significant change in the pore characteristics, however the specific surface area increased to $145 \text{ m}^2/\text{g}$. The additional surface area could stem from the ability for additional nitrogen adsorption lent by the more convoluted surface texture resulting from the addition of a silane coupling agent. For comparison, in another study using methoxy functionalized coupling agents with sol-gel derived fillers, a lower wear resistance results due to a pore volume which reduced from 0.8121 cc/g to as low as $.1776 \text{ cc/g}$, by applying the coupling agent [38] using a 95% ethanol and water solution at an adjusted pH of 4.5.

Conclusions

A composite interphase was designed to enhance the interactions between the phases of a particulate filler and the matrix by promoting mechanical and chemical interlocking through the formation of an interpenetrating network between the matrix and a methacrylate functionalized polymer silanated to the filler. For this purpose, a methacryloxypropyl triethoxysilane (MAMTES) coupling agent combined with a methyl triethoxysilane (MTES) coupling agent system was successfully silanated to the Bioglass® filler. A dependence on the ratio of methacrylate functionalized coupling agent to a non-functionalized coupling agent used during the silane treatment of the particles on the reinforcing capabilities of the filler was discovered.

At lower levels of methacrylate functionalized coupling agent in the silane system, there is no reinforcing effect by the addition of filler to the resin system as studied using tensile strengths. In fact, there is no significant difference between composites made using an unsilanated Bioglass® and one made with a 1 to 1 ratio of MAMTES to MTES coupling system. Slightly better tensile properties are evident in composites made with higher levels of methacrylate functionalized coupling agent, however, there is still a reduction in strength from the pure resin. At mid levels of MAMTES to MTES, i.e. at the 3 to 1 ratio, there is an increase in tensile strength from the pure resin showing the importance of the coupling system and not just the presence of a coupling system to the enhancement of a composite. Stabilization of the interface is also enhanced by the addition of the 3 to 1 coupling system, as indicated by both flexural and tensile strengths.

The weight change in the composite samples differed significantly in the salt solution compared to the pure water. Most obviously is the increased weight gain and the lack of an equilibrium weight for the salt solution soaked samples. A slightly lower weight gain rate is notice in the composite made in the silanated Bioglass®. If the diffusion of water is activating the glass filler, then the additional weight gain could be the result of the sorption of HCA forming ions (calcium and phosphate) from the salt solution. The lower weight gain rate for the silanated composite is in support of a shielding effect of the coupling agent to the bioactivity of the filler.

CHAPTER 4

DESIGNED INTERFACE FOR BIOACTIVE POLYMER COMPOSITES UTILIZING SULFONATED POLYSULFONE

Introduction

Among the thermoplastics, polysulfone (PSF) is widely used in medical applications because of its excellent mechanical properties and stability in the body environment [92]. Studies using polysulfone as a thermoplastic toughener in thermosetting materials has increased significantly [93] because improvements to fracture properties are achieved without sacrificing other useful properties such as high glass transition temperatures, modulus, and chemical resistance [94], [95]. In epoxy-sulfone systems, improvements in toughness as the polysulfone concentration increases are attained through the two-phase morphology that forms.

Polysulfone in its unmodified form will not wet a glass surface well simply because there is no affinity between the polar groups on a glass surface and the hydrophobic nature of polysulfone. Therefore, to improve an interfacial interaction between the polymer and the glass filler, polar groups can be added to the polymer backbone. For example, the addition of carboxyl groups increases hydrophilicity and alters the solubility characteristics, allowing greater water permeability and better separation [96]. In addition, functional groups added to polysulfone are an intrinsic requirement for ion affinity, ion exchange, and other specialty membranes used to expand the applications satisfied by polysulfone.

Introduction of sulfonic acid groups onto the PSF backbone has been achieved by using chlorosulfonic acid [14], a sulfur trioxide triethyl phosphate complex [97], [98], or a propane sulfone agent [99]. The reaction is reported to proceed with the substitution of a proton located on the aromatic ring close to the isopropylidene unit and the ether bond, by a sulfonic acid group. The selectivity of the sulfonating agent is considered to be a result of steric hindrances. The polysulfone repeat unit has the following structure:

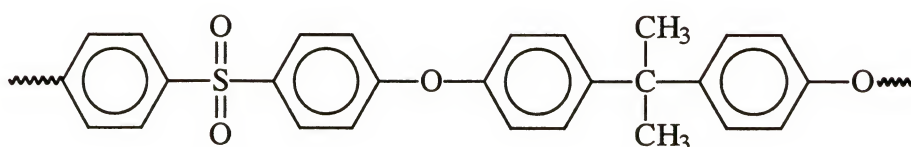


Figure 4.1. Polysulfone repeat unit

Polysulfone has been used as the matrix to form bioactive composites. The bioactive composites were developed by dispersing Bioglass® particles in a polysulfone matrix through the dissolution and precipitation of the polymer in the presence of the particles [14]. The in vitro study of these systems show that a HCA layer is deposited on the surface of a composite having 40% volume fraction of glass after 20 hour in SBF (simulated body fluid). Mechanical tests demonstrated that the properties of the polysulfone-Bioglass® composites are compatible with those reported for cortical bone. To improve the interaction between the filler and the matrix the polysulfone was sulfonated [14]. The resultant composites showed improved modulus, strength, and energy to failure.

In this work the procedure for chemically sulfonating polysulfone was revisited. The interphase of polymer/filler composites was modified by applying a polymer with

mechanically beneficial properties with respects to toughness and thermal stability but with a hydrophilic chemical group attached to it. In this study the sulfonated polysulfone (SPSF) is grafted to Bioglass® particles. The ionomeric nature of SPSF leads it to surround the glass particle and/or form complexes with the ions that leach from the glass. To improve the mechanical properties of the composite, this SPSF layer must be able to dissipate stresses that occur between the resin and particle that would otherwise be relieved either by cracking of the composite or debonding from the filler. For this to occur, the SPSF must be able to form a pathway for energy dispersion from the resin. If adequate diffusion can be achieved between the crosslinking resin and the linear polysulfone this pathway could occur via physical crosslinks as the SPSF becomes entangled in the curing resin. The sulfonic acid chemical group will ideally improve both physical and chemical interactions between the filler and matrix. Thus the resultant composite will be improved.

Experimental

Preparation of sulfonated polysulfone

The sulfonation of polysulfone was performed by first dissolving a commercially available polysulfone (Udel® from Union Carbide) in dichloroethane. Several batches of sulfonated polysulfone were prepared with differing levels of sulfonation. The method of preparation started with dissolving the desired amount of polysulfone (10 w%) in 1,2-dichloroethane (Fisher) in an argon environment and low humidity (11-14%). The solution was placed in a cold bath of dry ice and methanol to slow the reaction. The procedure to sulfonate polysulfone comes from the work of Orefice [14] performed at the University of Florida. However, the decision to cool the reaction was added due to the

high reactivity of the reaction. Chlorosulfonic acid was mixed into the solution, the amount of which was determined by the mole ratio of acid to the polysulfone repeat unit. As the acid was mixed, the polymer precipitated from solution. Mixing continued for 30 min. after which the reaction was halted by adding copious amounts of methanol. The resulting material was rinsed three times with methanol then dried in a vacuum oven held at 75°C.

Methods of Polysulfone Analysis

Spectroscopic techniques

Modified polysulfones were cast into films using dimethyl formamide (DMF) and dried overnight at 75°C under vacuum. Transmission Fourier-transform infra-red (FTIR) spectroscopy was performed with a Nicolet 20SX spectrometer using 128 scans at a 4 cm⁻¹ resolution. A background spectrum was taken before each sample and subtracted from the acquired sample scans.

After rinsing and drying the polymer, samples were dissolved in 1-3ml of deuterated-dimethyl formamide (d-DMF) and filtered down to 40μm into NMR tubes. Proton nuclear magnetic resonance (¹H NMR) 200 MHz spectra were obtained with a Varian XL-Series NMR superconducting spectrometer system. Tetramethyl silane was used as an internal reference material.

Thermal techniques

Thermogravimetric analysis (TGA) on synthesized polymers was performed using a TG/DTA 320 Seiko apparatus. The heating rate used was 10°C/min in a nitrogen flow of 200 ml/min. The sample and an alumina reference were introduced into a platinum crucible to be heated from 30 to 1000°C.

Dynamic scanning calorimetry (DSC) analysis was performed in a DSC 220 Seiko thermoanalysis system. The analysis was performed at a heating rate of 10°C/min with a continuous flow of nitrogen gas (80 ml/min). The sample and an alumina reference were sealed in aluminum pans for testing. A background, acquired by running the same program on an empty pan and alumina reference, was subtracted from each sample scan.

Grafting Sulfonated Polysulfone

Bioglass® particulate was treated with an aminopropyl triethoxysilane (APS) by first introducing 0.5 v% APS into dry-toluene for 10 minutes at room temperature. The Bioglass® particles were then added and mixed for 75 minutes. Afterwards the mixture was centrifuged and rinsed with toluene three times before being allowed to dry under vacuum at 120°C overnight.

The silanated Bioglass® particles were then introduced into a solution of sulfonated polysulfone (1 w%) in ethanol (95% in water) and mixed for 2 hours. The ethanol and non-reacted SPSF was centrifuged off then the resultant particles rinsed 3 times with ethanol. The collected particles were dried at 120°C for 24 hours under vacuum.

Preparation of Composites

Materials

As in the previous chapter the matrix material is comprised of 2,2'-bis-(4-methacryloyloxyphenyl)propane (Bis-MEPP), tri-ethylene glycol dimethacrylate (TEGDMA), and nadic methyl anhydride (NMA). The initiator system used was 0.5 w% camphoroquinone (CQ) and 0.5 w% N,N-dimethyl-p-toluidine (DMPT). To initiate the

ring opening of NMA, 2.5 w% diaryl iodonium hexafluoroantimonate relative to NMA was added.

The resin was mixed on a Genie Vortex mixer in containers that exclude light. 30 v% Bioglass® ($d < 20 \mu\text{m}$) was then hand mixed into the resin. Composites were processed using vacuum to facilitate particle wetting and resin degassing.

The uncured composites were then molded between glass plates separated from the material by polyethylene terephthalate film. The mold was then illuminated using a UniXS twin Xenon strobe lamp light cure oven manufactured by Heraeus Kulzer on both sides for 180 seconds. If necessary the samples were then cut using a slow speed diamond saw. To produce tensile samples an aluminum mold made to ASTM type 5 dogbone specifications was used so that no post cure cutting was necessary.

Samples designated as 'dry' were placed in sample bags and stored in desiccators. Alternate post cure environments included a water soak in ultrapure ($17\text{-}18 \text{ M}\Omega\text{-cm}$) water and a salt-water soak, both held at 37°C for 5 weeks.

The composition of the salt-water soak (Table 4.1) is based on artificial saliva but lacking in proteins. The pH of the solution is adjusted to 6.7 with NaOH or HCl and the volume increased to 1L using ultrapure water.

Table 4.1. Composition of salt-soak for a 1 L of solution

Salt	Concentration
Potassium phosphate	25 mM in 0.1 L
Sodium dibasic phosphate	24 mM in 0.1L
Potassium hydrogen carbonate	150 mM in 0.1 L
Sodium chloride	100 mM in 0.1 L
Magnesium chloride hexahydrate	1.5 mM in 0.1 L
Citric acid	25 mM in 0.006 L
Calcium chloride dihydrate	15 mM in 0.1 L

Mechanical testing of composites

The ASTM D790-81 four-point bend procedure was used to measure flexural properties. An Instron 1122 fitted with a four-point fixture with a support span of 40 mm and a load span of 20 mm. The crosshead speed used was 1 mm/min. The sample size was 7 x 2 x 45 mm.

Tensile testing was performed according to ASTM D638-89 using the Type 5 sample geometry. An Instron 1122 was fitted with pneumatic grips with a clamping force of 80 psi. The crosshead speed was 0.05 inches/min (1.3 mm/min) corresponding with an elongation rate of 5% per minute.

Characterization of Sulfonated Polysulfone

Sulfonation of polysulfone was first confirmed in the prepared samples by noting changes in the material's solubility. First of all the sulfonated polysulfone crashes out of 1,2-dichloroethane, unlike PSF. In addition, SPSF is insoluble in tetrahydrofuran, unlike PSF. The sulfonated polysulfone, however, could be dissolved in solvents that are not solvents for the original polysulfone. Samples prepared using lower amounts of chlorosulfonic acid were insoluble in water but showed some solubility in ethanol, unlike

the highly substituted polymers that dissolve in water. Varying the initial concentration of chlorosulfonic acid produced a range of polymers with different degrees of substitution. The solubility changes after sulfonation indicates that as the degree of sulfonation increases, so does the solubility parameter of the polymer. None of the samples produced indicated signs of gelation by an inability to be dissolved in solvents such as dimethylformamide.

The hydrophilicity of the sulfonated polysulfone is illustrated by the water sorption behavior of cast films. Moisture pickup from the atmosphere at ambient conditions (40-44% humidity, 27°C) ranged from 0% for polysulfone to 14% for a moderately sulfonated polysulfone.

Two methods were used to determine the degree of sulfonation (DS), elemental sulfur analysis (performed by Atlantic Microlab, Inc.), and nuclear magnetic resonance (NMR). In addition to confirming the sulfonation process, NMR can be used to determine the new structure of the modified polysulfone. The degree of sulfonation was calculated from NMR data [14] using the following expression that basically ratios the areas under the peaks associated with the chemical modification:

$$DS = \frac{12 - 4R}{2 + R}$$

where R is the sum of the area under peaks a , b , a' , b' , and c divided by the sum of the area under peaks of d and e . Figure 4.2 shows the lettering scheme for the particular protons identified in the NMR scans for both the modified and unmodified polysulfones. The c and d protons are located on the rings of the diphenyl sulfone unit, while the a and b protons are found on the rings of the bisphenol-A unit.

The proton NMR spectrum acquired for the unmodified polysulfone sample is depicted in Figure 4.3. The aromatic portion of the spectrum is the most important because new chemical shifts due to the introduction of the acidic side group occur in the aromatic portions of the spectrum. Due to both steric hindrances and the electron withdrawing nature of the sulfone chemical group, which deactivates the adjacent phenyl rings to electrophilic attack by the sulfonating agent, the most likely position for the sulfonic acidic group to add is the *a* position of the bisphenol-A rings (Figure 4.2).

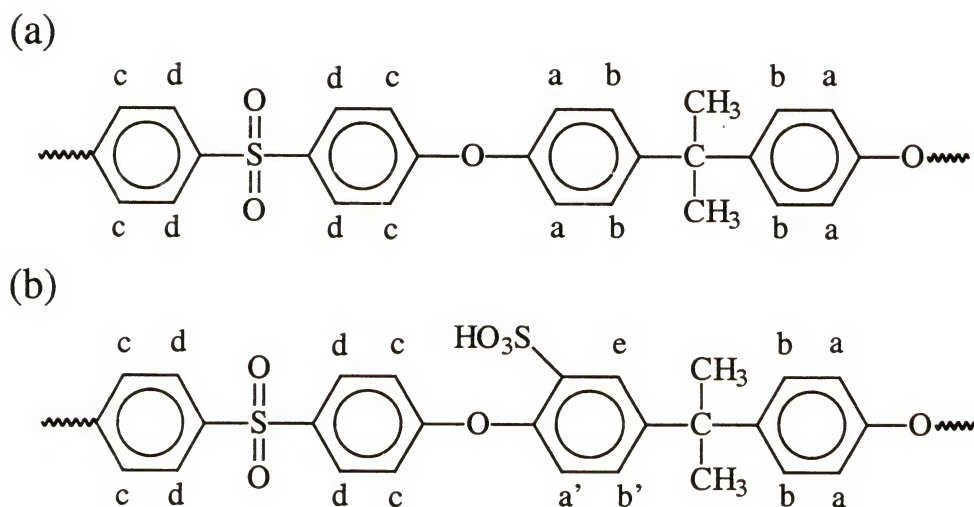


Figure 4.2. (a) unreacted polysulfone, (b) sulfonated polysulfone.

The predicted scheme for the sulfonation of polysulfone is represented in Figure 4.4.

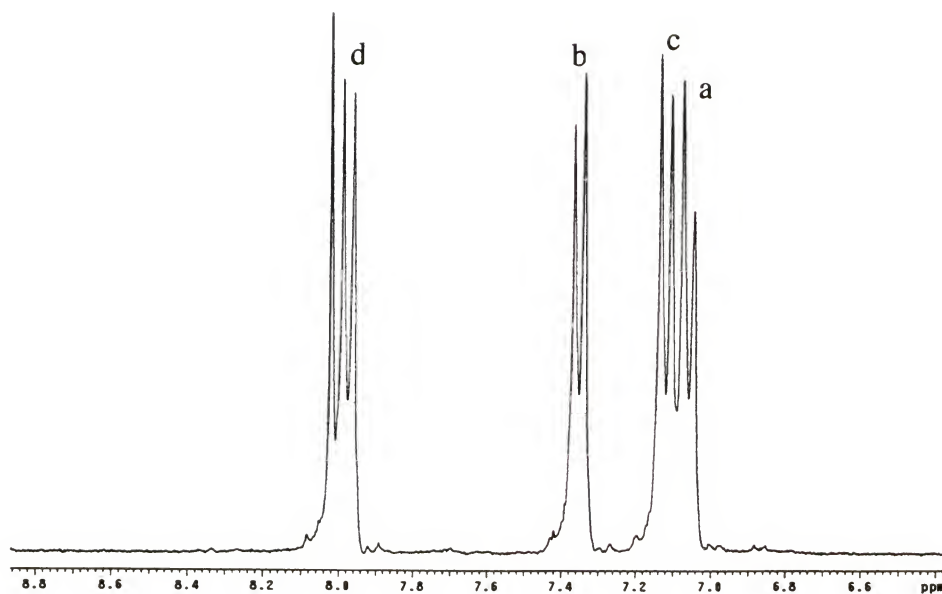


Figure 4.3. Proton NMR of unreacted polysulfone

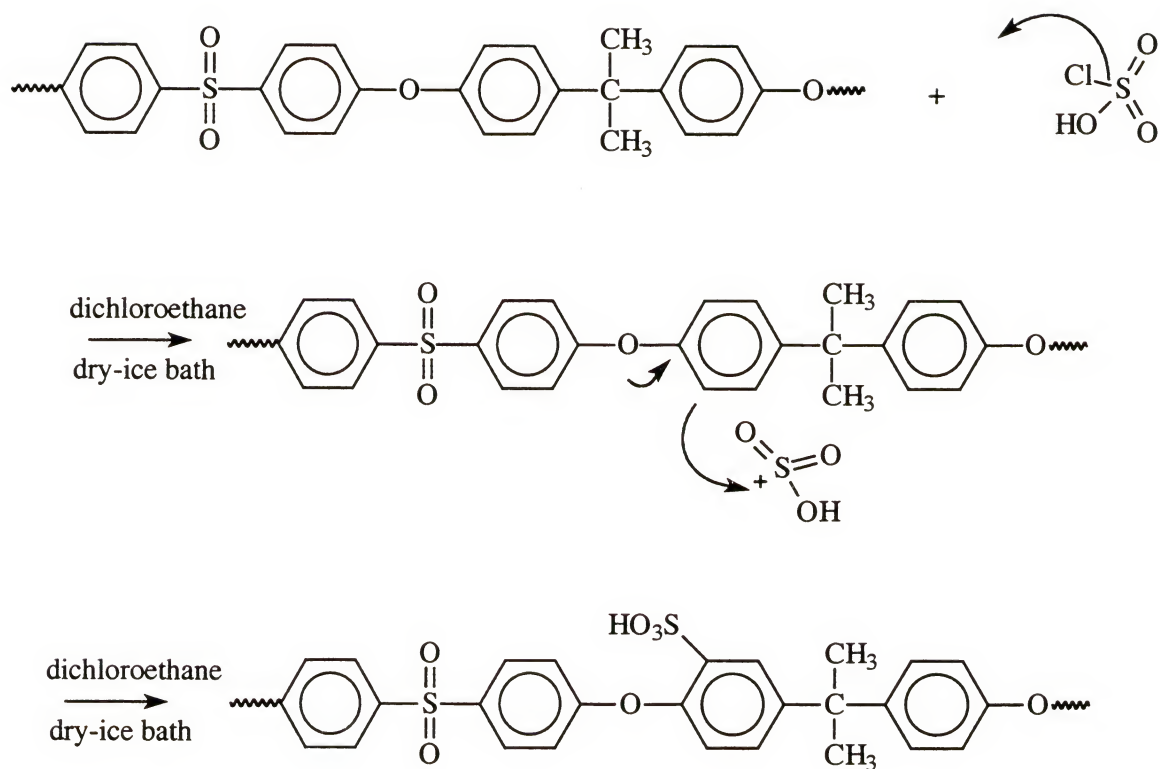


Figure 4.4. Predicted scheme for the sulfonation of polysulfone via chlorosulfonic acid

New peaks are present on the proton NMR spectra of the modified polysulfones (Figures 4.5-4.7). The amount of peak shifting is increased as the degree of sulfonation is increased. In Table 4.2 both the chemical shifts and the areas under the peaks are reported. Protons located nearer to the ether linkage (peaks *c* and *a*) have the largest upfield shift after modification.

Table 4.2. Proton NMR data and degree of sulfonation for unmodified and modified polysulfone. Lightly, moderately and highly sulfonated polysulfones refer to samples made with 1:1, 6:5, and 2:1 molar ratios, respectively, of ClSO₃H to PSF repeat unit

Type of proton	Polysulfone		Lightly Sulfonated Polysulfone		Moderately Sulfonated Polysulfone		Highly Sulfonated Polysulfone	
	Peak (ppm)	Area (%)	Peak (ppm)	Area (%)	Peak (ppm)	Area (%)	Peak (ppm)	Area (%)
<i>a</i>	7.044 7.072	20	7.072 7.047	19	7.088	15	7.064	10
<i>b</i>	7.364 7.336	27	7.342	21	7.352	10	7.374	9
<i>c</i>	7.132 7.103	28	7.135 7.107	26	7.145 7.118	32	7.093 7.115	26
<i>d</i>	7.989 7.959	25	7.966 7.992	25	7.976 8.002	19	7.932 7.958	30
<i>a'</i>	-	-	7.000	2	6.960	2	6.980	10
<i>b'</i>	-	-	7.368	4	7.376	11	7.403	12
<i>e</i>	-	-	7.920	3	7.917	10	7.845 7.872	4
NMR DS	0.01		0.38		.56		1.05	
El. Anal. DS	0.0		0.4		0.6		1.4	

For the lightly sulfonated polysulfone the degree of sulfonation is equal to 0.4. The sulfonated polysulfone used in this analysis was prepared by reacting chlorosulfonic acid and polysulfone in a ClSO_3H :PSF repeat unit molar ratio of 1:1, producing an efficiency of 40%. The moderately sulfonated polysulfone with a $\text{DS}=0.6$ was prepared using a molar ratio of 6:5 for an efficiency of 50%. Finally, the highly sulfonated polysulfone with a $\text{DS}=1.4$ was prepared using a molar ratio of 2:1 for an efficiency of 70%.

For samples with lower degrees of sulfonation (Figures 4.5 and 4.6), protons associated with the *a* position shift to form a shoulder, indicated by *a'*. Protons associated with the *d* position shift to form a new peak indicated by the letter *e*, and the ratio of intensities for protons in the *b* position become closer to unity.

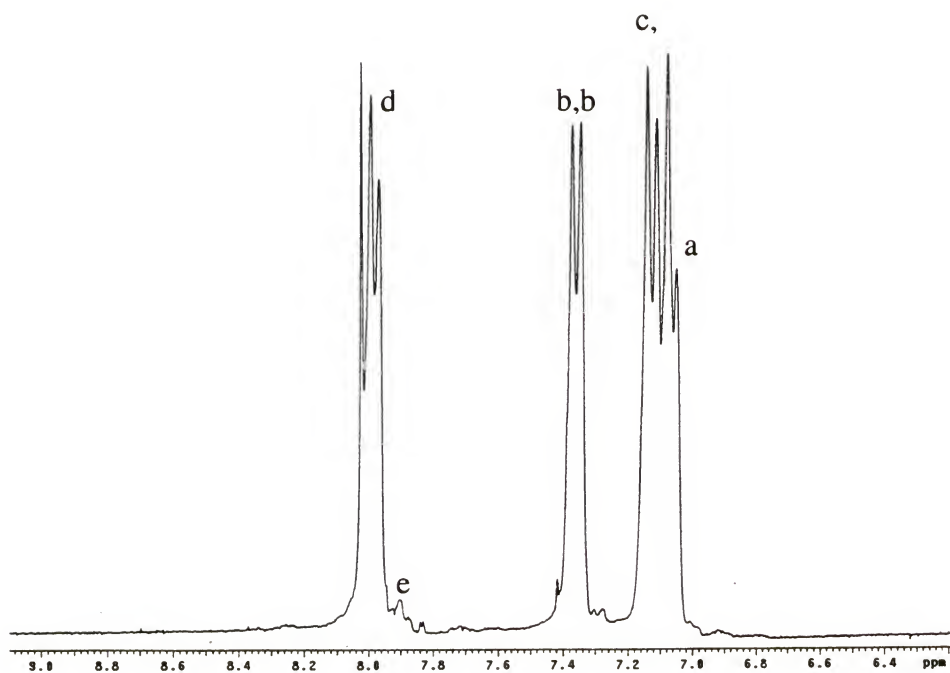


Figure 4.5. Proton NMR scan of lightly sulfonated polysulfone

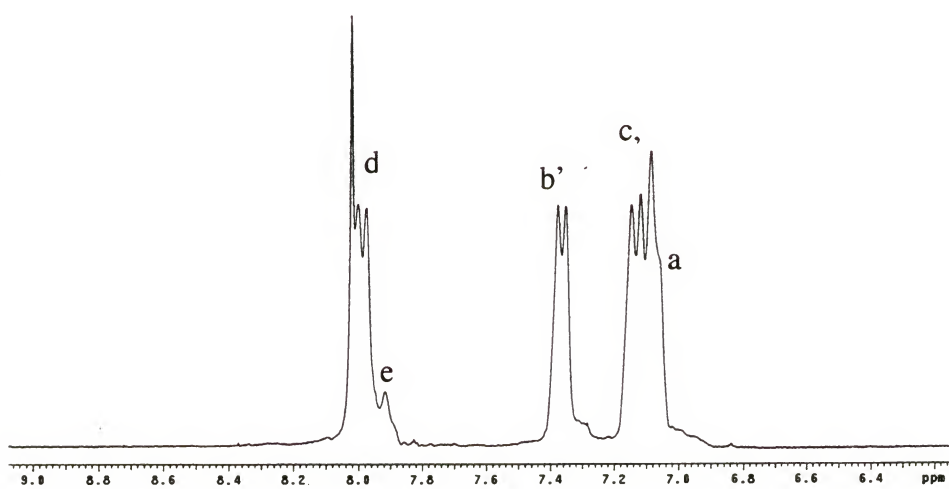


Figure 4.6 Proton NMR scan of moderately sulfonated polysulfone

As the mole percent of chlorosulfonic acid used increases, the peak shifting and intensity differences become more apparent. Water soluble samples (Figure 4.7) exhibit major peak shifts and some additional peaks. Major peak shifting is noted for protons indicated by *d*, *c*, and *a*. Less shifting is noted on peaks associated with *b* protons. This is in some agreement with the results of Noshay and Robeson in that sulfonation seems to occur to a higher degree at the bisphenol-A portion of the repeat unit, but unlike Noshay and Robeson it may not be limited to this position. The more heterogeneous sulfonation of the polysulfone in this study likely results from the less sterically hindered acid used as a sulfonating agent compared to the sulfur trioxide/triethyl phosphate complex used by Noshay, et al. Another possibility is that the environment of the protons changes not because of the acid group bonding in positions other than that indicated by the *a* proton, but rather because the repeat unit of the SPSF begins to fold in on itself due to ionic interactions thus producing the increased peak shifting.

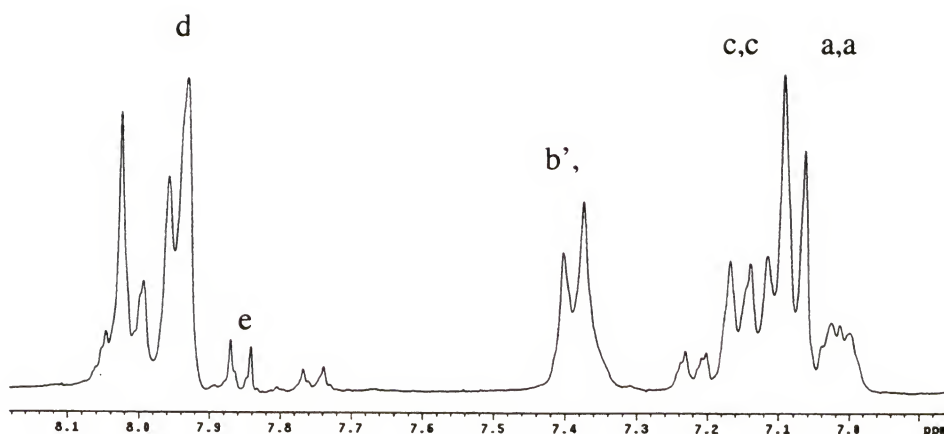


Figure 4.7. Proton NMR scan of highly sulfonated polysulfone

The FTIR transmission spectra of polysulfone and several sulfonated polysulfones are reproduced in Figure 4.8. Table 4.3 reveals the FTIR peak usually associated with polysulfone spectra and its sulfonated form. In the spectrum of SPSF, peaks within the region 2800 to 2200 cm^{-1} are usually seen in compounds with sulfonic acid groups, while the broad absorption around 3400 cm^{-1} is commonly related to hydroxyl groups. The addition of sulfonate groups also affects the absorbencies related to the aromatic rings as well. Differences between the spectra are notable in the 835 , 855 and 875 cm^{-1} regions and are attributed to the C-H out-of-plane bending motions between para-substituted and tri-substituted aromatics.

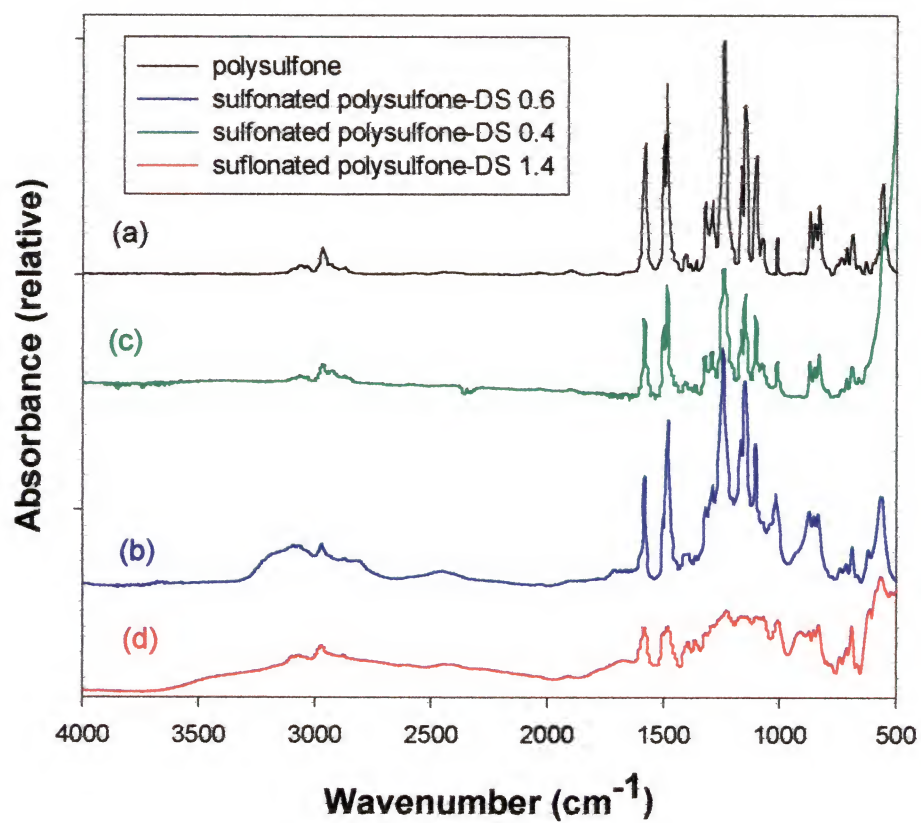


Figure 4.8. FTIR spectra of sulfonated and unmodified polysulfones

Table 4.3. Infrared assignments of polysulfone and its sulfonated derivative

Frequency (cm^{-1})	Assignments
3100 3078 3042	Aromatic C-H stretching vibrations
2980 2880	Asymmetric and symmetric C-H stretching vibrations involving entire methyl group
2800 2458	SOH vibrational modes
1590 1508 1490	Aromatic C=C stretching
1412	Asymmetric C-H bending deformation of methyl group
1393 1368	Symmetric C-H bending deformation of methyl group
1325 1298	Doublet resulting from asymmetric O=S=O stretching of sulfone group
1245	Asymmetric C-O-C stretching of aryl ether group
1172	Asymmetric O=S=O stretching of sulfonate group
1152	Symmetric O=S=O of sulfone group
1108 1092	Aromatic ring vibrations
1028	Symmetric O=S=O stretching of sulfonate group
1010	Ring vibration of para-substituted aryl ether
874 850	Out of plane C-H deformation of isolated hydrogen in 1,2,4 substituted phenyl ring
832	Out of plane C-H deformation characteristic of para-substituted phenyl
710 689 624	C-S stretching vibrations

Thermal Analysis of Sulfonated Polysulfone

The addition of acidic groups to the PSF backbone means that the modified material has a very strong affinity for water. This water bonds strongly to the sulfonated polysulfone and acts as a plasticizer to lower the glass transition temperature. In Figure 4.9 the dynamic scanning calorimetry scans of PSF and sulfonated polysulfone with different degrees of sulfonation are reproduced. The glass transition temperature for unmodified polysulfone is recorded to be 186°C. A degree of sulfonation of 0.4 results in a drop in the T_g to 170°C. Increasing the degree of sulfonation to 0.6 further decreases the T_g to 165°C. Finally, at a degree of sulfonation high enough to elicit water solubility (DS=1.4), the glass transition temperature reduces to 152°C.

In addition to measuring the T_g of the polysulfone samples, another major result of the DSC studies is that there is no evidence of phase separation. Phase separation may be an indication of the presence of low molecular weight species that would be an indication of degradation during the sulfonation process.

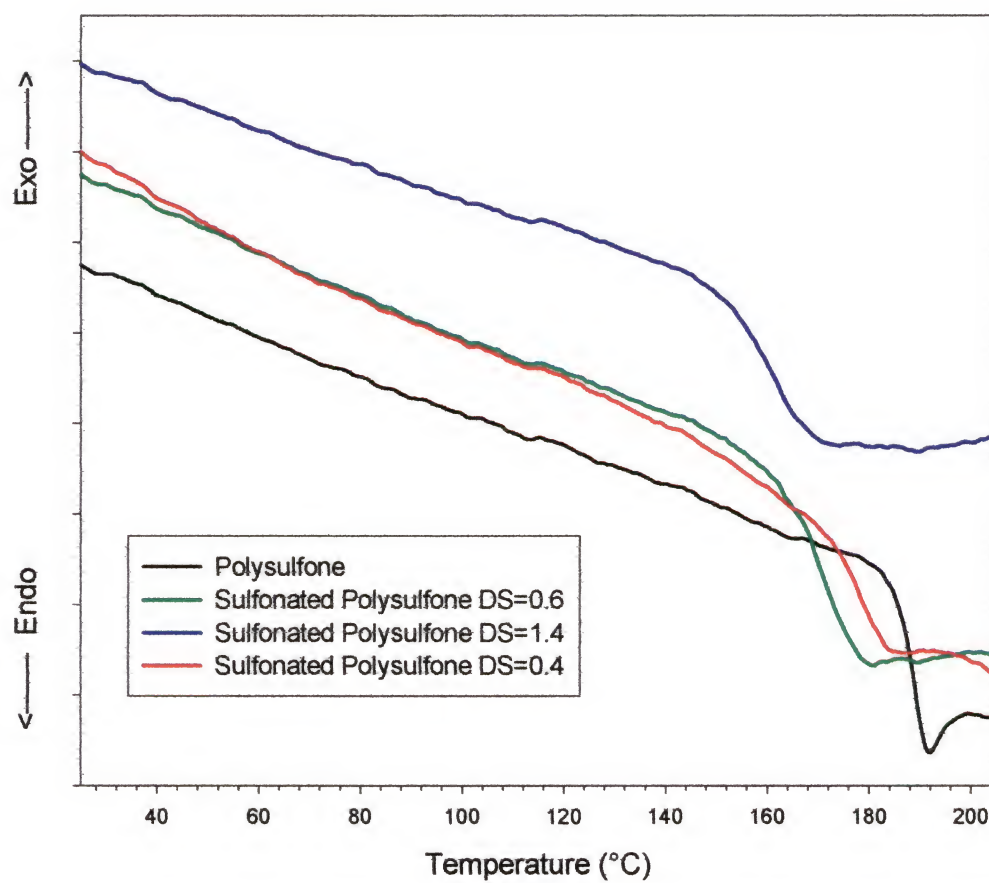


Figure 4.9. Differential scanning calorimetry scans for unmodified and sulfonated polysulfones

Determination of Processing Procedure for Grafting SPSF to Bioglass

In this section the question is asked whether the amount of SPSF present during the grafting procedure has an effect on the tensile strength of the composites. An experimental design (Table 4.4) was developed using the program Fusion Pro developed by S-Matrix Corp., with the content of NMA in the resin and the amount of SPSF used during the grafting procedure as variables. These two variables were not chosen because of any expected specific interaction between the two, although both have electronegative groups. For NMA the electronegative group is the carboxylic acid groups on the ring opened structure and for SPSF it is the sulfuric acid group. Both are expected to form ionic bonds with ions leached from the glass filler and therefore have an affinity for the glass. Figure 4.10 plots the tensile strengths acquired from composites filled with 30 v% modified or unmodified Bioglass®. The modified Bioglass® was grafted with SPSF as described earlier but with either a 1 or 5 w% concentration of SPSF in ethanol during the procedure. Also plotted in Figure 4.10 are the results of the experimental design showing the curve fitted to the acquired data. The r^2 values, or the fraction of data that can be explained by the data, for the two curves are .9776 and .9562 for the 1 w% and 5 w% processed Bioglass®, respectively, indicating a fairly good fit for the model.

Table 4.4. Design of experiment to determine the effect of SPSF concentration during grafting procedure

Run Number	SPSF (DS=1.4) w% in ethanol	NMA w% of resin
1	1.0	30
2	5.0	30
3	5.0	10
4	5.0	10
5	5.0	20
6	1.0	20
7	1.0	20
8	1.0	10
9	1.0	10

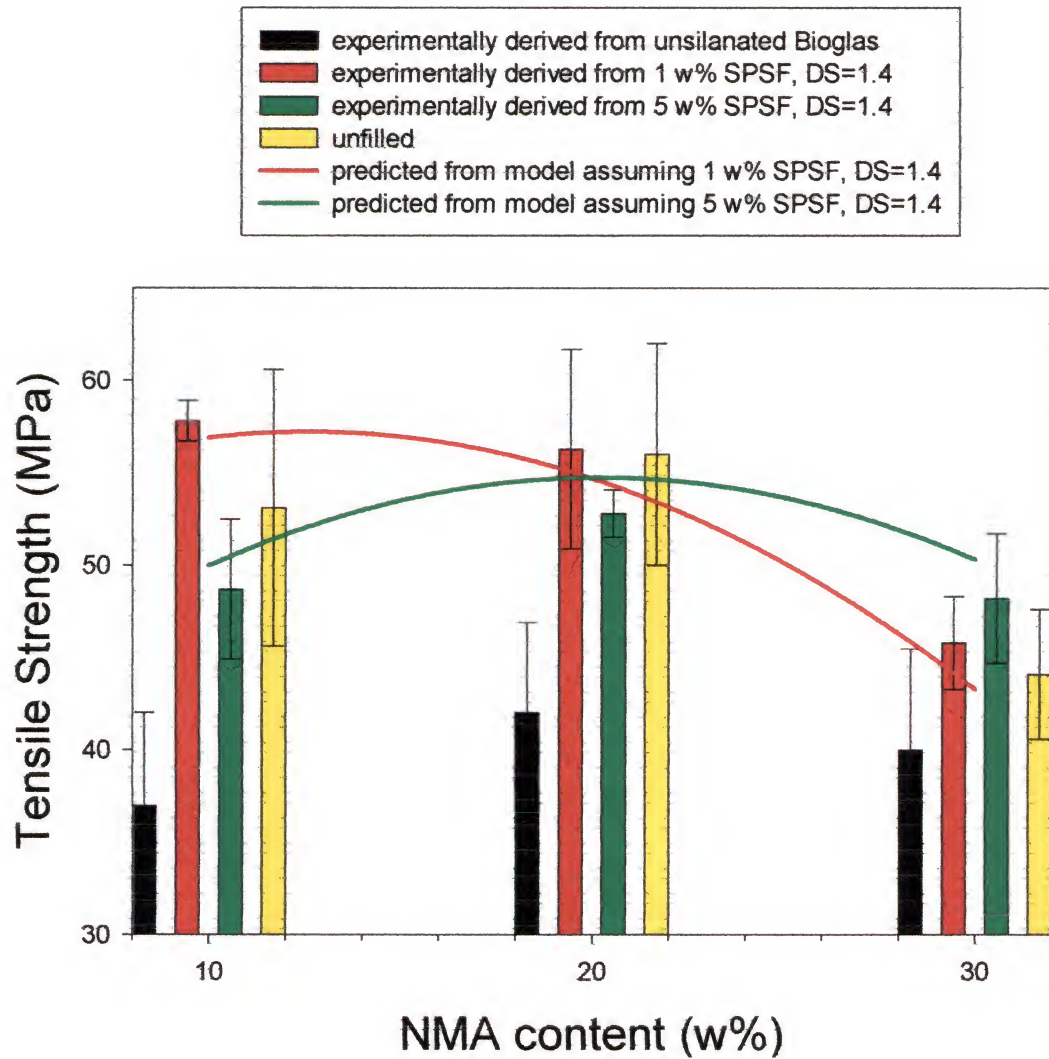


Figure 4.10. Tensile strength of dry composites varying the amount of nadic methyl anhydride in the resin and the grafting procedure of the filler

There are a couple of factors that contribute to the lower tensile strength witnessed in the high NMA content composites. In the dry condition the affect of NMA is to lower the tensile strength of the composites. It is thought that the reactivity of NMA is less than TEGDMA and Bis-MEPP [10]. As a result, composites containing NMA have higher levels of unreacted monomer or material that is not incorporated into the network structure. The unreacted material can act as a plasticizer for the system causing a reduction in the breaking strength of the composites. In addition, the addition of NMA increases the overall density of the resin prior to cure [10]. This increase in density could make it more difficult for the resin to form an interpenetrating network with the grafted polymer.

Glass particles are introduced into the system as a reinforcing phase. The silanation of the particles has a significant effect on increasing the breaking strength of the composites regardless on the amount of SPSF used to produce the filler. Conversely, for the unsilanated filler the tensile strength is significantly lower indicating the effective reinforcement by the surface treatment.

At 10 and 20 w% NMA, the composites comprised of the filler grafted in 1 w% SPSF has a significantly higher tensile strength compared to that grafted in 5 w% SPSF. At the 30 w% NMA composition, all samples, including the unsilanated filled composites, are not significantly different suggesting that the NMA content is the most important variable. Besides acting as a plasticizer, unreacted pools of NMA can act as flaw sites to lower the tensile strength.

The values obtained for the treated composites are not significantly below the tensile strength of the neat resin. The untreated filler, however, acts as a stress

concentrator that leads to crack initiation to lower the tensile strength. The modified filler does not lead to significant loss in strength indicating that fewer defects are introduced in the matrix such as voids in the interphase. A possible reason for the improved properties is the formation of an interpenetrating network formation between the grafted SPSF and the resin during the cure of the resin. Monomer, which commingles with the grafted polymer prior to cure, locks in the polymer after cure.

Mechanical Properties of Sulfonated Polysulfone Modified Bioglass Composites

Once the optimum level of SPSF to use during the grafting was determined the next question is to determine the effect of the degree of sulfonation on mechanical properties of the composites and the stability of these properties resulting from any post-cure treatment.

The tensile strengths of three, 20 w% NMA composites using fillers modified with three different SPSF samples are compared to an unmodified Bioglass® filled composite and an unfilled resin sample (Figure 4.11). In Figure 4.11 the affect of a 5-week soak in a salt solution is also recorded.

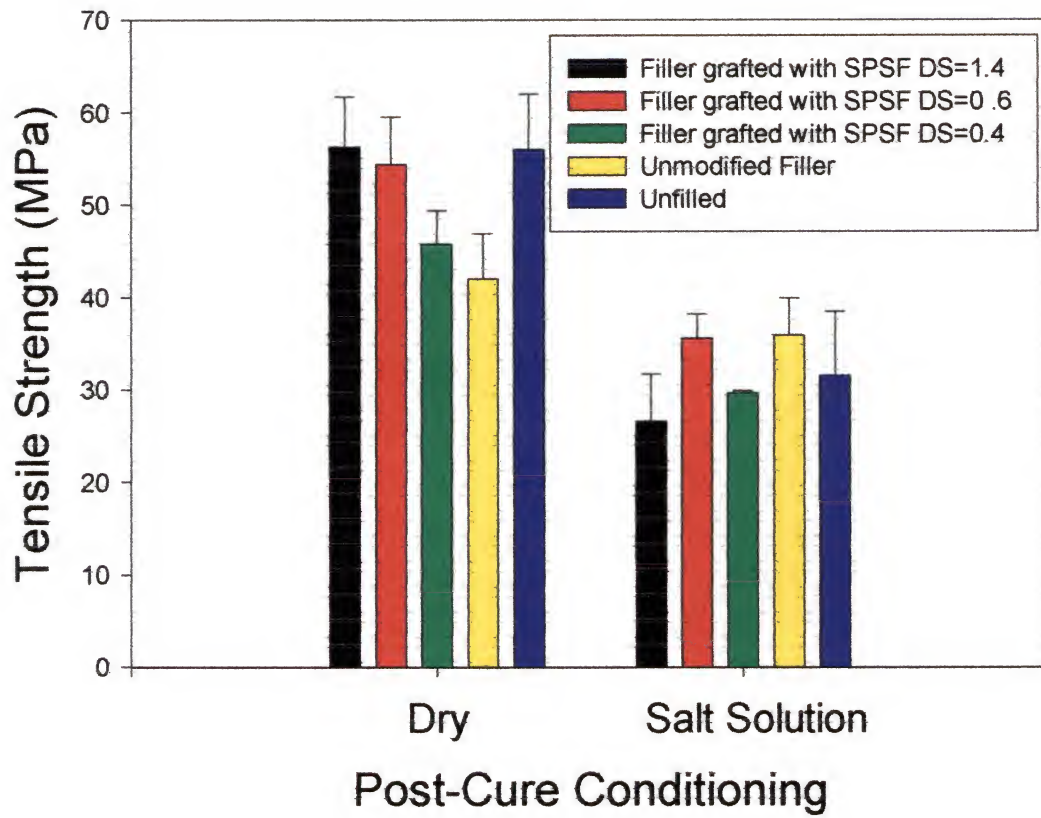


Figure 4.11. Tensile strength of composites varying the post-cure treatment and the degree of sulfonation used to modify the filler

All the materials in Figure 4.11 have their highest tensile strength values in the dry state. Dry composites made using an SPSF with degrees of sulfonation equal to 1.4 and 0.6 show none of the debilitating effects that the unmodified Bioglass® filler composites show. A t-test comparing the tensile strengths of the various samples shows no significant difference between the 1.4, 0.6, and unmodified Bioglass® filled composites ($\alpha=.05$).

Higher degrees of sulfonation means more interaction between the polymer and the filler suggesting that the ability to overcome the negative affects of the unmodified filler stems from the interaction between the SPSF and the matrix. One mechanism leading to the improved tensile strengths over the composites filled with unmodified Bioglass®, is the successful tethering of the grafted polymer to the matrix and filler. Less interaction between the grafted SPSF and the filler, as in the case of the DS=0.4 sample, could mean that there are fewer SPSF grafts available to form a significant interpenetrating network to effectively improve the tensile strength of the composites.

The strength of the pure resin specimens as well as the filled specimens all decrease upon exposure to the salt solution. The reduction in mechanical properties for the pure resin can be explained by the polar nature of the NMA molecule. Water swelling and plasticization by water of the matrix will cause a reduction in strength [100].

As reported earlier, the surface of the bioactive glass is dynamic when exposed to an aqueous environment. Compounded to this is the non-equilibrium state of the silane-coupling agent at the glass surface. Organic polymers with polar functional groups can form oxane bonds with mineral hydroxide surfaces. These covalent bonds can provide adhesive strength greater than the cohesive strength of the materials involved, but tend to

have poor resistance to water [75]. After soaking in the salt solution, each composite appears to be comparable in tensile strength regardless of filler modification. This could be an indication of the degradation of any effect to improve the tensile mechanical properties of the composite through surface treatment. The least amount of degradation (14.5%) due to post-cure environment is seen in the unmodified filler composite, but this is because it has the lowest tensile strength to begin with. The decrease in tensile strength in all the composites to a common level after soaking indicates a similar mechanism of reinforcement in all the composites independent of the surface treatment.

In the dry state, the addition of the unmodified Bioglass® filler acts as flaw sites to reduce the tensile strength of the composites by an average of 14 MPa when compared to the neat resin. After aging in the salt solution there is no significant difference in the tensile strengths of the composite samples and the resin indicating that the filler is no longer acting as the flaw site. Since there is no loss of tensile strength with the addition of the Bioglass® filler for the soaked samples there is still a reinforcing effect with the addition of the filler. This supports the idea of the resin's ability to form a mechanical bond with the filler.

Since there is no significant decrease in the salt-soaked-state tensile strength and in some cases a trend of increasing tensile strength, with the addition of the Bioglass® filler, the reinforcing nature of the filler is supported. There are two conflicting characteristics stemming from the degree of sulfonation, which may affect the reinforcing properties of the filler. The first is significant interaction between the grafted polymer and the filler so that an interpenetrating network can form between the grafted polymer and the matrix. The second is the hydrophilicity of the grafted polymer that may promote the

sorption of water to the possible detriment of the composite interface. For this reason, the composite with the moderate degree of sulfonation ($DS=0.6$) seems to be the more optimal material for use in the production of the composites. This composite not only results in one of the higher post-soak tensile strengths but also in one of the higher dry tensile strengths (Figure 4.11).

To further examine the mechanisms leading to the variations in strength, scanning electron microscopy (SEM) was used to image the fracture surfaces of the samples after breaking. Figure 4.12 shows the fracture surface of the composite containing unmodified Bioglass® filler after soaking. The fracture of the sample occurs only through the resin with no exposed particles to indicate a failure at the interface or through the particle. Therefore, there is no evidence of a transfer of stress from the resin to the particle.

Figure 4.13 shows the fracture surface of a dry composite filled with Bioglass® that has been modified with the SPSF with the 0.6 degree of sulfonation. In this figure there is evidence of a transfer of stress to the filler particle. Fracture occurs through the particles with no evidence of particle pullout, which would indicate a comparatively weak interface. After soaking the sample, however, the fracture of the sample occurs through the resin with no exposed particles (Figure 4.14) indicating the degradation of the reinforcing effect of the particle on the tensile strength. Since the fracture occurs through the resin, the resin can be identified as the weakest link rather than the degradation of the interface as a result of the sorption of water.

As discussed in previous chapters, one reason for choosing a bioactive filler was in the hope of producing a composite with the ability to bond with the natural tissues. Bonding of the filler material occurs through the formation of a biologically active

hydroxy-carbonate apatite (HCA) layer when exposed to an aqueous medium. This HCA phase is chemically and structurally equivalent to the mineral phase in bone so that it provides direct bonding by bridging the tissue with the implant. In this way it may be possible to take advantage of the sorption of water that is otherwise viewed as a purely negative consequence. Figure 4.15 is a micrograph of a portion of the fracture surface for a composite filled with Bioglass® modified with SPSF having a degree of sulfonation equal to 1.4. The higher degree of sulfonation means that the interface has a higher affinity for water, as discussed previously. In addition, this composite shows the lowest mean tensile strength (Figure 4.11), indicating a higher propensity for hydrolytic degradation. In Figure 4.15 there is evidence of the growth of a HCA layer from exposed particles. Energy dispersive x-ray (EDX) analysis was used to qualitatively determine the elemental composition of the structure. Results from the EDX analysis show a majority of the elemental composition to be calcium and phosphate, which is as expected in the HCA layer. There is, however, a Si peak present from the presence of silicon so that complete coverage of the particle in a hydroxy apatite layer has not occurred. The intensity of the major peaks in the spectra of the surface for the unreacted Bioglass was Si>Ca>P, it was replaced by Ca>P>>Si.

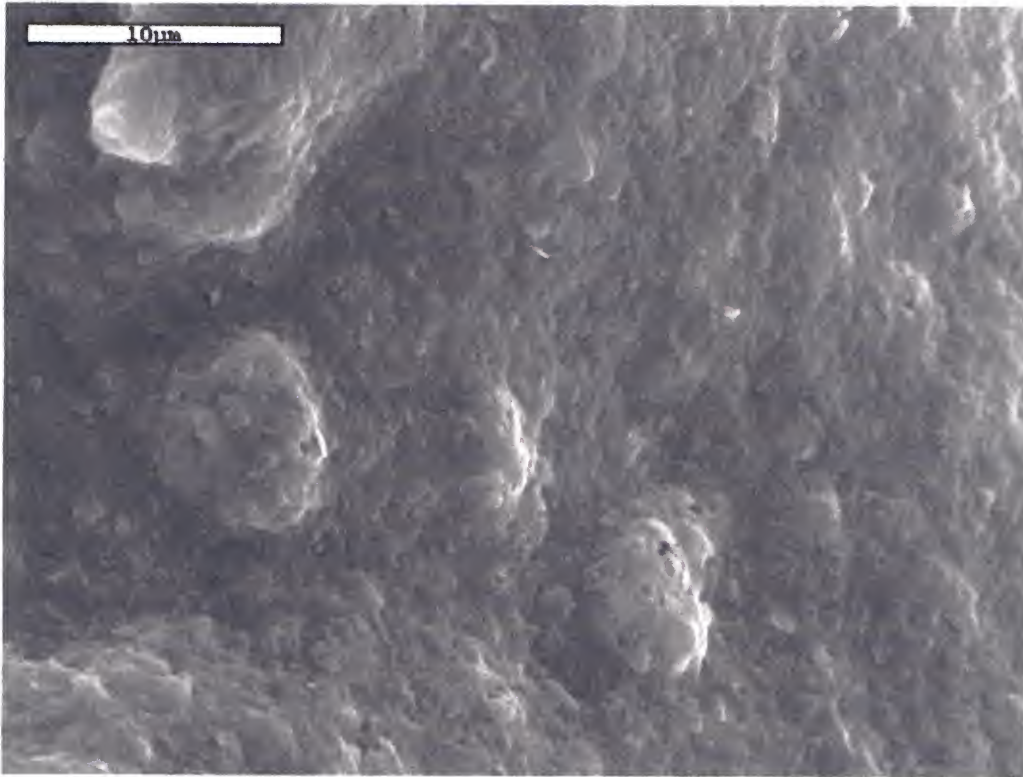


Figure 4.12. SEM fracture surface of a soaked composite containing 30 v% unmodified Bioglass®

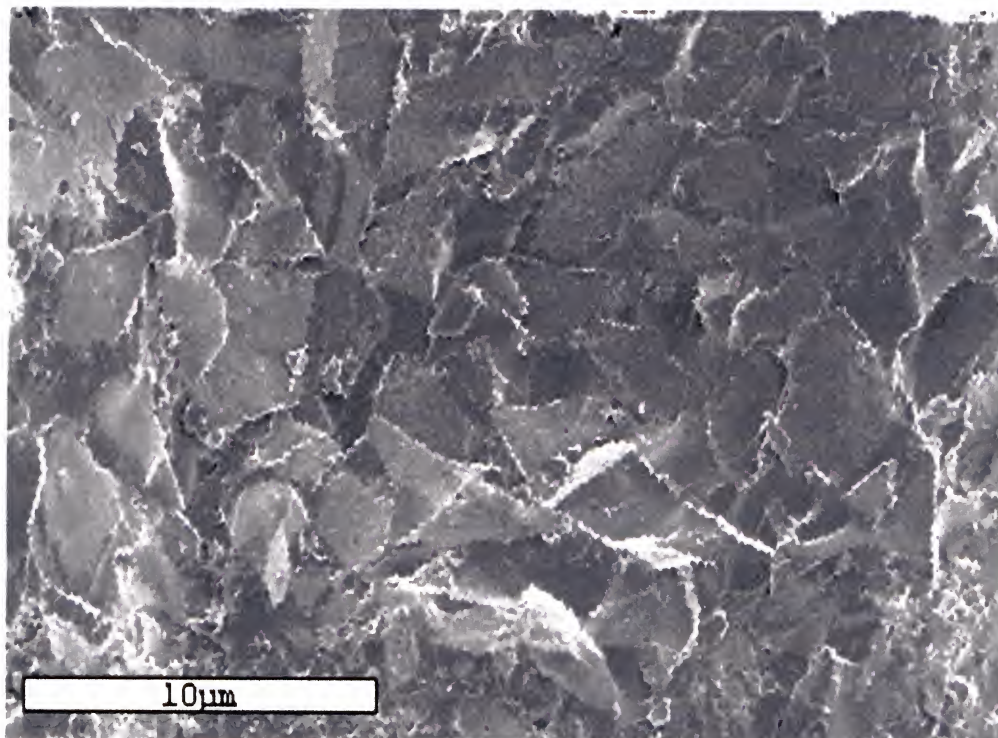


Figure 4.13. SEM fracture surface of a dry composite containing 30 v% Bioglass® modified with SPSF (DS=0.6)

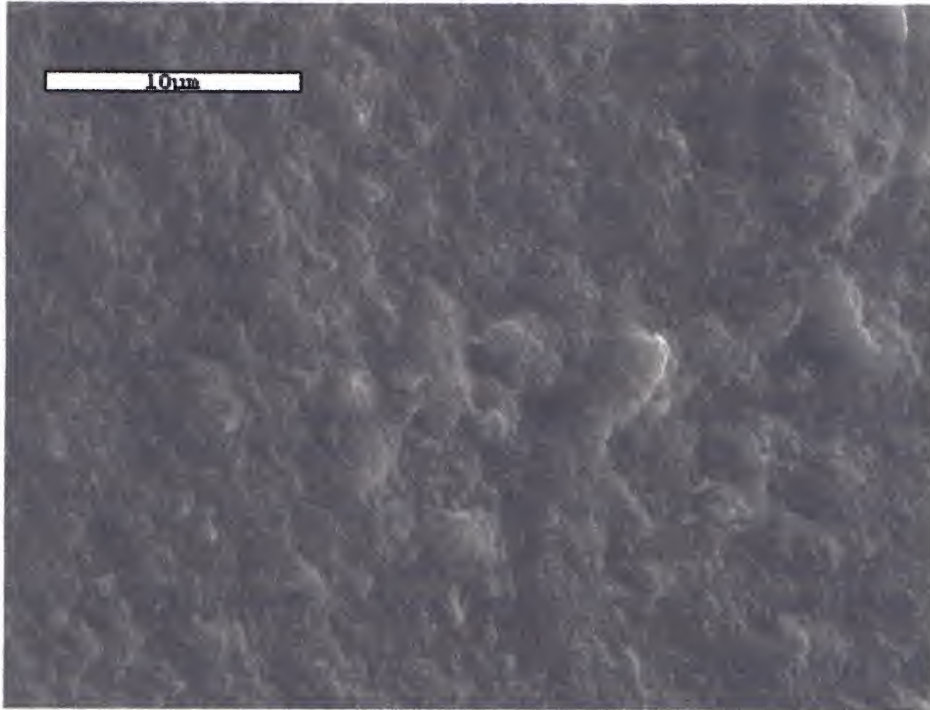


Figure 4.14. SEM fracture surface of a soaked composite containing 30 v% Bioglass® modified with SPSF (DS=0.6)

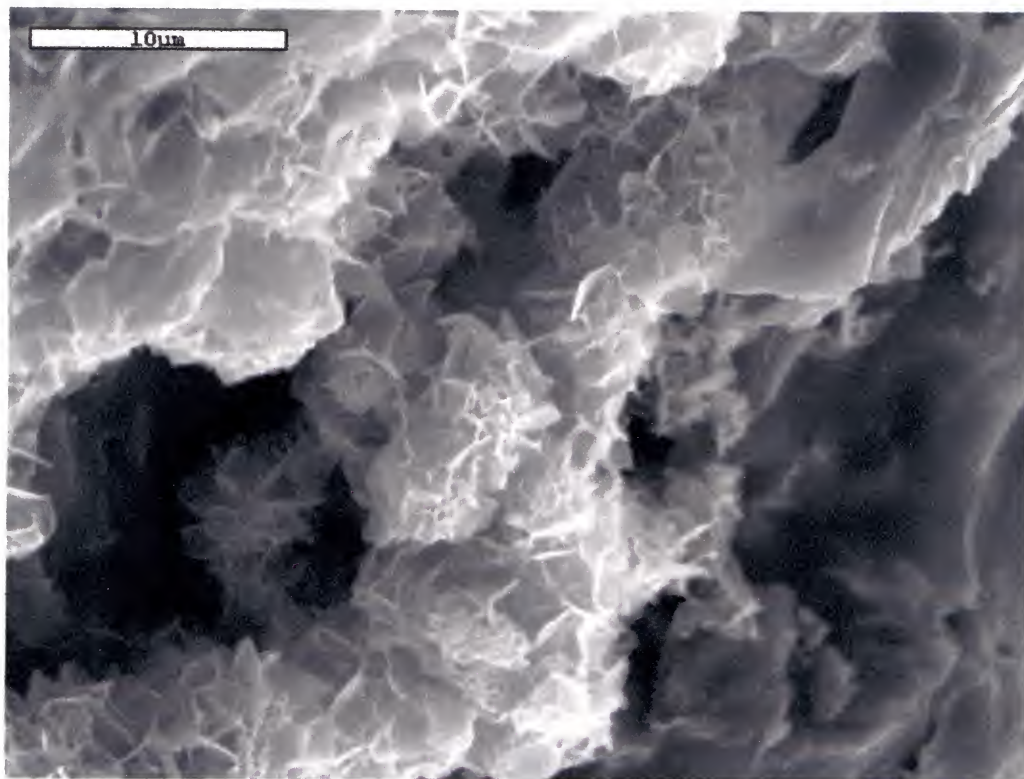


Figure 4.15. SEM fracture surface of a soaked composite containing 30 v% Bioglass® modified with SPSF (DS=1.4) showing evidence of HCA growth

The flexural properties of three, 20 w% NMA composites using fillers modified with three different SPSF samples are compared to an unmodified Bioglass® filled composite and an unfilled resin sample in Figures 4.16 and 4.17. In these figures the affect of a 5-week soak in either a salt solution or nano-pure water is also recorded. Note that in Figure 4.16 the flexural strength of the pure resin sample is not recorded. This is because during testing these samples bottomed out on the fixtures before failing.

Many of the tensile strength trends are seen in the flexural strength tests; specifically, the loss of strength due to hydrolytic degradation of the interface and resin failure due to plasticization. The trend in the dry state of lower flexural strength with degree of sulfonation used during the filler processing is the same as for tensile strengths.

Samples have been aged in a salt solution to mimic more closely the oral environment and to facilitate hydroxy apatite formation. Because the salt solution contains ions which may help in the production of a HA layer it is predicted that composites soaked in this solution will appear more bioactive. In addition, ions either leaching from the filler or sorbed from the salt solution may also be forming specific bonds with the polar groups of either the dicarboxylic acid from the ring opened NMA or the acid groups of the grafted SPSF. This type of ionic crosslinking could be a reason for the slightly higher flexural strengths seen in samples soaked in the salt solution verses water.

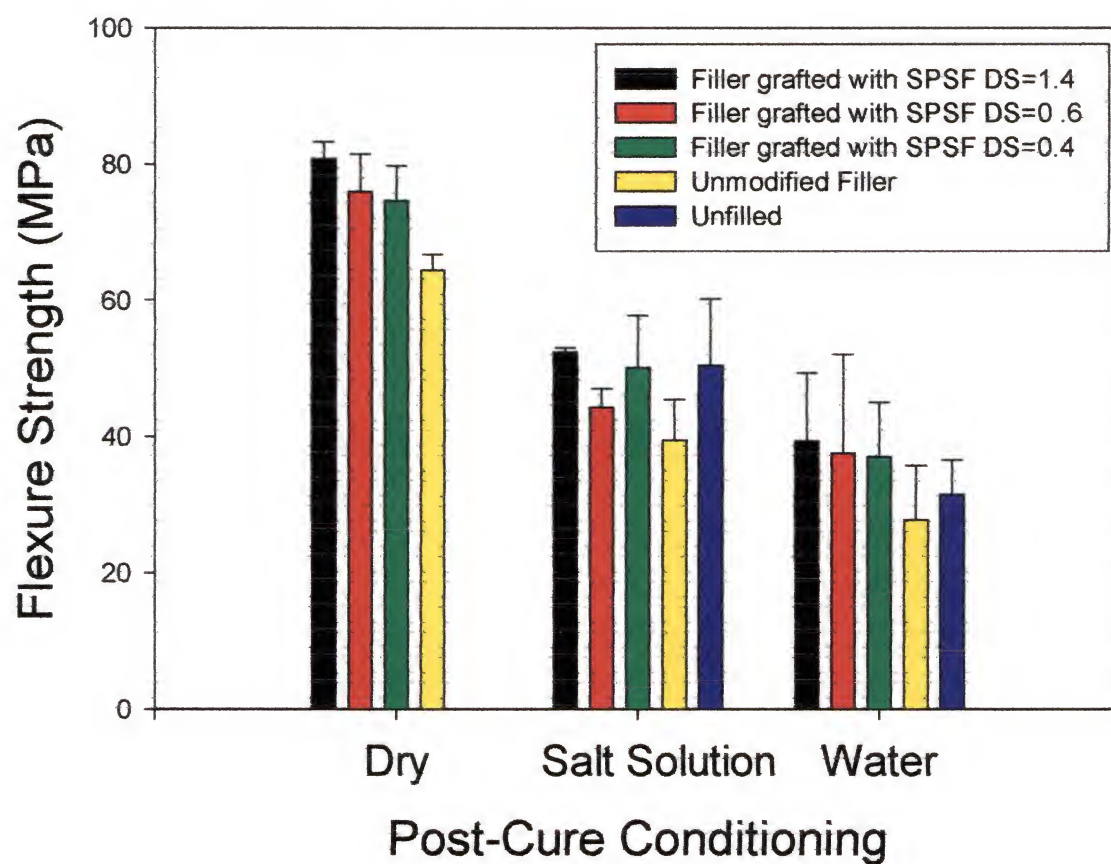


Figure 4.16. Flexural strength of composites varying the post-cure treatment and the degree of sulfonation used to modify the filler

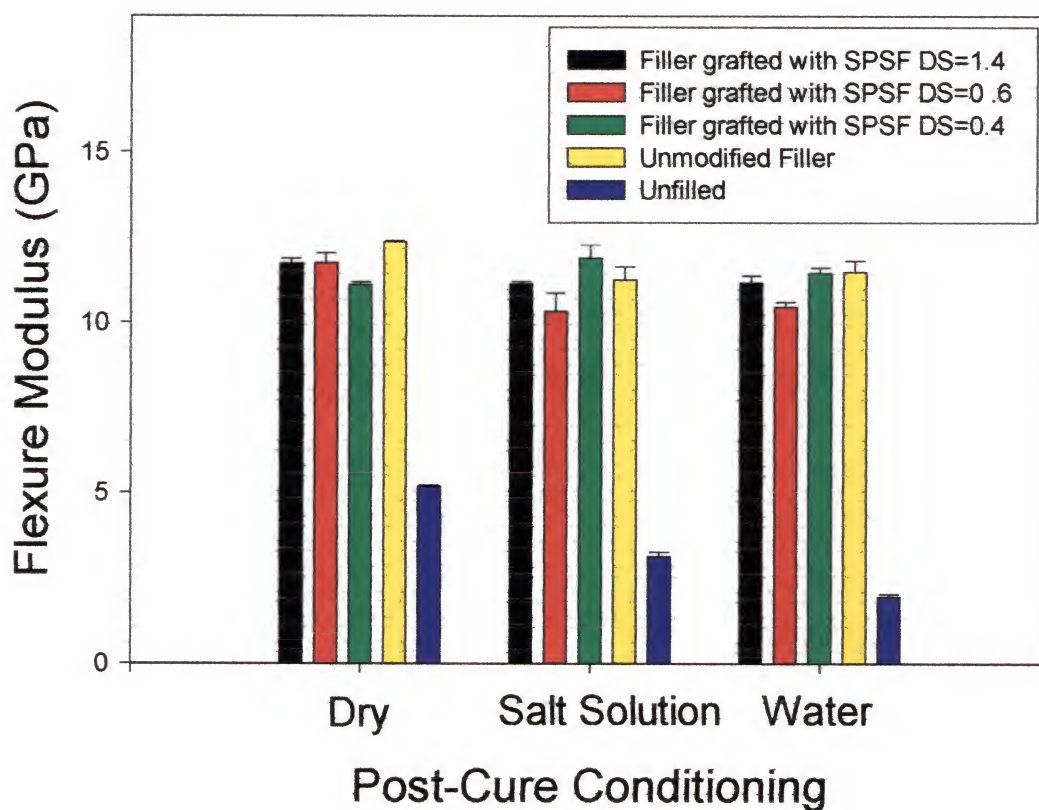


Figure 4.17. Flexural modulus of composites varying the post-cure treatment and the degree of sulfonation used to modify the filler

The reported change in modulus of dental composites aged in water ranges from a decrease [28], [10], [101] to an increase [102], and no change [101]. Most attribute the decrease in the modulus of the neat resin system, which is aged in either a water or salt-solutions, to plasticization by the solvent [10]. In general, the chemistry of the matrix polymer, the volume fraction of reinforcing phase and polymer/filler stress transfer governs the modulus of a composite. The moduli of the composites show no significant differences within each post-cure environment, this indicates the presence of a dominating variable that is the same in all the samples. Since the surface treatment is different for each composite and the resin has a significantly lower modulus, then the filler particle itself is the dominant variable. Indicating the importance of mechanical interlocking between the filler and the resin. All that is required for maximum stiffness is that there be contact between the two phases so that load transfer can occur between the matrix and the filler [67]. Therefore, any voids at the interface may effect the modulus of a composite, thus matrix wetting of the filler plays a key role in increasing the modulus. No decrease in the flexural moduli of the composite samples with post-cure treatment indicates that the plasticization affecting the neat resin system does not affect the matrix/filler interface. The similar flexural modulus values for the composites also indicate little change in the wetting properties of the matrix material in relation to surface modification.

The elastic modulus measured in polysulfone composites containing Bioglass® grafted with the sulfonated polymer show a higher modulus (5.1 ± 0.15 GPa) than composites made with untreated particles (4.6 ± 0.14) [14]. The higher modulus values could stem from improved wetting of the filler because of structural similarities between

the grafted polymer and the matrix material. In addition, the tensile strengths and energy to failure of these composites also increased when the filler was modified with SPSF. Differences in the degree of sulfonation on the mechanical properties of these composites were not examined, however, intersegmental interactions between the polymer chains of the grafts and matrix couple with entanglements are likely responsible of the high levels of stress transfer obtained.

Conclusions

A composite interphase was designed to enhance the interactions between the phases of a particulate filler and the matrix by promoting mechanical interlocking through the formation of an interpenetrating network between the matrix and a polymer grafted to the filler. For this purpose, sulfonated polysulfones were successfully prepared and grafted onto the Bioglass® filler. A dependence of the level of sulfonation on the reinforcing capabilities of the filler was discovered. A degree of sulfonation below a certain level, about 0.6, does not provide the necessary interaction between the matrix and the filler to allow sufficient stress transfer between the resin and particulate. At higher degrees of sulfonation (DS~1.4) there is a potential for increased water attraction at the interface that leads to a higher propensity for hydrolytic degradation of the interface and lowered mechanical properties. Along with the lowered mechanical properties, however, there is evidence of hydroxy-carbonate-apatite growth that is necessary for the condition of bioactivity.

In the dry state, the addition of the unmodified Bioglass® filler results in flaw sites reducing the tensile strength of the neat resin from an average of 56 ± 6.0 MPa to 42 ± 4.9 MPa. All the samples examined in this study have their highest tensile strength

values in the dry state. Dry composites made using an SPSF with degrees of sulfonation equal to 1.4 ($TS = 56.3 \pm 5.4$ MPa) and 0.6 ($TS = 54.5 \pm 5.1$) show none of the debilitating effects that the unmodified Bioglass® filler composites show.

Unlike in the dry state, samples aged in the salt solution show no loss of tensile strength with the addition of the unmodified Bioglass® filler ($TS = 35.9 \pm 4.0$) when compared to the neat resin ($TS = 31.5 \pm 7.0$). Although all the samples examined in this study decrease in tensile strength after soaking, the tensile strengths of the composites do not drop significantly below the tensile strength of the soaked-neat resin. This indicates that there is a reinforcing effect with the addition of the filler supporting the idea of the resin's ability to form a mechanical bond with the filler.

A trend in the data, however, suggests that the composite made from Bioglass® filler grafted with SPSF having a DS of 0.6, has the best matrix/filler adhesion resulting in a higher tensile strength within the dry and salt-soaked conditions. The sample trending with the lowest tensile strength after aging in the salt solution is the composite made from Bioglass® filler grafted with SPSF having a DS of 1.4. The higher degree of sulfonation means that the interface may have a higher affinity for water, which may add to the propensity for hydrolytic filler-matrix degradation. This higher affinity for water, however, may also facilitate in the growth of a HCA layer.

No decrease in the flexural moduli of the composite samples with post-cure treatment indicates that the plasticization affecting the neat resin system does not affect the matrix/filler interface. The similar flexural modulus values for the composites also indicate little change in the wetting properties of the matrix material in relation to surface modification.

CHAPTER 5

CHARACTERIZATION OF THE COMPOSITE INTERFACE BY DYNAMIC MECHANICAL AND WEAR ANALYSIS

Introduction

In the previous chapters several different surface modifications to the Bioglass® filler were examined. It has been shown that not only is the structure of the modifying agent important, but also the manner with which it is applied.

Since the usage of polymer composites for tooth restorations began in the sixties, clinical trials have identified wear as a major problem for occluding surfaces of teeth [103], [104], [105], [106], [66]. Both friction and wear are due to forces that arise from the contact of solid surfaces in relative motion. Solid bodies subjected to increasing load deform elastically until the yield stress is reached, at higher stresses they then deform plastically. In most contact situations some asperities, or the peaks of surface undulations usually on the order of micrometers, generally deform elastically in the bulk, while at the tips there is local plastic deformation where actual contact occurs, depending on the load [107]. The wavelength of these asperities has been conventionally described as roughness.

The wear mechanisms of dental composites has been identified by resin wear, filler exposure and filler loss [108]. Variations in the mechanisms of wear can be attributed to the development of a transfer layer, lubrication, filler-matrix debonding and hydrolytic degradation. Almost all currently employed inorganic fillers for dental

composites are non-porous solid structures. However, inadequate wear resistance limits the use of these fillers in posterior restorations [38].

Roughness

There are two parameters that are most often used to describe surface roughness, one is the roughness average (R_A) value and the other is root mean square (RMS) value. The R_A is the mean vertical deviation of the profile from the centerline, treating deviations both above and below the center line as positive (Eq. 5.1). The RMS value is defined as the square root of the mean of the square of these deviations (Eq. 5.2).

$$R_A = \frac{1}{n} \sum_{i=1}^n |z_i| \quad \text{Eq. 5.1}$$

$$RMS = \left[\frac{1}{n} \sum_{i=1}^n (z_i)^2 \right]^{\frac{1}{2}} \quad \text{Eq. 5.2}$$

These parameters are concerned only with the relative departures from the center line in the vertical direction, therefore they do not provide any information about the shapes, slopes and sizes of the asperities or about the frequencies of their occurrence.

Wear

The mechanisms leading to wear are complex and many. The classification of wear mechanisms is also complex and many and has included as many as twelve classifications [109] to as few as 2 classifications, mechanical and chemical [107]. Three

major mechanisms of mechanical wear include adhesive wear, abrasive wear, and surface fatigue, a major mechanism of chemical wear includes corrosive wear.

Dynamic Mechanical Analysis and Three Phase Modeling of Composites

As demonstrated in the previous chapters, the mechanical properties of composites are strongly influenced by the interfacial properties. The particle/matrix adhesion is a function of the surface characteristics of the filler, i.e. surface topography and roughness, surface energetics and wettability, and chemical bonding along the interface. The contribution of each of these characteristics to the level of adhesion is additive [110]. The moduli of elasticity of a composite material can be used to indicate the effectiveness of the stress/strain transfer from the matrix to the filler particles. Composites made with 0, 20, and 40 v% Bioglass®, containing SiO₂, NaO₂, CaO, and P₂O₅, and a matrix of a 60/40 mixture by weight of Bis-GMA and TEGDMA showed an increasing storage modulus (6.3, 9.0, and 16.1 GPa, respectively) when analyzed by dynamic mechanical spectroscopy [12]. The increasing storage modulus gives evidence to the reinforcing effect of the Bioglass® filler. The tan δ response of the composites shows that the addition of Bioglass® to the dental resin also significantly reduces damping effects. In a composite, the molecular motions at the interfacial region generally contribute to the damping of the material apart from those of the individual materials. Composites made from 40 v% Bioglass® and polysulfone analyzing the effect of particle size on the elastic modulus found that the modulus is not largely affected by a change from 125-106 micron to 45-38 micron sized particles [111]. A simple analysis [112] using Equation 5.3 was used by Orefice et al. to investigate the role of the interface

between the polysulfone matrix and bioactive filler on the stress transfer efficiency of the composite.

$$\tan \delta_c = (1 - BV_g) \tan \delta_m \quad \text{Eq. 5.3}$$

In the above equation the subscript c is related to the composite, g to the glass and m to the matrix. V_g is the volume fraction of glass and $\tan \delta$ is the loss tangent and B is the parameter that quantifies the difference between the expected result using the Rule of Mixtures and the one obtained experimentally. Increasing B values indicate a larger interfacial response to the mechanical properties of the composites. For the smaller particles the B value is larger (.48 compared to .25) most likely stemming from the increased surface area to bulk volume ratio for smaller particles.

The boundary layer between the filler and the matrix of the composite has been used to explain shifts in the glass transition temperature of the polymer matrix with the addition of a reinforcing phase [113], [114], [52]. Interactions between the filler and the matrix can result a phase of higher modulus and Tg due to lowered matrix chain mobility from the anchoring of the matrix material to the filler. Interactions can also result in a decreased Tg, possibly resulting from the formation of two well-separated regions, as in reported cases where epoxy was combined with either glass or carbon fibers [115], [116]. To account for the additional effects of the boundary layer, models have been developed to include additional terms to the Rule of Mixtures expression. The more simplistic two-phase models assume perfect adhesion [113]. By accounting for the third, boundary layer

phase, a better representation of the contributions of modifications to the filler surfaces can be made.

One of the goals of this research is to evaluate the interface of the composites characterized in previous chapters using three-phase-block models. The reinforcing effects of the bioactive fillers have been identified through both tensile and flexure tests, now the efficiency of this reinforcement will be quantified by examining the dynamic mechanical responses of the composites. An additional goal of this chapter is to use a rapid measurement of wear resistance under well-controlled environmental conditions, for the purpose of identifying the effect of specific material properties on the potential modes of material failure responsible for abrasive wear of a surface.

Experimental Procedure

Composite and resin sample bars were prepared as described in previous chapters in the form of rectangular bars 45 x 7 x 2 mm. For the wear tests, the samples were then placed in a salt solution held at 37°C for five weeks with a periodic replacement of the solution. Prior to testing the samples were rinsed with nano-pure water.

Dynamic mechanical spectroscopy (DMS) was performed on specific samples using a Seiko DMS 110 double cantilever type module interfaced with a Seiko SDM5600H Rheostation. DMS imposes a sinusoidal strain at various frequencies on a sample over a range of temperature. As a result, any relaxation processes occurring in the samples can be identified from data collected in the form of the storage modulus (E'), the loss modulus (E'') and the $\tan \delta$ ($\tan \delta = E''/E'$). Multifrequency experiments were performed at 0.1, 0.5, 1, 5, and 10 Hz over a temperature range of -140 to 230°C at a rate of 0.75°C/min in a nitrogen environment (200ml/min. flow rate).

A tribological pin-on-table apparatus involving reciprocal motion was used. Samples were secured in a polyethylene trough of nanopure water while a 4 mm² 316 stainless steel pin (Figure 5.1) polished to 0.03 microns, slid across the sample at a constant load. A metal contact was used because of the incompatibility of the mating materials as well as the good heat transfer characteristics of the metallic material. A water circulation system was set up and maintained at 37°C. Wear testing ran for 10 hours along a 25 mm wear track under a force of 10.5 N. Three specimens of each sample were tested.

After 10 hours the water from the test was collected, as well as any wear debris. The water was dried off and the wear debris weighed. The wear track was analyzed using a Veeco Instruments, Inc Wyko NT1000 light profilometer.

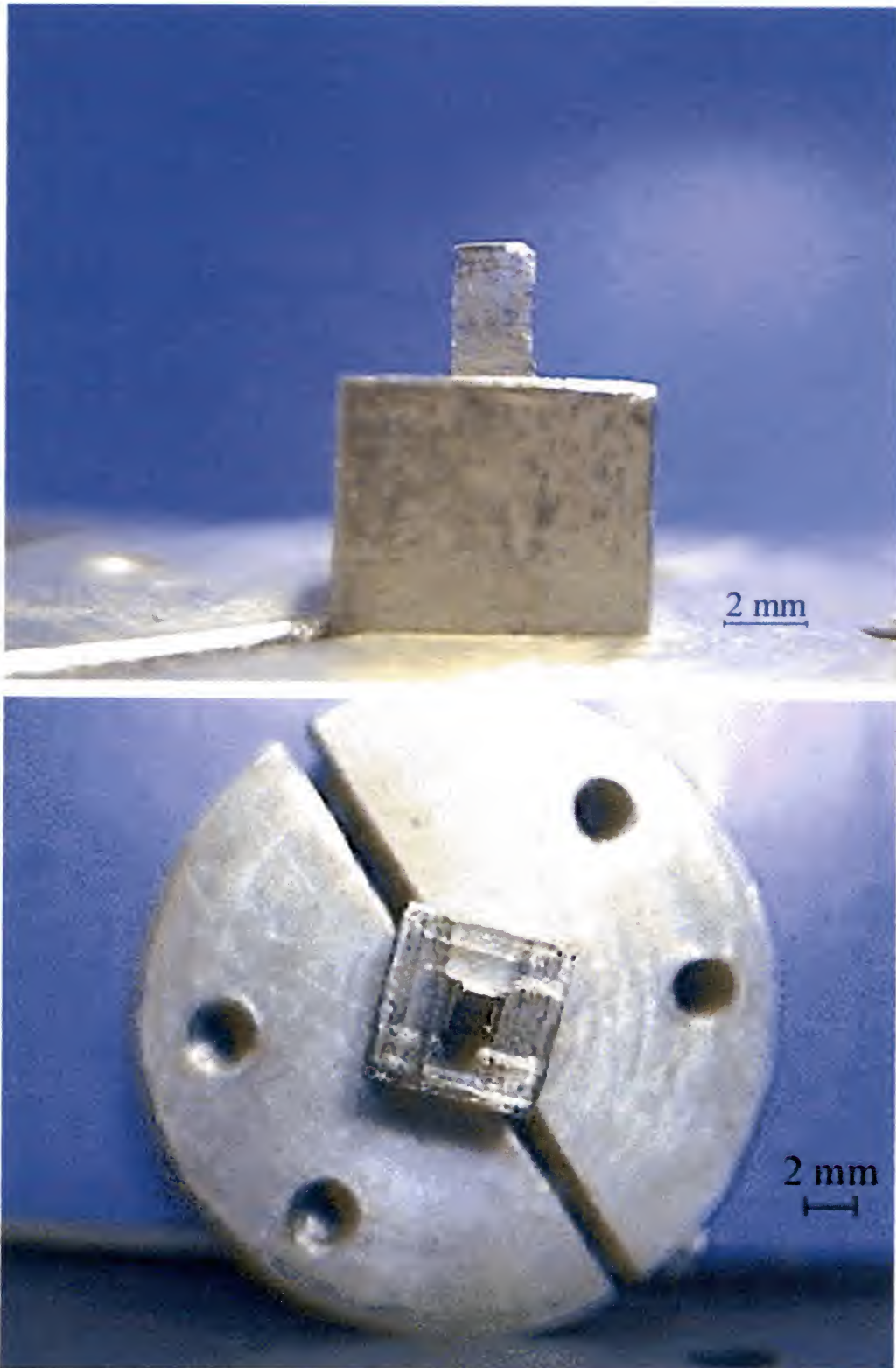


Figure 5.1. 316 steel pin prior to wear test

Dynamic Mechanical Spectroscopy

Dynamic mechanical spectroscopy (DMS) gives the response of a sample as a function of temperature and frequency by applying a periodic stress. Since stress and strain values are generally not in phase, two values can be measured, a modulus value and a phase angle which can be related to the damping of the sample. Figure 5.2 shows the $\tan \delta$ plot, at a frequency of 1 Hz, comparing several composites with varying filler modifications to the neat resin. The peak in the loss tangent corresponds to the onset of molecular mobility in the matrix. For each sample there is no significant change in the peak temperatures except for the composite made with the unmodified Bioglass®. For the Bioglass® filled composite, the $\tan \delta$ peak temperature increases 15% from the neat resin or from 147 °C to 169 °C. The magnitude of the $\tan \delta$ peak is decreases from the neat resin with the addition of filler. The largest decrease in magnitude is for the unmodified filler composite while the smallest decrease is seen in the composite made with the Bioglass® which has been modified with sulfonated polysulfone (DS = 0.6). The reduction in the magnitude of the $\tan \delta$ peak with the addition of Bioglass® has also been noted in composites based on a Bis-GMA system [12]. The reduction can be associated with a decrease in the damping ability of the composites. Decreased damping can be an indication of increasing mobility restrictions, specifically for the resin nearest a particle, If the interparticle distance should decrease, regions of a continuous phase of restricted mobility can form to lower the material's damping capabilities [117]. The larger decrease in the magnitude of the $\tan \delta$ curve for the unmodified Bioglass® composite when compared to the modified composites, could be an indication of particle agglomeration

which would increase the amount of the restricted resin phase and increase the level of heterogeneity for the macrophase composite.

A shoulder present in the $\tan \delta$ plots between 50 and 100°C for all the samples is found to be independent of frequency. A β -relaxation has been identified in methacrylates relating to the rotation of the $-\text{COOCH}_3$ side group [118] which appears to correspond with the shoulders recorded in this work. Therefore, a similar transition may be expected for the dimethacrylate-based resins used in this study even though a true ethylene oxide segment is not present. For the composites measured in this work, however, the temperature and magnitude at which this shoulder appears to be dependent on the surface treatment of the fillers. Similar trends in β transitions have also been reported in Bis-GMA-based polymers [119] including the independence with frequency. These peaks were regarded as the onset of vitrification, which is an artifact of the polymerization temperature. Therefore, the β relaxations observed in this work are likely related to the composites' cure conditions.

The addition of a filler material and its silanation has been shown to affect the cure properties of a composite [67], [80], [120]. Vaidyanathan, et al. [121] looked at the α and β relaxations of a PMMA based dental composite containing a microfine silica. The presence of the filler resulted in a shift to higher temperatures and a broadening of the peaks. A broadening of the $\tan \delta$ peak is an indication of the heterogeneity of the samples. With the broadening of the α peak the β peak becomes less noticeable.

For the neat resin in Figure 5.2 a sub-T_g relaxation, or γ relaxation, is evident at temperatures near -80°C. A similar relaxation is evident for the composite samples at temperatures reaching the lower limit of the DMS test. Unlike the β -relaxation, the

temperature of the γ -relaxation is dependent on frequency and has been identified as likely occurring as a result of ethylene oxide segment mobility.

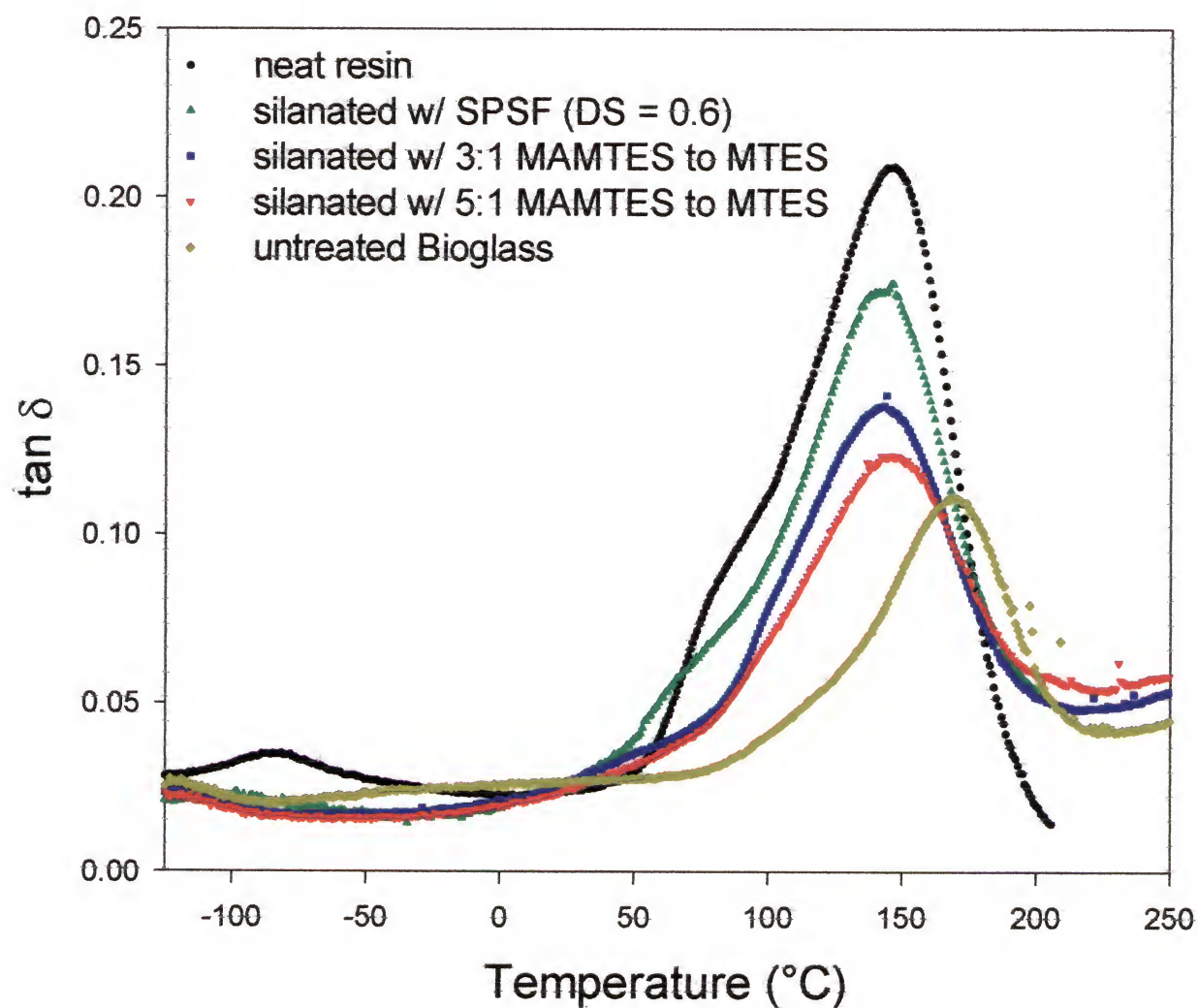


Figure 5.2. Tan δ response of neat resin and Bioglass® composites at 1 hertz

Figure 5.3 shows the storage modulus, at a frequency of 1 Hz, comparing composites made with Bioglass® either as made or with a 3 to 1 or a 5 to 1 ratio of methacryloxypropyl triethoxysilane (MAMTES) to methyl triethoxysilane (MTES) coupling system, to the neat resin. In all cases, the addition of filler increases the modulus of the sample in both the rubbery regime (above the T_g) and in the glassy regime (below the T_g). The changes in the dynamic storage modulus values are more pronounced than the changes of the flexure modulus reported in Chapter 3 for the same composites. Although the flexure test can theoretically give the same information as the dynamic test, the dynamic tests are especially sensitive to the chemical and physical structure of plastics [122]. At 37°C, or normal body temperature, the modulus increases 97% from the neat resin with the addition of Bioglass® modified with the 3:1 coupling system. With unmodified Bioglass® there is only a 63% increase in modulus, confirming the reinforcing ability of the modified filler.

One unexpected result from the dynamic mechanical response is the lack of increasing glass transition temperature with the addition of the modified filler. The increase in the composite made from the unmodified Bioglass® follow the results of other studies [113] where the increase is usually related to a reduction in molecular mobility by a densification around the filler. This explanation, however, is generally used in thermoplastic materials where the mobility is commonly less restricted than in an already crosslinked resin. The addition of the coupling system to the particles could be such that this densification does not occur to the point of affecting the glass transition temperatures of the composites.

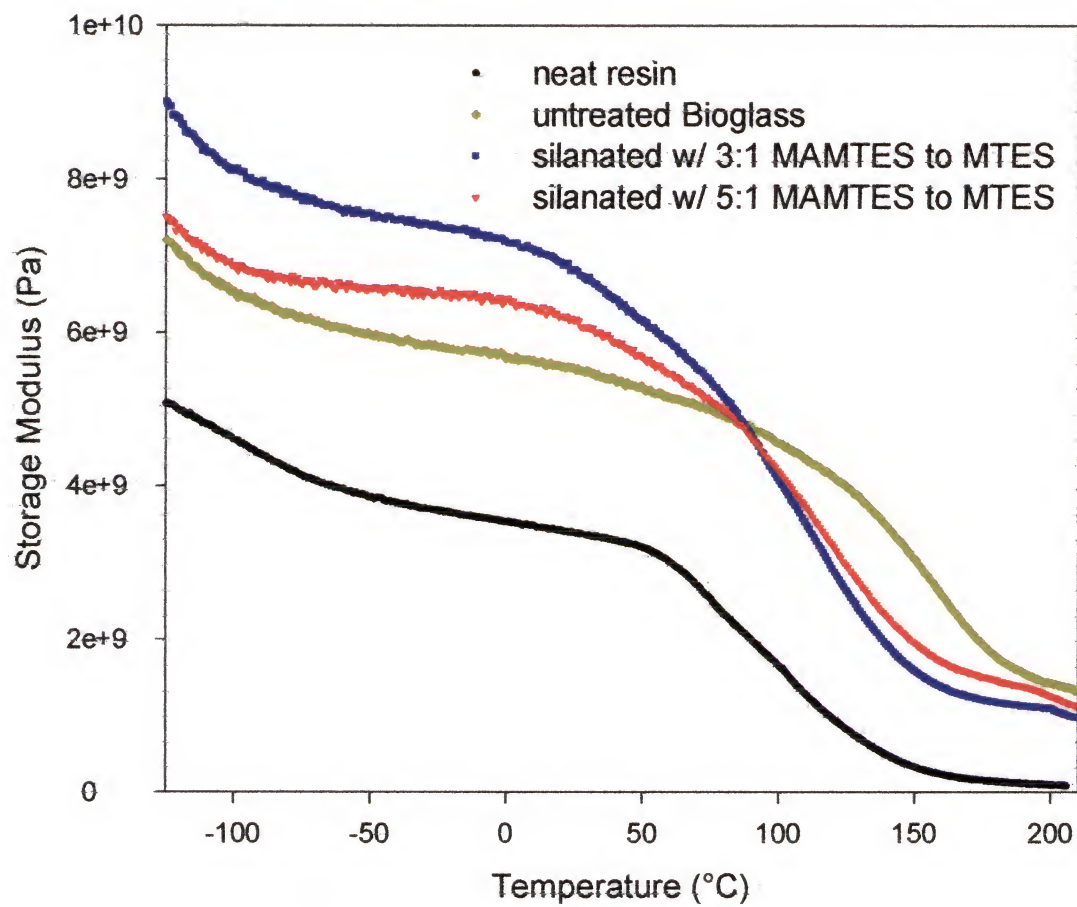


Figure 5.3 Storage modulus of neat resin and Bioglass® composites at 1 hertz

Three-Phase Model

It is well known that the quality of the adhesion between phases governs the static and dynamic mechanical properties of composites. Using a model originally developed by Takayanagi [123], the observed $\tan \delta$ responses of the composites were modeled. The development of the three-phase model comprises three regions, or blocks (Figure 5.4), two of which are in parallel and a third in series. The two blocks in parallel represent attributes referring to the matrix and the fillers. The third block, in series, accounts for additional strains such as orientation, clamping effects, or skin effects. The skin effect is attributed to the non-uniform strain at the surface relative to the bulk due, in part, by the characteristic of composites to be covered by a layer of matrix as a result of the processing procedure of the composite. These additional strains are represented by the term λ . The K term accounts for imperfect filler and matrix adhesion. From the block model an equation for the complex composite modulus can be derived by a combination of the parallel and series rules of mixture. From the complex modulus equation, the $\tan \delta$ response can be derived (Equations 5.4-5.9).

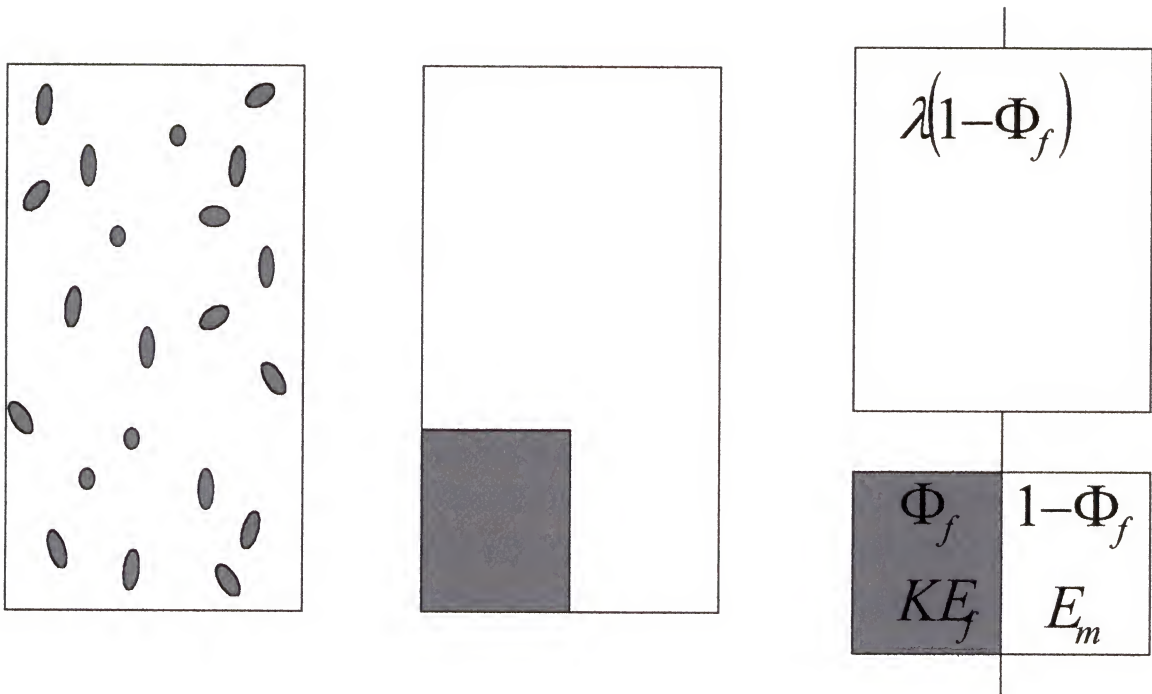


Figure 5.4. The three-phase block model: f and m refer to filler and matrix attributes, respectively, Φ refers to the volume fraction, K and λ describe the reinforcement efficiency and the amount of matrix material, respectively, and E refers to the modulus.

$$\frac{1}{E_c^*} = \frac{1 - \xi}{K\Psi E_f^* + (1 - \Psi)E_m^*} + \frac{\xi}{E_m^*} \quad \text{Eq. 5.4}$$

$$\tan \delta_c = \frac{(M'' E_m' + M' E_m'')(\xi M' + (1 - \xi)E_m') - (M' E_m' - M'' E_m'')(\xi M'' + (1 - \xi)E_m'')}{(M' E_m' - M'' E_m'')(\xi M' + (1 - \xi)E_m') + (M'' E_m' + M' E_m'')(\xi M'' + (1 - \xi)E_m'')} \quad \text{Eq. 5.5}$$

$$M' = K\Psi E_f' + (1 - \Psi)E_m' \quad \text{Eq. 5.6}$$

$$M'' = K\Psi E_f'' + (1 - \Psi)E_m'' \quad \text{Eq. 5.7}$$

$$\Psi = \frac{\Phi_f}{1 - \xi} \quad \text{Eq. 5.8}$$

$$\xi = \lambda(1 - \Phi_f) \quad \text{Eq. 5.9}$$

The subscripts c , f , and m refer to the composite, filler and matrix properties, respectively. The terms E^* , E' , and E'' denote the complex, storage, and loss modulus components, respectively. The volume fractions of the matrix and filler phases are

represented by Φ . The ξ term equals the volume fraction of the skin, or the fraction of the matrix phase that is in series. Ψ is the volume fraction of the filler, excluding any skin material.

Before the simulation of the dynamic mechanical response of a composite can be achieved, the thermomechanical response of both the filler and matrix material needs to be determined. In this study the thermomechanical scan of Bioglass® could not be achieved. However, since the filler is relatively non-viscoelastic, the loss modulus could be assumed to be zero. In addition, it was assumed that there are no significant transitions in the filler at the temperature range used for testing the composite. The corresponding loss and storage moduli temperature profiles from DMS runs of the resin were used to simulate the $\tan \delta$ response. The K and λ values were then chosen to provide the best fit between the simulated and experimental $\tan \delta$ responses of the composites.

Figures 5.5 through 5.8 show the relation between the pure resin, the actual composite, and the simulated composite $\tan \delta$ responses for composites with either unmodified Bioglass® or Bioglass® modified with SPSF (DS=0.6), or MAMTES to MTES coupling systems with ratios of 5 to 1 and 3 to 1, respectively.

To achieve the best fit between the simulated and experimental $\tan \delta$ responses, both the K and λ values need to be adjusted simultaneously. Variations in the λ term indicate a difference in the filler dispersion between the samples. Although the simulated spectra can match the magnitude of the $\tan \delta$ depression with the addition of filler, the K and λ solutions do not provide a very good match for the spectra, specifically the temperature at which the glass transition of the composite occurs and the breadth of this transition.

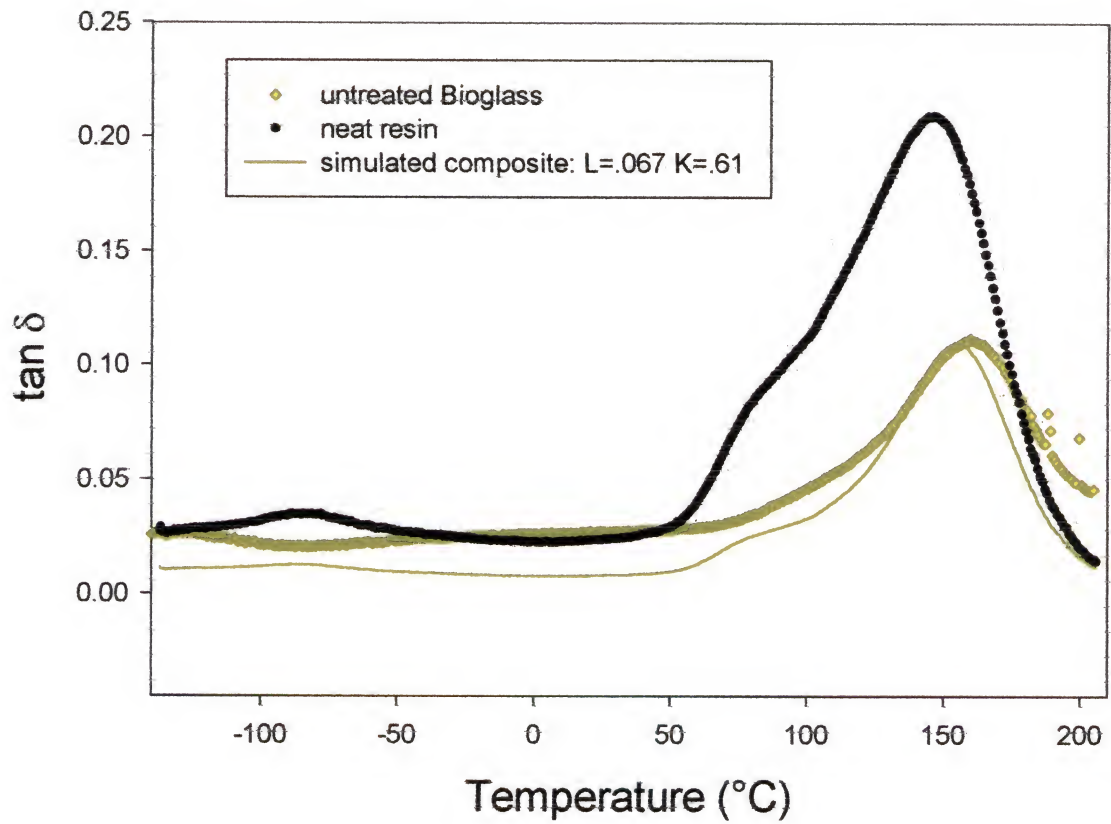


Figure 5.5. Comparison between the neat resin system, a composite made with 30 v% unmodified Bioglass®, and the simulated $\tan \delta$ response of the composite.

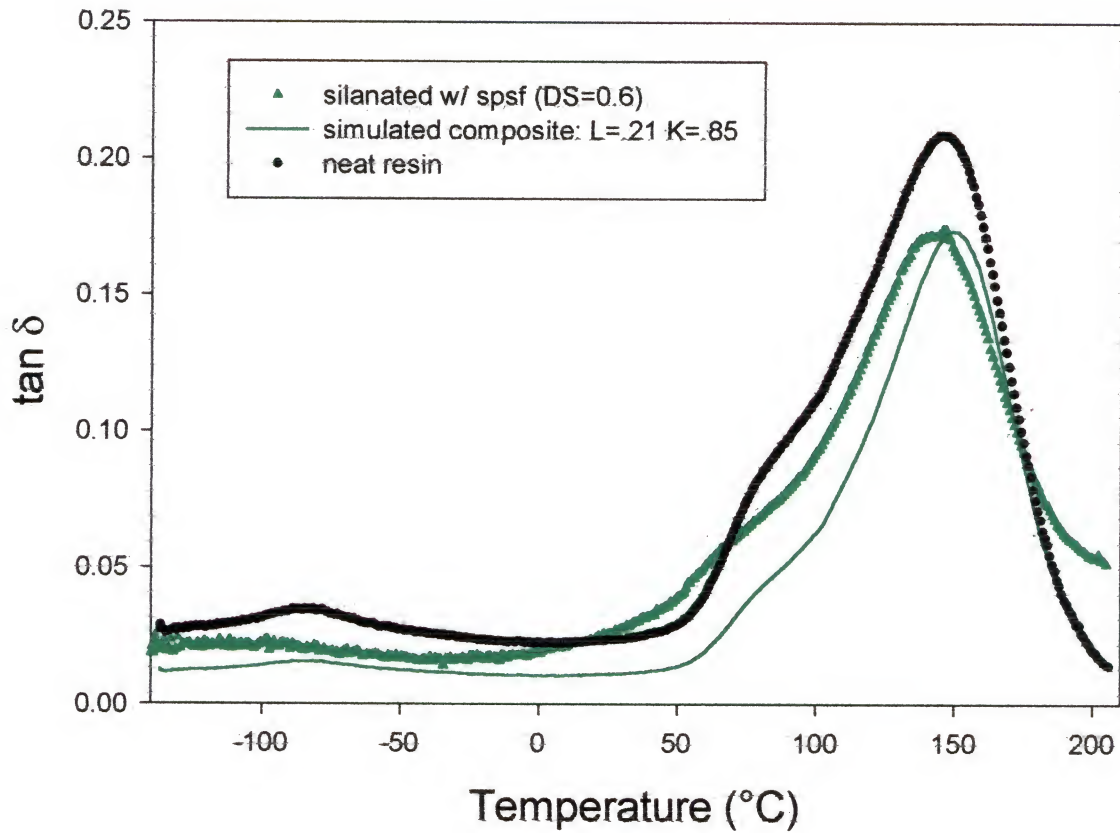


Figure 5.6. Comparison between the neat resin system, a composite made with 30 v% Bioglass® modified with SPSF (DS = 0.6), and the simulated $\tan \delta$ response of the composite.

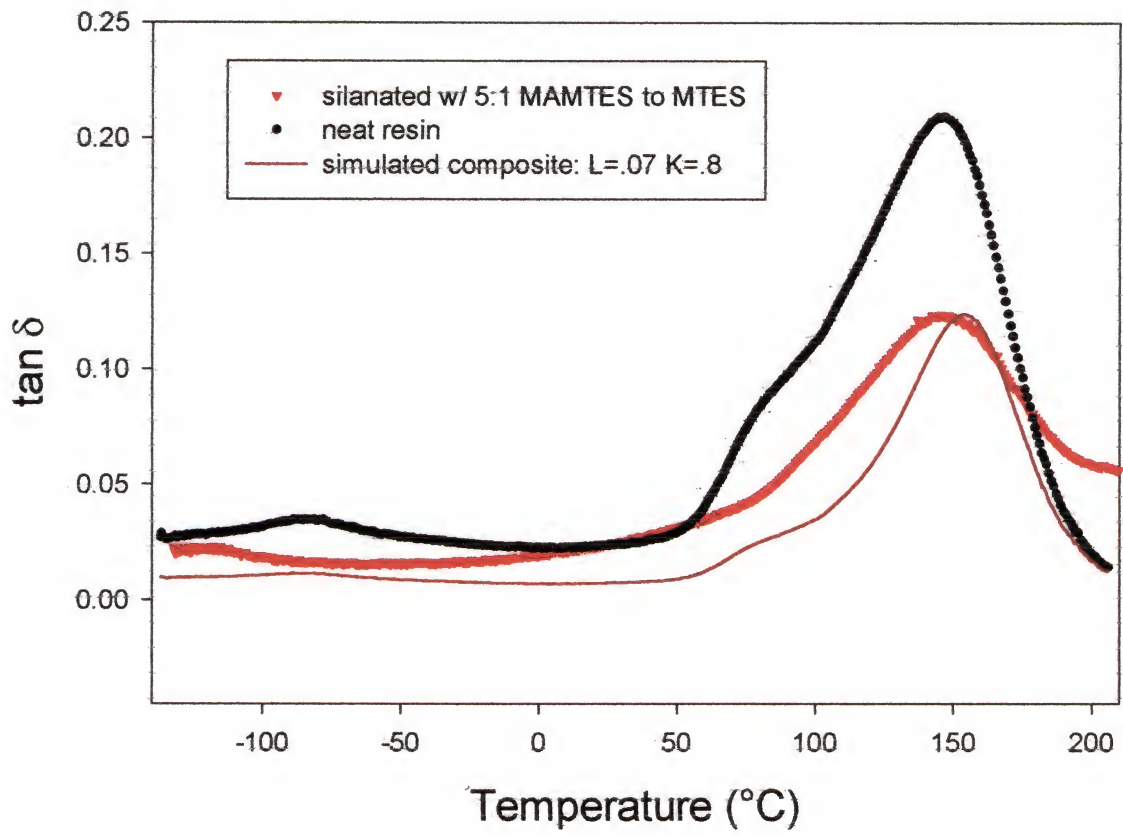


Figure 5.7. Comparison between the neat resin system, a composite made with 30 v% Bioglass® modified with the 5:1 MAMTES to MTES coupling system, and the simulated $\tan \delta$ response of the composite.

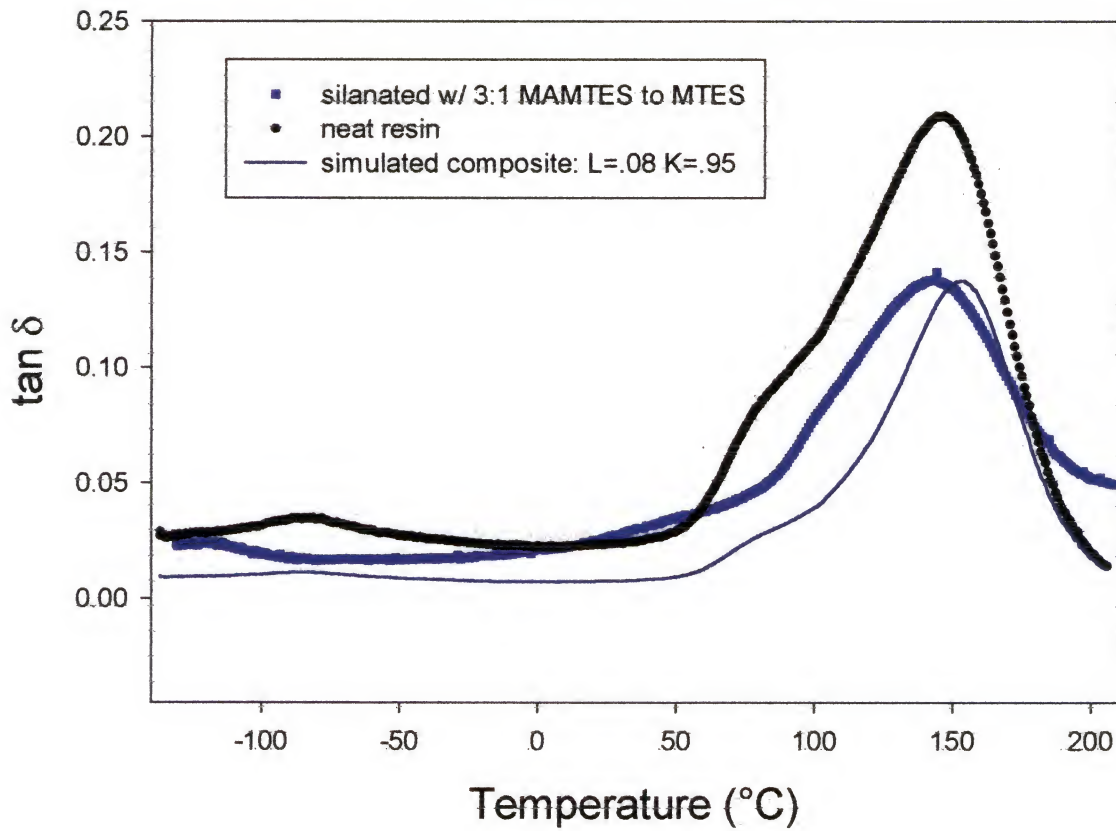


Figure 5.8. Comparison between the neat resin system, a composite made with 30 v% Bioglass® modified with the 3:1 MAMTES to MTES coupling system, and the simulated $\tan \delta$ response of the composite.

Even with the disagreement between the simulated composite scans and the actual composites scans, trends in the differences of the λ and K values can be explained from the tensile and flexure mechanical results examined in the earlier chapters. Table 5.1 records the K and λ values for the different composites for easier discussion.

The low lambda value for the unmodified Bioglass® sample composite could be an indication of the better dispersive properties of the glass after it has been silanated. The highest lambda value was determined for the sulfonated polysulfone modified glass. This could be a result of the number of polar groups added in this modifying system compared to the methacrylate based coupling system, allowing for better filler dispersion.

K values range from 0 to 1 where a $K = 1$ indicates perfect adhesion and $K = 0$ indicates poor filler/matrix adhesion. A significant increase in the K value is noted with the addition of a modifying agent. The K value for the unmodified Bioglass®, however, is not so low as to assume that no reinforcing effect results from the addition of this filler. The K values for the MAMTES:MTES coupling systems follow the trends of the tensile strengths discussed earlier in Chapter 3, i.e. increasing K values depict improved filler adhesion for better mechanical reinforcement. In addition, the K value for the SPSF modified filler increases from the unmodified Bioglass®, supporting the results of the tensile strengths reported in Chapter 4.

Small changes to decrease the number for lambda while keeping K constant results in a larger decrease in damping than if the K value is decreased while keeping lambda constant. This is an indication that the effect of particle dispersion has more of an effect on the $\tan \delta$ response of a composite than does adhesion of the resin to the filler. A larger decrease in the K value, however, results in an increased predicted broadening of

the $\tan \delta$ peak. The broadening of the $\tan \delta$ peak has been difficult to predict from this model, therefore quantifying the adhesion via this method is only partially successful.

Because the fit of the three-phase block model was less than absolute, another method was implemented to elucidate further the effect of the interface on the relaxation processes of the matrix. Parameters from a Cole-Cole plot have been used in physical models that relate the dynamic, or complex modulus, to the un-relaxed and relaxed modulus times to quantify the interface efficiency [124], [52], [125], [126].

A Cole-Cole plot was originally developed to study the dielectric properties of materials, but it can also be applied to viscoelastic properties because of the similar time-energy relationships. The magnitude of changes in the relaxation phenomena due to the presence of the filler and the changes in the interfaces are related to the degree of interaction between phases of the composites. The parameters determined from the Cole-Cole plot for the different composites are recorded in Table 5.1 along with the fitting parameters from the block model.

The values h and k represent the long and short time parameters, respectively, obtained from the Cole-Cole plot. In the Cole-Cole plot the storage modulus is plotted against the loss modulus. Both parameters are then calculated from the angles in which the curves are extrapolated to the storage modulus axis.

$$h = \frac{2\theta_r}{\pi} \quad \text{Eq. 5.10}$$

$$k = \frac{2\theta_u}{\pi} \quad \text{Eq. 5.11}$$

Table 5.1. Fitting parameters for modeling and quantifying the filler adhesion in composites with 30 v% Bioglass® with various surface treatments.

Model terms	Bioglass® modifications				
	Resin	Unmodified	SPSF (DS = 0.6)	5:1 MAMTES to MTES coupling system	3:1 MAMTES to MTES coupling system
K	---	0.61	0.85	0.80	0.95
λ	---	0.07	0.21	0.07	0.08
h	0.86	0.89	---	0.88	0.92
k	0.77	0.60	---	0.65	0.55

The angles Θ_r and Θ_u are defined in Figure 5.9. Both h and k parameters can be related to inhomogeneities within the material that would disturb the relaxation processes. In this way, the Cole-Cole plot can be used to help describe the change in breadth of the alpha transition of the $\tan \delta$ plots that was not accounted for by the block model. Lower values for h and k can represent a less gaussian distribution of relaxation times with more pronounced tails. In terms of a composite, the interface is a type of inhomogeneity that can lower the values of k and h by interfering in the relaxation phenomena of nearby chains.

Figure 5.10 shows the Cole-Cole plots for the dynamic mechanical data at 1 Hz of the resin and composites made with unmodified Bioglass® and glass modified with the MAMTES:MTES coupling systems. The calculations for the h and k values are based on the glass transitions. Because of this, the Cole-Cole plot was extrapolated through the sub- T_g transitions to calculate h and k .

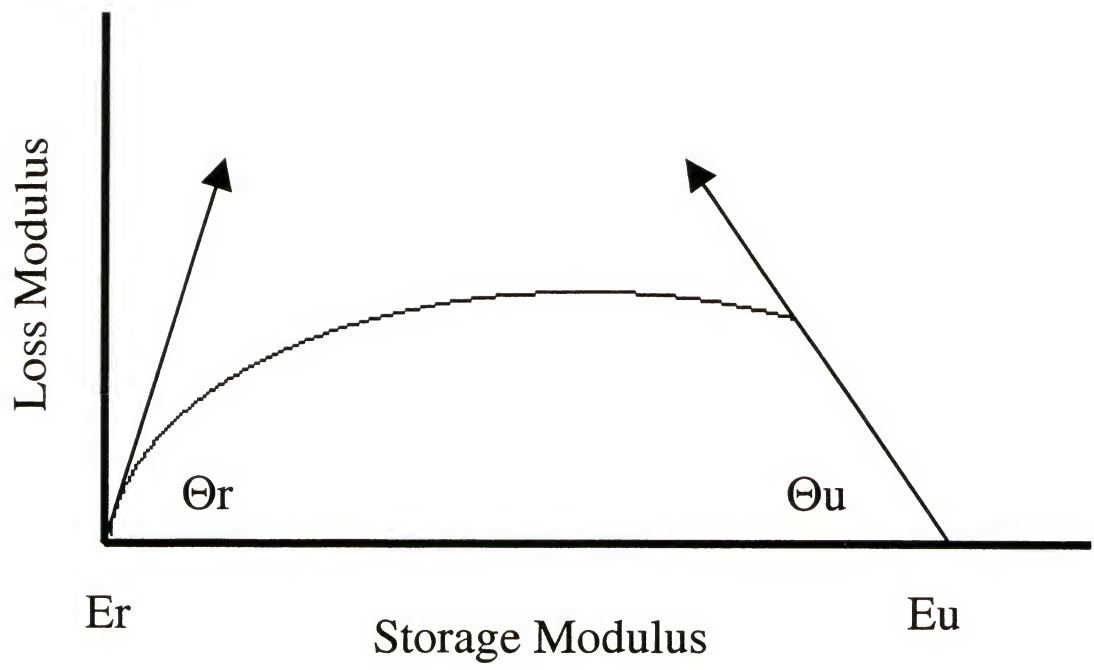


Figure 5.9 Diagram of a Cole-Cole plot.

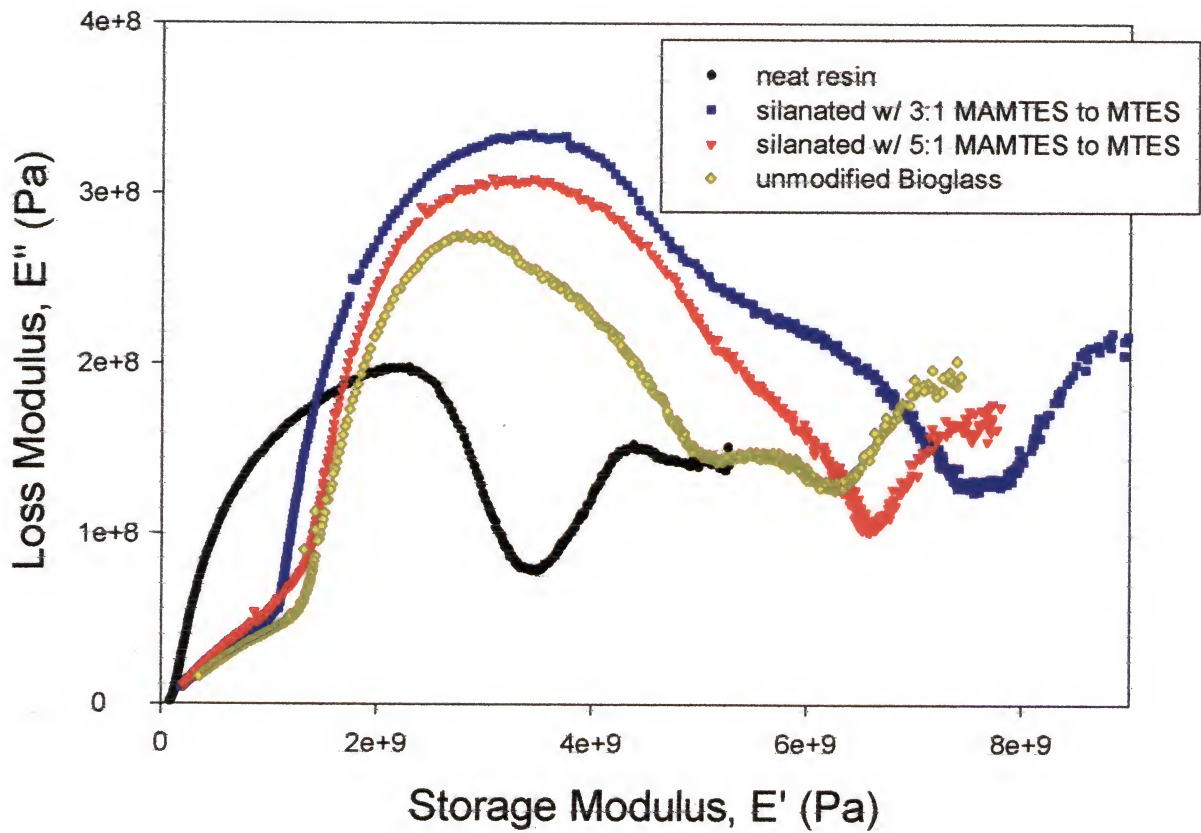


Figure 5.10. Cole-Cole plot for resin and composites with 30 v% Bioglass®

As recorded in Table 5.1, the k values decrease from the resin to the composites made with the 5:1 MAMTES to MTES coupling system, to the unmodified filler, to the composites made with the 3 to 1 coupling system. This is the opposite trend calculated for the h value, which increases in that same order. The parameter k ($0 < k < 1$) is consistent the motional ability of the chains and hence the material density. The increasing h ($0 < k < h < 1$) values is related to the presence of junction points, for example inclusion or chemical and/or physical crosslinks, which hinder the molecular motion on a large scale. This could help explain the lack of increasing T_g that is usually seen with the addition of a coupling agent to the filler in a composite.

Wear of Dental Samples

Tribological studies have shown the importance of the formation of a transfer layer consisting of compacted debris. The transfer layer can act as a lubricant so that the coefficient of friction is lowered [127], [128], [129], [130]. The influence on the importance of lubrication during the wear of materials is depicted in Figure 5.11 where the wear track of an initial resin sample is shown. This sample was run without the water that was used to analyze every other sample in this study. Without water to aid as a lubricant the stresses are such that fractures occur in the resin that are not evident in the subsequent samples. The majority of these fractures occur at the edges of the samples. This is as expected since the highest tensile stresses would be where the steel pin changes direction. The force on the sample if static translates into 2.625 MPa, assuming a 2 mm^2 contact area, which is approximately 5% of the ultimate tensile strength (56 MPa) of the neat resin stated in the previous chapters. At the beginning of the wear test, only a few of

the large asperities could come into contact with the counterface, or steel pin. Applying pressure to the specimen results in plastic deformation that occurs at the tips of these asperities. Because of the relative movement of the two counterfaces (the sample and the steel pin) some of the asperities fracture and form debris while others can move back and forth to take up some

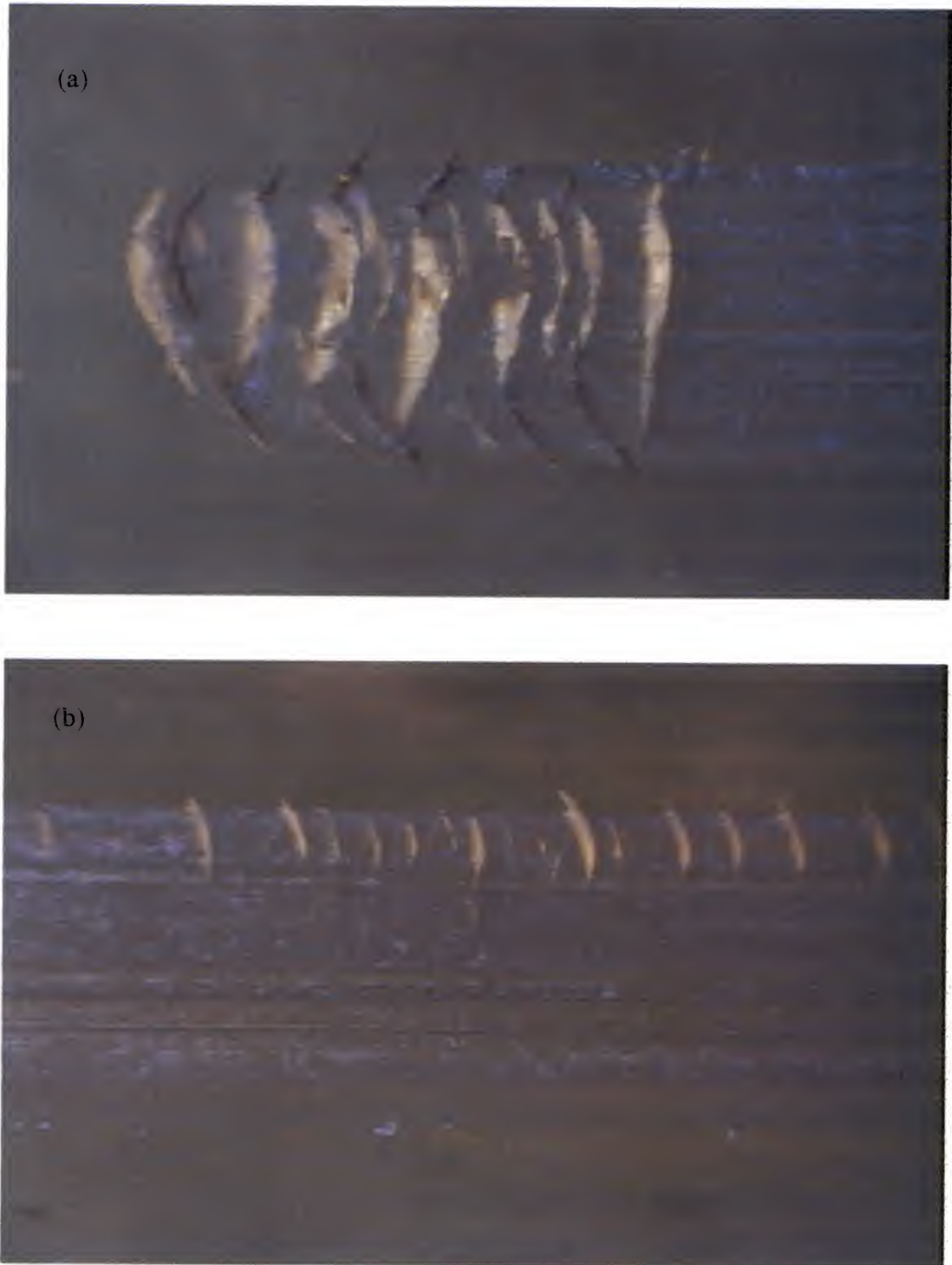


Figure 5.11. Wear track of unlubricated resin sample (a) at the end of wear track, (b) in the middle of wear track.

tangential movement by elastic deformation. Delamination and abrasive wear are the main wear mechanisms. Cracking of the contact area and delamination is significant. At this stage plowing becomes significant because the debris formed cannot escape from the contact area and acts as abrasives between the two surfaces. Score marks on the surface can be seen on the sample surface as well as on the pin surface (Figure 5.12). Evidence of debris trapped on the pin surface is clearly visible in the photoimages.

All subsequent tests were run in a water bath held at 37°C. Figure 5.13 shows the wear track of another resin sample of the same composition. Although score marks are clearly visible on both the wear track and the steel pin, there is no evidence of the crack formation in the lubricated sample.

To quantify the wear of the samples, profiles were taken of the width and height of the middle of the wear track the light profilometer to measure the volume of wear loss. The volume was then compared to the weight of wear collected from each test. The amount of variance in the data is too large to make any definite conclusions, however, there are trends towards improved wear with the addition of a filler particle. In addition, by comparing the volume to the weight of the recovered material, it is likely that the majority of wear material comes from the resin material. This is expected for two reasons. The first reason is the formation of the 'skin-layer' on the surface of the

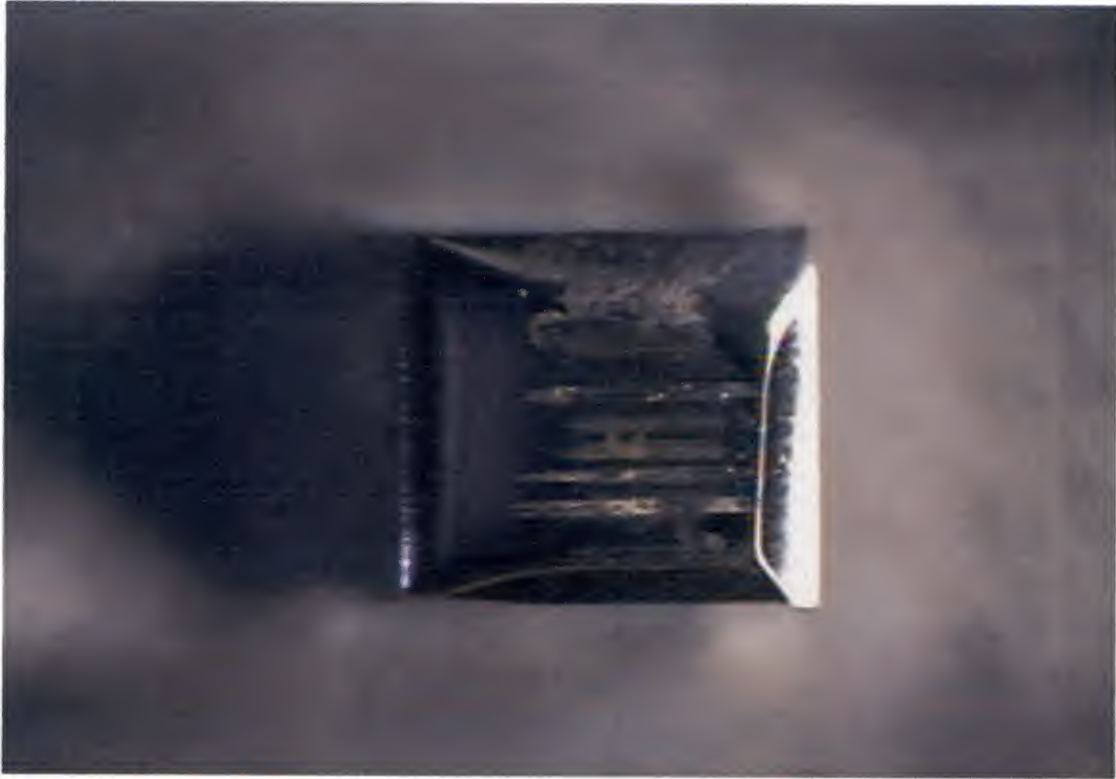


Figure 5.12. Surface of steel pin after wear test without lubrication



Figure 5.13. End of wear track of lubricated resin sample

Most of the debris is immediately removed, in the case of experiments performed in water, reducing the probability of film formation. Also lubrication is provided by the water, which reduces the adhesion forces and ultimately the wear rate. Because of a constant flushing action by saliva in the oral cavity and the sliding motion between teeth during chewing, a stable third-body interfacial layer probably does not form on dental restorations. Therefore, the wear data from tribometers that employ a continuous flushing action during testing could provide a better simulation as compared to tribometers that rely on a stagnant fluid environment.

The amount of wear was quantified two ways, by the volume of the material removed to produce the wear track, and the weight of the wear debris collected after the test. Figure 5.14 shows the relationships between these two methods. By comparing the wear volume and weight of the resin sample to the wear volume and weight of the composite samples, a better idea of the wear mechanisms can be discerned. Although there is no significant difference in the wear volume of the composites with respect to different filler surface treatments, there is a marked decrease of approximately 32% in the wear volume with the addition of 30 v% Bioglass® compared to the neat resin. The wear weight, however, shows no significant decrease with the addition of filler. Because the density of the filler is higher than the density of the resin, if filler is debonding as a result of the wear test this would result in a larger than expected wear weight, skewing the data in favor of the pure resin sample. In addition, there is the wear debris from the steel pin to contend with. All in all, the weight of the wear debris is not a very accurate account of the wear mechanisms of materials tested.

The edge of the wear track of the neat resin sample is shown in Figure 5.15. From this image the evidence of wear by an adhesive mechanism is evident in the pile up of wear debris at the end of the wear track. By comparison, the edge of the wear track for the Bioglass® sample (Figure 5.16) is more sharp. The lack of debris piling-up at the edge of the composite samples is an indication of the greater wear resistance of these samples over the neat resin.

Another method to quantify the wear process of the materials is the change in the roughness resulting from the wear test. Table 5.2 records the roughness data before and after 10 hour measurements of wear for the resin and composites and compares the different filler surface treatments. The addition of filler to the resin increases the initial roughness of the samples.

Rough surfaces have a higher plasticity index than smooth surfaces, so some plastic deformation would occur at the tips of the asperities [131]. The rougher surface wears more than the smooth surface. Work hardening is likely to prevent these deformed asperities from being completely flattened so that the sharper asperities on a rough surface would be able to accumulate more of the tangential movement by elastic deformation.

The initial flatness of the samples goes to rough because wear debris has less ability to escape causing leading to the plowing of the samples. Conversely, more rough surfaces go to flat because wear debris has a greater chance to escape from the contact areas into adjacent hollows. The surface can become worn flatter.

In addition to the effects of the initial roughness of the samples is the transfer of stress from the matrix material to the filler material as discussed in earlier chapters. The

reinforcing effect of the filler allows for greater stresses before material failure; thus resulting in the lower wear volumes of the composites verses the neat resin.

Examples of the wear track of a neat polymer resin sample and a Bioglass® filled sample are provided in Figures 5.17 and 5.18, respectively, using the light profilometer. From these images, the roughness and volume of removed material could be measured.

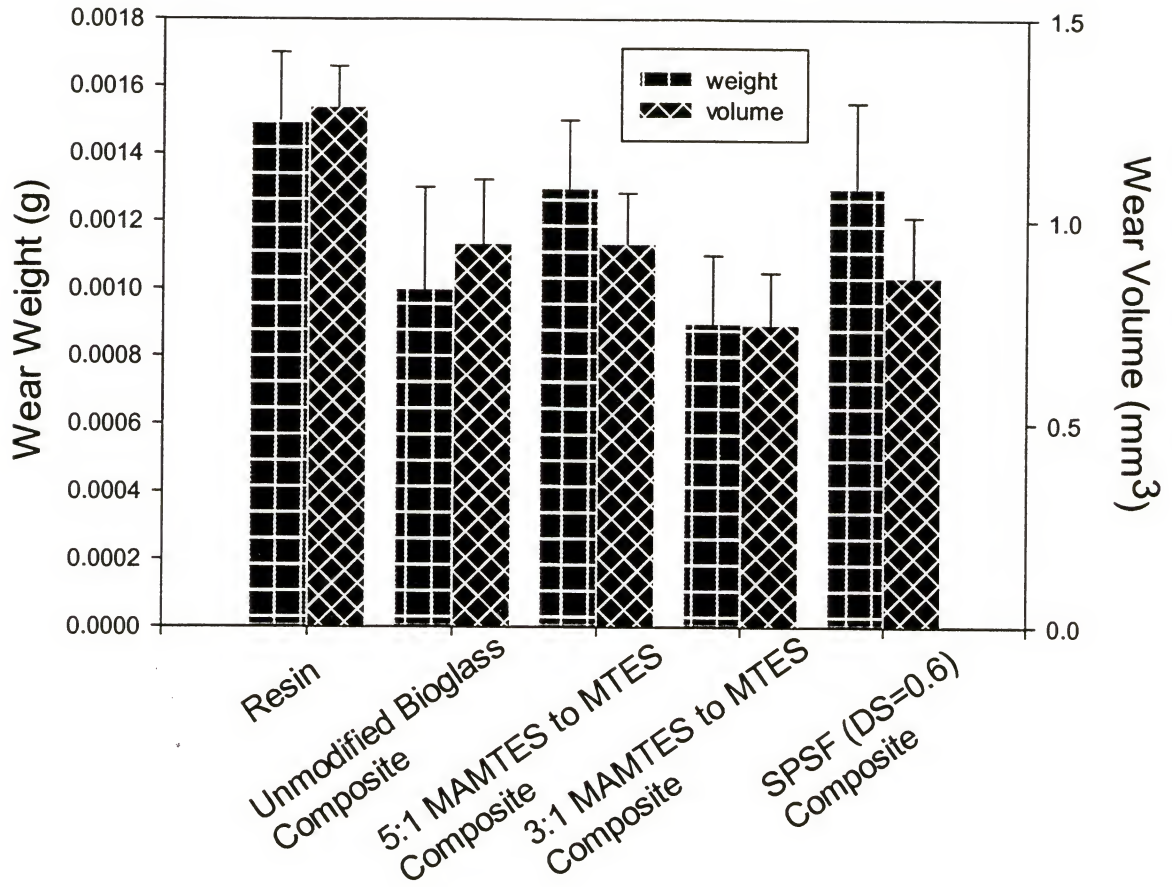


Figure 5.14. Wear weight and volume of resin and composites comparing different filler surface treatments after 10 hour wear runs.

Table 5.2. Roughness data before and after 10 hour wear runs for the resin and composites comparing different filler surface treatments

Sample	Initial R_A (μm)	R_A (μm) after wear run
Neat resin	0.07 ± 0.03	8.02 ± 0.50
Composite with unmodified Bioglass®	0.55 ± 0.06	5.95 ± 0.82
Composite with Bioglass® modified with 3:1 MAMTES to MTES coupling system	0.49 ± 0.05	5.01 ± 0.62
Composite with Bioglass® modified with 5:1 MAMTES to MTES coupling system	0.50 ± 0.08	4.95 ± 1.02
Composite with Bioglass® modified with SPSF (DS = .06)	0.52 ± 0.12	4.55 ± 0.83

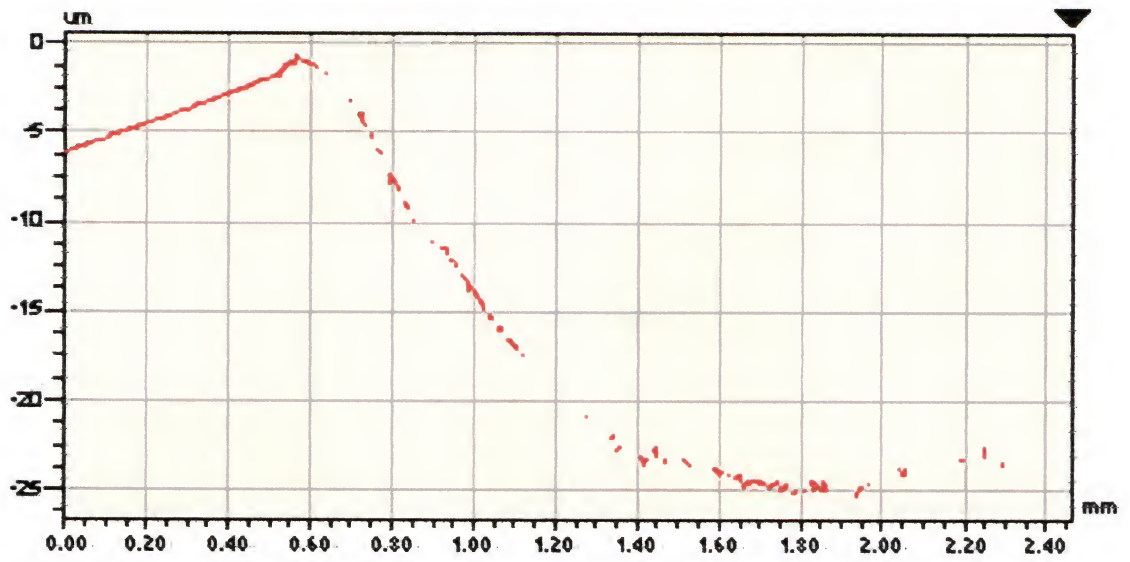


Figure 5.15. Profile of the end of the wear track for a neat resin sample.



Figure 5.16. Profile of the end of the wear track for 30 v% Bioglass® filled composite.

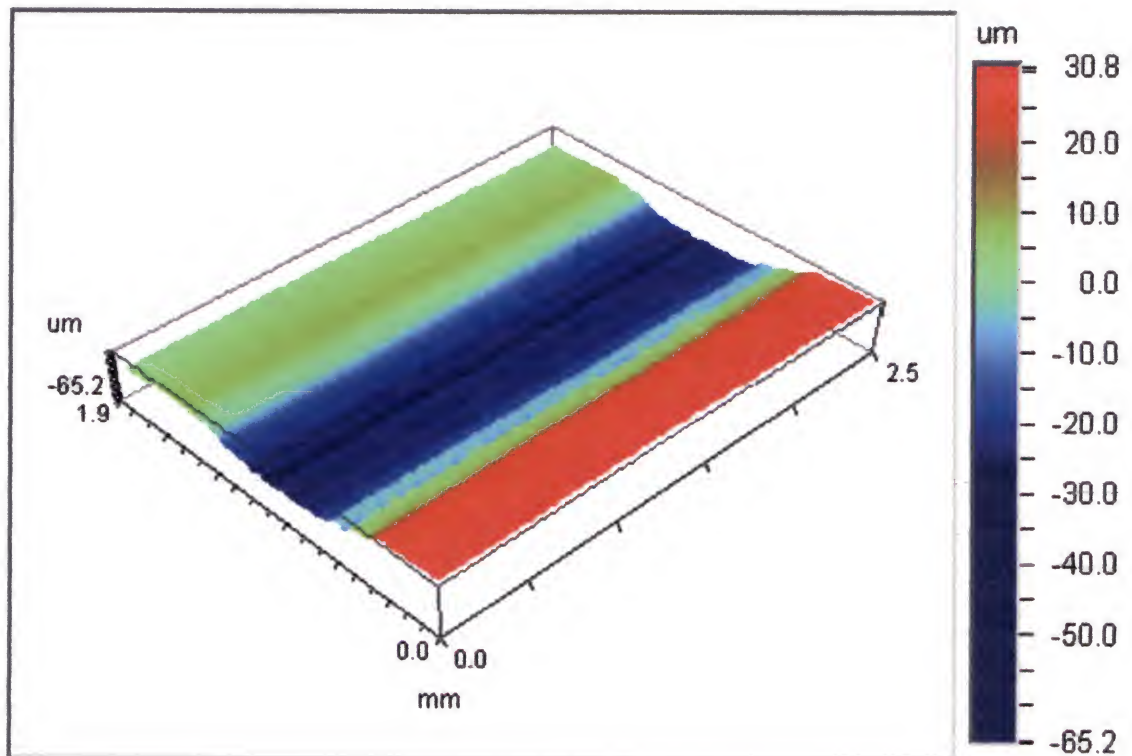


Figure 5.17. Example wear track of neat resin

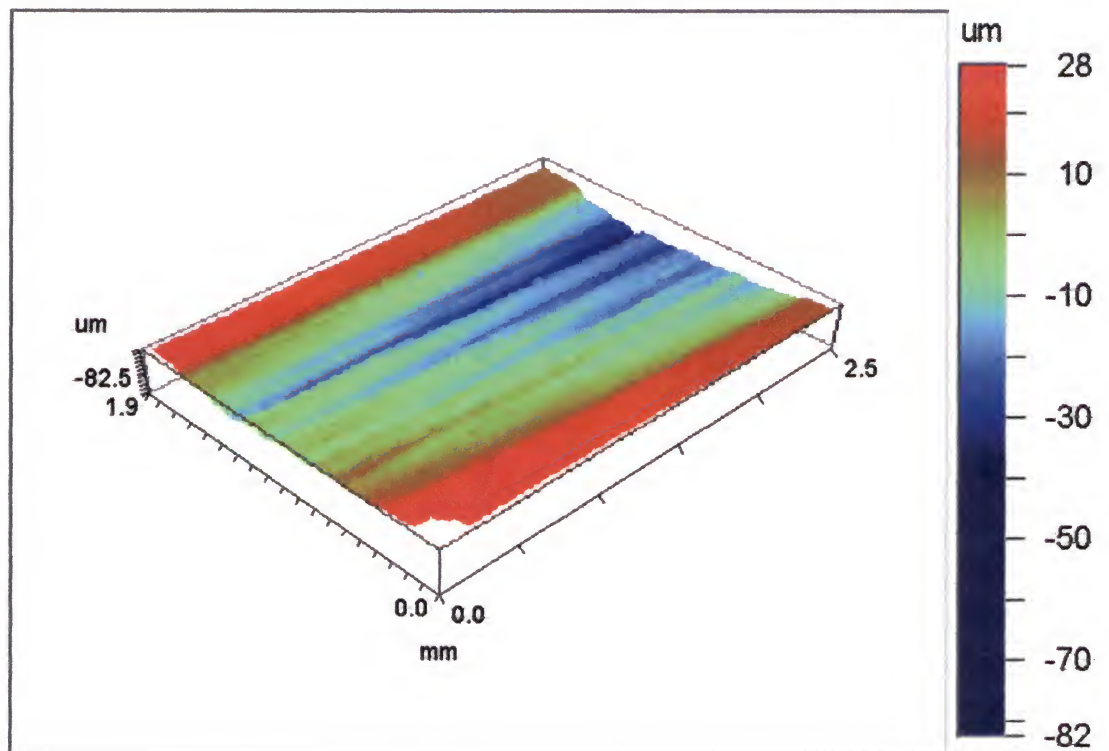


Figure 5.18. Example wear track of composite filled with 30 v% Bioglass®

Conclusions

The surface modification of Bioglass® filler has a significant effect on the enhancement of mechanical and physical properties of the composites studied in the previous chapters. Using a 3:1 MAMTES to MTES resin system, the dry-state tensile strength increases from an average of 56.0 ± 6 MPa for the pure resin to 60.1 ± 3.7 for the composite. The 5:1 MAMTES to MTES resin system shows a lower tensile strength (49.8 ± 1.9 MPa), however, not as low as the unmodified Bioglass® (42.0 ± 4.9 MPa). Grafting a sulfonated polysulfone ($DS = 0.6$) onto the Bioglass® particle results in a average tensile strength of 54.5 ± 5.1 MPa, thus also prevented the decrease in tensile strength seen by adding unmodified filler to the resin.

To help quantify and compare the two different surface modifying systems, two types of modeling were used based on the dynamic mechanical responses of the materials. Using the more effective coupling systems determined from Chapters 3 and 4 and a model originally developed by Takayanagi [123], the observed $\tan \delta$ responses of the composites were modeled. Even with the disagreement between the simulated composite scans and the actual composites scans, trends in the differences of the λ and K values can be explained from the tensile and flexure mechanical results examined in the earlier chapters. The low λ value for the unmodified Bioglass® sample composite could be an indication of the better dispersive properties of the glass after it has been silanated. The highest λ value was determined for the sulfonated polysulfone modified glass. This could be a result of the number of polar groups added in this modifying system compared to the methacrylate based coupling system, allowing for better filler dispersion.

Because the fit of the three-phase block model was less than ideal, another method using a Cole-Cole plot was implemented to elucidate further the effect of the interface on the relaxation processes of the matrix. The k values decrease from the resin to the composites made with the 5:1 MAMTES to MTES coupling system, to the unmodified filler, to the composites made with the 3 to 1 coupling system. This is the opposite trend calculated for the h value, which increases in that same order. The parameter k ($0 < k < 1$) represents the mobility of the chains and hence the material density. The increasing h ($0 < k < h < 1$) values is related to the presence of junction points, for example inclusion or chemical and/or physical crosslinks, which hinder the molecular motion on a large scale. This could help explain the lack of increasing T_g that is usually seen with the addition of a coupling agent to the filler in a composite.

Using the wear volume as an indication of wear resistance, the addition of the glass filler reduces the wear volume by an average of 32%. There are, however, no trends in the wear volumes of the filled samples to conclude that one of the surface modifying systems is superior to another for wear resistance. The large change in roughness seen for the neat resin sample compared to the filled samples gives an indication of a possible wear mechanism, namely the ability for wear debris to escape from the wear track by falling into “pits” of the rougher composite samples. By allowing wear debris to escape from the wear track, the increased subsequent plowing of the samples from adhesive wear is limited.

CHAPTER 6 CONCLUSIONS

Three variations of surface treatment systems applied to particulate sol-gel derived Bioglass® filler were studied. The efficiency of the surface modifications was analyzed as it relates to the bioactivity and to the enhancement of mechanical properties of the composites studied. Among the filler surfaces studied are: (1) the hydroxyl groups contained on dried Bioglass® particulate, (2) methacryloxypropyl triethoxysilane (MAMTES) coupling agent combined with a methyl triethoxysilane (MTES) coupling agent (Chapter 3), and (3) grafted sulfonated polysulfone (SPSF) with different degrees of sulfonation (Chapter 4). Concerns include the ability of the coupling system to improve the mechanical properties of the composites and to investigate the effect of both the amount of coupling agent used during processing and the ratio of MAMTES to MTES. Other points of interest studied are the effects of the post-cure environment of the composites and how the submersion of the samples in either a water or salt solution affects the physical properties of the samples.

The resin system chosen is based on 2,2'-bis-(4-methacryloylethoxyphenyl) propane (Bis-MEPP) using triethylene glycol dimethacrylate (TEGDMA) as a diluent to improve processability and the degree of cure. To help offset the polymerization shrinkage in dental resins, nadic methyl anhydride (NMA), a cyclic anhydride with an unsaturated vinyl group has been added to the base resin system

A composite interphase was designed to enhance the interactions between the phases of a particulate filler and the matrix by promoting mechanical and chemical interlocking through the formation of an interpenetrating network between the matrix and a methacrylate functionalized polymer silanated to the filler. For this purpose, a methacryloxypropyl triethoxysilane (MAMTES) coupling agent combined with a methyl triethoxysilane (MTES) coupling agent system was successfully silanated to the Bioglass® filler. A dependence on the ratio of methacrylate functionalized coupling agent on the reinforcing capabilities of the filler was discovered.

At lower levels of methacrylate functionalized coupling agent in the silane system (less than the 3:1 ratio studied), there is no reinforcing effect by the addition of filler to the resin system as studied using tensile strengths. In fact, there is no significant difference between composites made using an unsilanated Bioglass® ($TS = 42 \pm 4.9$ MPa) and one made with a 1 to 1 ratio of MAMTES to MTES coupling system ($TS = 39.4 \pm 3.6$ MPa). Slightly better tensile properties ($TS = 49.8 \pm 1.9$ MPa) are evident in composites made with higher levels (above the 3:1 ratio) of methacrylate functionalized coupling agent, however, there is still a reduction in strength from the pure resin ($TS = 56.0 \pm 6$ MPa). At mid levels of MAMTES to MTES, i.e. at the 3 to 1 ratio, there is an increase in tensile strength ($TS = 60.1 \pm 3.7$ MPa) from the pure resin showing the importance of the coupling system, and not just the presence of a coupling system, to the enhancement of a composite.

The weight of the resin sample increases 4% and 6% when aged in water for samples made with 10 and 20 w% NMA. Samples made with 40 w% NMA crack before an equilibrium water uptake. Adding 30 v% untreated Bioglass® to the 10 w% NMA

resin system results in a decreasing weight change trending beyond the -1.6% final measurement in this study. Modifying the Bioglass® particulate, however, results in an increased weight gain of 0.23% . The lack of weight loss in the 3:1 silanated glass composite could be an indication of the effective binding of the skin-layer, or pure resin layer that surrounds a composite, to the bulk material through the reinforcing effect of the filler. In addition to weight reduction through the leaching of the resin material, the bioactive filler may also be leaching ions to the nano-pure water. The silane-coupling system is then acting as a shield to the diffusion of water, protecting the filler/matrix interface.

The weight change in the composite samples differed significantly in the salt solution compared to the pure water. Most obviously, is the increased weight gain and the lack of an equilibrium weight for the salt solution soaked composites, which increases from -1.6 to 2.9% for the composite made from unsilanated Bioglass® and 0.23 to 2.6 for the composite made from silanated Bioglass®. If the diffusion of water is activating the glass filler, then the additional weight gain shown for the salt soaked samples could be the result of the sorption of HCA forming ions (calcium and phosphate) from the salt solution.

A composite interphase was designed to enhance the interactions between the phases of a particulate filler and the matrix by promoting mechanical interlocking through the formation of an interpenetrating network between the matrix and a polymer grafted to the filler. For this purpose, sulfonated polysulfones were successfully prepared and grafted onto the Bioglass® filler.

In the dry state, the addition of the unmodified Bioglass® filler results in flaws reducing the tensile strength of the neat resin from an average of 56 ± 6.0 MPa to 42 ± 4.9 MPa. All the samples examined in this study have their highest tensile strength values in the dry state. Dry composites made using an SPSF with degrees of sulfonation equal to 1.4 (TS = 56.3 ± 5.4 MPa) and 0.6 (TS = 54.5 ± 5.1) show none of the debilitating effects that the unmodified Bioglass® filler composites show.

Unlike in the dry state, samples aged in the salt solution show no loss of tensile strength with the addition of the unmodified Bioglass® filler (TS = 35.9 ± 4.0) when compared to the neat resin (TS = 31.5 ± 7.0). Although all the samples examined in this study decrease in tensile strength after soaking, the tensile strengths of the composites do not drop significantly below the tensile strength of the soaked-neat resin. This indicates that there is a reinforcing effect with the addition of the filler supporting the idea of the resin's ability to form a mechanical bond with the filler.

A trend in the data, however, suggests that the composite made from Bioglass® filler grafted with SPSF having a DS of 0.6, has the best matrix/filler adhesion resulting in a higher tensile strength within the dry and salt-soaked conditions. The sample trending with the lowest tensile strength after aging in the salt solution is the composite made from Bioglass® filler grafted with SPSF having a DS of 1.4. The higher degree of sulfonation means that the interface may have a higher affinity for water, which may add to the propensity for hydrolytic filler-matrix degradation. This higher affinity for water, however, may also facilitate in the growth of a HCA layer.

No decrease in the flexural moduli of the composite samples with post-cure treatment indicates that the plasticization affecting the neat resin system does not affect

the matrix/filler interface. The similar flexural modulus values for the composites also indicate little change in the wetting properties of the matrix material in relation to surface modification.

The surface modification of Bioglass® filler has a significant effect on the enhancement of mechanical and physical properties of the composites studied in the previous chapters of this study. To help quantify and compare the two different surface modifying systems, two types of modeling were used based on the dynamic mechanical responses of the materials. Using the more effective coupling systems determined from Chapters 3 and 4 and a model originally developed by Takayanagi [123], the observed $\tan \delta$ responses of the composites were modeled. Trends in the differences of the model parameters can be explained from the tensile and flexure mechanical results examined in the earlier chapters. The parameters related to the unmodified Bioglass® composites indicate the better dispersive properties of the glass after it has been silanated. The sulfonated polysulfone modified glass showed the most enhanced parameters for filler matrix interactions. This could be a result of the number of polar groups added in this modifying system compared to the methacrylate based coupling system, allowing for better filler dispersion.

Parameters from a Cole-Cole plot were also examined to quantify the reinforcing quality of the filler particles. The model parameters indicate a decreasing motional ability of the chains going from the resin to the composites made with the 5:1 MAMTES to MTES coupling system, to the unmodified filler, to the composites made with the 3 to 1 coupling system and a increasing crosslinking effect of the filler in the same sample order, which hinder the molecular motion on a large scale. This could help explain the

lack of increasing T_g that is usually seen with the addition of a coupling agent to the filler in a composite.

Using the wear volume as an indication of wear resistance, the addition of the glass filler reduces the wear volume by an average of 32%. There are, however, no trends in the wear volumes of the filled samples to conclude that one of the surface modifying systems is superior to another for wear resistance. The large change in roughness seen for the neat resin sample compared to the filled samples gives an indication of a possible wear mechanism, namely the ability for wear debris to escape from the wear track by falling into “pits” of the rougher composite samples. By allowing wear debris to escape from the wear track, the increased subsequent plowing of the samples because of adhesive wear is limited.

In the dry condition the affect of NMA is unclear. It is thought that the reactivity of NMA is less than TEGDMA and Bis-MEPP [10]. As a result, composites containing NMA have higher levels of unreacted monomer or material that is not incorporated into the network structure. The unreacted material can act as a plasticizer for the system causing a reduction in the breaking strength of the composites. However, resin the samples with the highest average tensile strength contains 20 w% NMA. The tensile strength of the neat resins vary from 53.1 ± 7.5 MPa to 56.0 ± 6.0 to 44.1 ± 3.5 MPa for 10, 20, and 30 w% NMA, respectively. The increasing tensile strength with NMA concentrations between 10 and 20 w% may be due to an increase in the polarity of the system, which have been shown to increase the tensile strength through hydrogen bonding [19]. The competition between increased polarity and unreacted monomer leads to the lack of clear trends.

The addition of the grafted particles increases the breaking strength of the composites regardless on the amount of SPSF ($DS = 1.4$) used to produce the filler. Conversely, for the unsilanated filler the tensile strength is significantly lowered indicating the effective reinforcement by the surface treatment.

At 10 and 20 w% NMA, the composites comprised of the filler grafted in 1 w% SPSF has higher average tensile strengths (57.8 ± 1.1 and 56.3 ± 5.4 MPa, respectively) compared to that grafted in 5 w% SPSF (48.7 ± 3.8 and 52.8 ± 1.3 MPa, respectively). At the 30 w% NMA composition, all samples, including the unsilanated filled composites, are not significantly different suggesting that the NMA content is the most important variable in determining the tensile properties at this composition.

Closing Remarks

Including nadic methyl anhydride in this Bis-MEPP based resin system has been shown to help offset polymerization shrinkage by 0.7% [10]. Once hydrolyzed to its dicarboxylic acid, it also has the ability to form interact with leachable cations from the bioactive filler (Figure 6.1). For these reasons it was included in this study. The increased polarity of resin system with the addition of NMA has possibly led to some of the higher strengths discussed above.

Surface modification of the filler has also led to higher tensile strength, however, dependencies on the concentrations and compositions of the modification systems have been found. The MAMTES-co-MTES coupling system resulted in the highest dry tensile strengths seen in this study (~ 60 MPa). This tensile strength was achieved using a 3:1 ratio of MAMTES to MTES. This sample also had the highest tensile strength after being aged 5 weeks in a salt solution (~ 37 MPa).

A reinforcing effect was also found in composites made with Bioglass® grafted with a sulfonated polysulfone. The most efficient matrix/filler adhesion was found in composites made with Bioglass® that had been grafted with a SPSF having a degree of sulfonation equal to 0.6. At higher levels of sulfonation, direct evidence of hydroxy apatite growth was found. For the goal of a bioactive dental composite, these systems are worth further examination.

Specific areas for future examination are a determination of the leaching components after aging in a salt or water solution and an examination of mechanical properties over longer aging times.

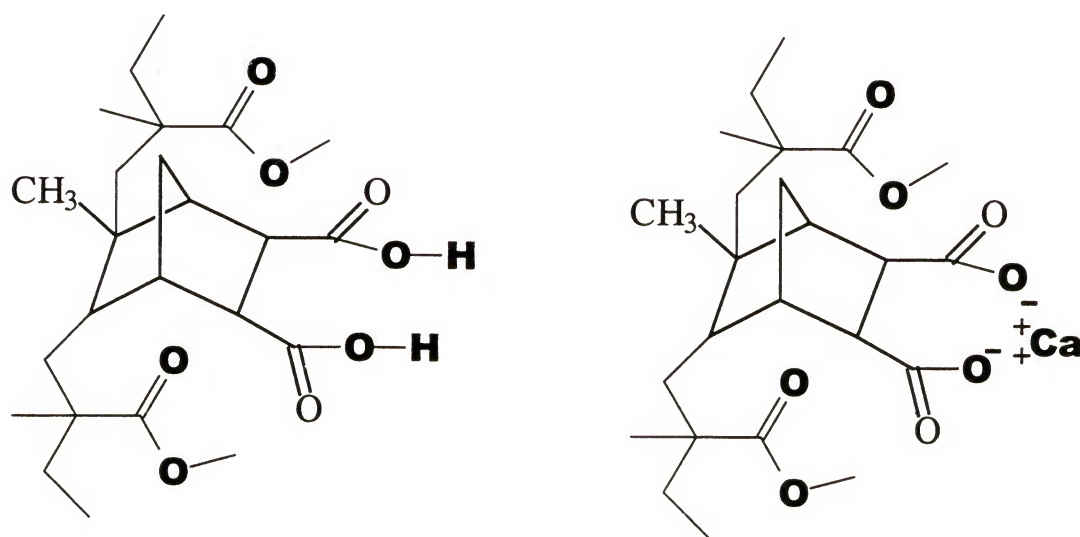


Figure 6.1. Schematic showing the incorporation and hydrolysis of nadic methyl anhydride and the interaction with a calcium ion

LIST OF REFERENCES

1. Craig, R.G., W.J. O'Brian, J.M. Powers, *Dental Materials: Properties and Manipulation*. 4th ed. 1987, St. Louis: The C.V. Mosby Company.
2. Liu, C.F., S.M. Collard, C.D. Armeniades, *American Journal of Dentistry*, 1990. **3**(2): p. 44-50.
3. Watts, D.C. A.J. Cash, *Meas Sci Technol*, 1991. **2**: p. 788-794.
4. Millich, F., L. Jeang, J.D. Eick, C.C. Chappelow, C.S. Pinzino, *Journal of Dental Resins*, 1998. **77**(4): p. 603-608.
5. Day, D., *American Ceramic Society Bulletin*, 1995. **74**(12): p. 64-68.
6. Prasad, S.V., P.D. Calvert, *Journal of Material Science*, 1980. **15**: p. 1746-1754.
7. Venhoven, B.A.M., A.J. de Gee, A. Werner, C.L. Davidson, *Biomaterials*, 1994. **15**(14): p. 1152-1156.
8. Bastioli, C., G. Romano, *Journal of Materials Science*, 1987. **22**(12): p. 4207-4214.
9. Davis, D.M., N.E. Waters, *Journal of Dental Research*, 1989. **68**(7): p. 1194-1198.
10. Mehlem, J.J., *The influence of nadic methyl anhydride on mechanical and thermomechanical properties of dental resins and composites*, in *Materials Science and Engineering*. 1999, Masters Thesis, University of Florida: Gainesville.
11. Lin, F.H., D.E. Day, *Biomedical Engineering Applications Basis Communications*, 1993. **5**(6): p. 784-795.

12. Zamora, M.P., J.J. Arnold, L.L. Hench, A.B. Brennan. *Bioglass Reinforced Dental Composites: Thermomechanical Properties*. Polymer Preprints, American Chemical Society Proceedings. 1995. ACS, Washington, DC.
13. West, J.K., S. Wallace, *Journal of Non-Crystalline Solids*, 1993. **152**(2-6): p. 109-117.
14. Orefice, R.L., *Bioactive composites with designed interfaces*, in *Materials Science and Engineering*. 1997, Doctorial Dissertation, University of Florida: Gainesville. p. 498.
15. Phillips, R.W., *Elements of Dental Materials*. 4th ed. 1984, Philadelphia: W.B. Suaunders Company.
16. Svare, C.W., L.C. Peterson, J.W. Reinhardt, D.B. Boyer, C.W. Frank, D.D. Gay, R.D. Cox, *Journal of Dental Research*, 1981. **60**: p. 1668-1671.
17. Soderholm, K.-J., *Resin-Based Composites*, in *Dental Materials for Clinical Practice*, K. Anusavice, C. Shen, and K.-J. Soderholm, Editors. 1992, University of Florida: Gainesville. p. 18-40.
18. Petersen, E.A., R.W. Phillips, M.L. Swartz, *Journal of the American Dental Association*, 1966. **73**: p. 1324-1336.
19. Kawaguchi, M., T. Fukushima, T. Horibe, *Dental Materials Journal*, 1988. **7**(2): p. 174-181.
20. Holter, D., H. Frey, R. Mulhaupt, J.E. Klee, *Branched bismethacrylates based on bis-gma-a systematic route to low shrinkage composites* in *Proceedings of The 1997 Las Vegas ACS Meeting*. 1997. Las Vegas, NV: Division of Polymer Chemistry, American Chemical Society.
21. Kalachandra, S., *Dental Materials*, 1989. **5**(4): p. 283-288.
22. Shobha, H.K., M. Sankarapandian, S. Kalachandra, D.F. Taylor, J.E. McGrath, *Journal of Materials Science: Materials in Medicine*, 1997. **8**: p. 583-586.

23. Chowdhury, N.A., K. Wakasa, R. Priyawan, M. Yamaki, *Journal of Materials Science: Materials in Medicine*, 1997. **8**: p. 149-155.
24. Ruyter, I.E., H. Oysaed, *Acta Odontologica Scandinavica*, 1982. **40**(3): p. 179-192.
25. Birdsell, D.C., P.J. Bannon, R.B. Webb, *Journal of the American Dental Association*, 1977. **94**(2): p. 311-314.
26. Kalachandra, S., "Glassy polymers as dental materials," in *Encyclopedia Handbook of Biomaterials and Bioengineering*, D.J.T.D.L. Wise, *et al.*, Editors. 1995, Marcel Dekker, Inc.: New York. p. 1545-1556.
27. Venhoven, B.A.M., A.J. de Gee, A. Werner, C.L. Davidson, *Biomaterials*, 1996. **17**(7): p. 735-740.
28. Jones, D.W. and A.S. Rizkalla, *Journal of Biomedical Materials Research: Applied Biomaterials*, 1996. **33**: p. 89-100.
29. Coombe, E.C., *Notes on Dental Materials*. 5th ed. 1986, Edinburgh: Churchill Livingstone.
30. Park, J.B., R.S. Lakes, *Biomaterials: An Introduction*. 2nd ed. 1992, New York: Plenum Press.
31. Soderholm, J.-J.M., *Journal of Dental Research*, 1983. **62**: p. 126-130.
32. Salz, U., P. Burtscher, K. Vogel, N. Moszner, V. Rheinberger, : p. 143-144.
33. Peutzfeldt, A., E. Asmussen, *Journal of Dental Resins*, 1991. **70**(12): p. 1537-1541.
34. Zamora, M.P., K.B. Wagener, A.B. Brennan. *Copolymer compositions designed to offset polymerization shrinkage in dental composites: I. Maleic anhydride*. 1994: Division of Polymer Chemistry, American Chemical Society.
35. Hotz, P., J.W. McLean, *British Dental Journal*, 1977. **142**: p. 41.

36. Hench, L.L., *Journal of the American Ceramic Society*, 1991. **74**(7): p. 1487-1510.
37. Hench, L.L., R.J. Splinter, W.C. Allen, T.K. Greenlee, *Biomedical Materials Research Symposium*, 1971(2 (Part 1)): p. 117-141.
38. Luo, J., R. Seghi, J. Lannutti, *Materials Science & Engineering C: Biomimetic Materials, Sensors and Systems*, 1997. **5**(1): p. 15-22.
39. Hench, L.L., O. Andersson, "Bioactive glasses", in *Advanced Series in Ceramics*, M. McLaren and D.E. Niesz, Editors. 1993, World Scientific Publishing Co. Pte. Ltd.: Singapore. p. 41-62.
40. Li, P., K. Nakanishi, T. Kokubo, K. de Groot, *Biomaterials*, 1993. **14**: p. 963-967.
41. Labella, R., M. Braden, K.W.M. Davy, *Biomaterials*, 1992. **13**(13): p. 937-943.
42. Saito, M., A. Muraoka, T. Mora, N. Sugano, K. Hino, *Biomaterials*, 1994. **15**: p. 156-160.
43. Shinzato, S., M. Kobayashi, W.F. Mousa, M. Kamimura, M. Neo, K. Choju, T. Kokubo, T. Nakamura, *Journal of Biomedical Materials Research*, 2000. **53**(1): p. 51-61.
44. Fujita, H., K. Ido, Y. Matsuda, H. Lida, M. Oka, Y. Kitamura, T. Nakamura, *Journal of Biomedical Materials Research*, 2000. **49**(2): p. 273-288.
45. Fujita, H., H. lida, K. Kawanabe, Y. Okads, M. Oka, T. Masuda, Y. Kitamura, T. Nakamura, *Journal of Biomedical Materials Research, Applications in Biomaterials*, 1999. **48**(43-51).
46. Hench, L.L., G.P. LaTorre, *Bioceramics*, 1992. **5**: p. 67-74.
47. Jang, J., J.Y. Lee, J.K. Jeong, *Journal of Applied Polymer Science*, 1996. **59**: p. 2069-2077.
48. Ko, Y.S., W.C. Forsman, T.S. Dziemianowicz, *Polymer Engineering and Science*, 1982: p. 805-814.

49. Wagner, H.D., A. Lustiger, *Composites*, 1994. **25**: p. 613-616.
50. Brennan, A.B., J.J. Arnold, M.P. Zamora, *Journal of Adhesion Science and Technology*, 1995. **8**: p. 1031-1048.
51. Boven, G., R. Folkersma, G. Challa, A.J. Schouten, M. Bosma, *Polymer*, 1992. **33**(1): p. 83-88.
52. Bergeret, A., N. Alberola, *Polymer*, 1996. **37**(13): p. 2759-2765.
53. Soderholm, K.J., M. Zigan, M. Ragan, W. Fischlschweiger, M. Bergman, *Journal of Dental Resins*, 1984. **63**(10): p. 1248-1254.
54. Martin, N., N. Jedynakiewicz, *Biomaterials*, 1998. **19**(1-3): p. 77-83.
55. Bowen, R.L., J.E. Rapson, G. Dickson, *Journal of Dental Research*, 1982. **61**(5): p. 654-658.
56. Rueggeberg, F.A., Y.H. Bagis. "Effect of post cure temperature and heat duration on monomer conversion in a photo-activated dental resin composite," in *Proceeding of The 1997 Las Vegas ACS Meeting*. 1997. Las Vegas, NV USA: Division of Polymer Chemistry, American Chemical Society.
57. Ferracane, J.L., J.K. Hopkin, J.R. Condon, *Dental Materials*, 1995. **11**: p. 354-358.
58. Yamaga, T., Y. Sato, Y. Akagawa, M. Taira, K. Wakasa, M. Yamaki, *Journal of Oral Rehabilitation*, 1995. **22**: p. 857-863.
59. Ruyter, E.I., S.A. Svendsen, *Acta Odontologica Scandinavica*, 1977. **36**: p. 75-82.
60. Ferracane, J.L., V.A. Marker, *Journal of Dental Research*, 1992. **71**(1): p. 13-19.
61. Wu, W., J.E. McKinney, *Journal of Dental Research*, 1992. **61**: p. 1180-1183.
62. Ferracane, J.L., J.R. Condon, *Dental Materials*, 1990. **6**: p. 282-287.

63. Li, Y., M.L. Swartz, R.W. Phillips, B.K. Moore, T.A. Roberts, *Journal of Dental Research*, 1985. **64**(12): p. 1396-1401.
64. Peutzfeldt, A., E. Asmussen, *Scandinavian Journal of Dental Research*, 1992. **100**(5): p. 296-298.
65. de Gee, A.J., P. Pallav, A. Werner, C.L. Davidson, *Dental Materials*, 1990. **6**: p. 266-270.
66. Ferracane, J.L., J.C. Mitchem, J.R. Condon, R. Todd, *Journal of Dental Research*, 1997. **76**(8): p. 1508-1516.
67. Kardos, J.L., "The role of the interface in polymer composites - Some myths, mechanisms, and modifications," in *Molecular Characterization of Composite Interfaces*, H. Ishida and G. Kumar, Editors. 1985, Plenum Press: New York. p. 1-11.
68. Mohsen, N.M., R.G. Craig, *Journal of Oral Rehabilitation*, 1995. **22**(3): p. 183-189.
69. Plueddemann, E.P., "Catalytic effects in bonding thermosetting resins to silane-treated fillers," in *Fillers and Reinforcements for Plastics*, R.D. Deanin and N.R. Schott, Editors. 1974, American Chemical Society: Washington, D.C. p. 86-94.
70. Erickson, P.W., A.A. Volpe, E.R. Cooper. . in *19th Annual Technical Conference of Reinforced Plastics*. 1974.
71. Kumins, C.A., J. Roteman, *Journal of Polymer Science: Part A*, 1963. **1**: p. 527.
72. Plueddemann, E.P., *Silane Coupling Agents*. 2nd ed. 1991, New York: Plenum Press.
73. Ishida, H., J.L. Koenig, *Journal of Polymer Science*, 1979. **17**: p. 615.
74. Plueddemann, E.P., H.A. Clark, L.E. Nelson, K.R. Hoffmann, *Modern Plastics*, 1962. **39**: p. 136.

75. Plueddemann, E.P., "Bonding through coupling agents," in *Molecular Characterization of Composite Interfaces*, H. Ishida and G. Kumar, Editors. 1985, Plenum Press: New York. p. 13-23.
76. Ishida, H., "Structural gradient in the silane coupling agent layers and its influence on the mechanical and physical properties of composites," in *Molecular Characterization of Composite Interfaces*, H. Ishida and G. Kumar, Editors. 1985, Plenum Press: New York. p. 25-50.
77. Eliades, G.C., G.J. Vougiouklakis, A.A. Caputo, *Dental Materials*, 1987. **3**: p. 19-25.
78. Urabe, H., K. Wakasa, Yamaki, *Journal of Materials Science*, 1991. **26**: p. 3185-3190.
79. Wang, M., L.L. Hench, W. Bonfield, *Journal of Biomedical Materials Research*, 1998. **42**(4): p. 577-586.
80. Ferracane, J.L., J.R. Condon, B. Suh, Polymer Preprints, *Abstract #1003*, 1994.
81. Labella, R., M. Braden, S. Deb, *Biomaterials*, 1994. **15**(15): p. 1197-1200.
82. Muller, H., S. Olsson, K.J. Soderholm, *European Journal of Oral Science*, 1997. **105**(4): p. 362-368.
83. Spahl, W., H. Budzikiewicz, W. Geurtsen, *Journal of Dentistry*, 1998. **26**(2): p. 137-145.
84. Soderholm, K.J., *Journal of Biomedical Materials Research*, 1984. **18**(3): p. 271-279.
85. Nicholson, J.W., *Journal of Materials Science: Materials in Medicine*, 1997. **8**(11): p. 691-695.
86. Xu, Z., Q. Liu, J.A. Finch, *Applied Surface Science*, 1997. **120**(3-4): p. 269-278.

87. Vandenberg, E.T., L. Bertilsson, B. Liedberg, K. Uvdal, R. Erlandsson, H. Elwing, I. Lundstroem, *Journal of Colloid and Interface Science*, 1991. **147**(1): p. 103-118.
88. Michalske, T., S.W. Freiman, *Nature*, 1982. **295**: p. 511-512.
89. Michalske, T., S.W. Freiman, *Journal of the American Ceramic Society*, 1983. **66**: p. 284-288.
90. Soderholm, K.J., *Journal of Dental Research*, 1983. **62**(2): p. 126-130.
91. Soderholm, K.J., R. Mukherjee, J. Longmate, *J-Dent-Res.*, 1996. **75**(9): p. 1692-1699.
92. Spector, M., "Porous Implants," in *Non-cemented total hip arthroplasty*. 1988, Raven Press: New York. p. 227.
93. Oyanguren, P.A., C.C. Riccardi, R.J.J. Williams, I. Mondragon, *Journal of Polymer Science, Part B: Polymer Physics*, 1998. **36**(8): p. 1349-1359.
94. Min, B.G., J.H. Hodgkin, Z.H. Stachurski, *Journal of Applied Polymer Science*, 1993. **50**(6): p. 1065-1073.
95. MacKinnon, A.J., R.A. Pethrick, S.D. Jenkins, P.T. McGrail, *Polymer*, 1994. **35**(24): p. 5319-5326.
96. Guiver, M.D., P. Black, C.M. Tam, Y. Deslandes, *Journal of Applied Polymer Science*, 1993. **48**(9): p. 1597-1606.
97. Noshay, A., L.M. Robeson, *Journal of Applied Polymer Science*, 1976. **20**: p. 1885-1903.
98. Johnson, B.C., I. Yilgor, C. Tran, M. Iqbal, J.P. Wightman, D.R. Lloyd, J.E. McGrath, *Journal of Polymer Science Part A: Polymer Chemistry*, 1984. **22**(3): p. 721-737.
99. Higuchi, A., N. Iwata, M. Tsubaki, T. Nakagawa, *Journal of Applied Polymer Science*, 1988. **36**: p. 1753.

100. Soderholm, K.-J.M., P.D. Calvert, *Journal of Materials Science*, 1983. **18**: p. 2957-2962.
101. Mitra, S.B., *Journal of Dental Research*, 1991. **70**(1): p. 72-74.
102. Bastioli, C., G. Romano, C. Migliaresi, *Properties of Dental Composites*, 1990.
103. Eames, W.B., J.D. Strain, R.T. Weitmann, A.K. Williams, *Journal of the American Dental Association*, 1974. **89**(1111-1117).
104. Leinfelder, K.F., T.B. Sluder, C.L. Sockwell, W.D. Strickland, J.T. Wall, *Journal of Prosthetic Dentistry*, 1975. **33**: p. 407-416.
105. Osborne, J.W., E.N. Gale, G.W. Ferguson, *Journal of Prosthetic Dentistry*, 1973. **30**(795-800).
106. Phillips, R.W., D.R. Avery, R. Mehra, M.L. Swartz, R.J. McCune, *Journal of Prosthetic Dentistry*, 1973. **28**: p. 164-169.
107. Arnell, R.D., P.B. Davies, J. Halling, T.L. Whomes, *Tribology: Principles and Design Applications*. 1993, New York: The Macmillan Press.
108. Kusy, R.P., K.F. Leinfelder, *Journal of Dental Restorations*, 1977. **56**: p. 544.
109. Godfrey, D., *Wear Control Handbook*. 1980, New York: ASME.
110. Nardin, M., I. Ward, *Materials Science and Technology*, 1987. **3**: p. 814-826.
111. Orefice, R.L., J.K. West, L.L. Hench, A.B. Brennan "Thermomechanical analysis of bioactive glass-polysulfone composites," in *Polymer Preprints*. 1996. Orlando, FL: American Chemical Society.
112. Dong, S., R. Gauvin, *Polymer Composites*, 1993. **14**(5): p. 414-420.
113. Theocaris, P., P. Ponirides, *Journal of Applied Polymer Science*, 1986. **32**: p. 6267-6279.

114. Rasmussen, S.T., *International Journal of Adhesion and Adhesives*, 1996. **16**: p. 147-154.
115. Gerard, J.F., *Polymer English Science*, 1988. **28**: p. 568.
116. Chauchard, J., B. Chabert, P. Jeanne, G. Nemoz, *Journal of Chemical Physics*, 1987. **84**: p. 239.
117. Tsagaropoulos, G., A. Eisenberg, *Macromolecules*, 1995. **28**(18): p. 6067-6077.
118. McCrum, N.G., B.E. Read, G. Williams, "Anelastic and dielectric effects," in *Polymeric Solids*. 1991, New York: Dover Publications, Inc. 452.
119. Clarke, R.L., *Biomaterials*, 1989. **10**(September): p. 494-498.
120. Urabe, H., K. Wakasa, M. Yamaki, *Journal of Materials Science: Materials in Medicine*, 1990. **1**: p. 55-59.
121. Vaidyanathan, J., T.K. Vaidyanathan, *Journal of Materials Science: Materials in Medicine*, 1995. **6**: p. 670-674.
122. Nielsen, L.E., R.F. Landel, *Mechanical properties of polymers and composites*. 2nd ed. 1994, New York: Narcel Dekker, Inc.
123. Takayanagi, M., H. Harima, Y. Iwata, *Mem. Fac. Eng. Kyushu Univ.*, 1963. **XXIII**: p. 1-13.
124. Bergeret, A., A. Agbossou, N. Alberola, P. Cassagnau, T. Sarraf, *European Polymer Journal*, 1992. **28**(10): p. 1201-1218.
125. Harris, B., G. Braddell, D.P. Almond, C. Lefebvre, J. Verbist, *Journal of Materials Science*, 1993. **28**: p. 3353-3366.
126. Ibarra, L., A. Macias, E. Palma, *Journal of Applied Polymer Science*, 1995. **57**(7): p. 831-842.
127. Bahadur, S., *Wear*, 2000. **245**(1): p. 92-99.

128. Ravikiran, A., S. Jahanmir, *Journal of the American Ceramic Society*, 2000. **83**(7): p. 1831-1833.
129. Michael, P.C., E. Rabinowicz, Y. Iwasa, *Cryogenics*, 1991. **31**.
130. Fu, Y., A.W. Batchelor, K.A. Khor, *Wear*, 1999. **230**(1): p. 98-102.
131. Fu, Y., A.W. Batchelor, Y. Wang, K.A. Khor, *Wear*, 1998. **217**(1): p. 132-139.

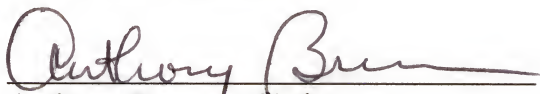
BIOGRAPHICAL SKETCH

Jeanne Macdonald was born Jeanne Hampton to Dean and Jan Hampton on June 1, 1973, in Seattle, Washington, the middle child of two sisters. She grew up mainly in Pittsburgh, Pennsylvania, with frequent road trips to the West Coast and Ohio to visit relatives. During high school Jeanne was involved in many extracurricular activities including swimming, volleyball, German and Latin club, and crew.

After graduating from high school in 1991, Jeanne attended the Virginia Tech, in Blacksburg, Virginia, graduating with a Bachelor of Science degree in materials science and engineering in December of 1995.

After an internship with Vistakon, Johnson & Johnson, under the supervision of Dr. Jim Jen in Jacksonville, Florida, Jeanne began graduate studies at the University of Florida in 1995. During her tenure at the University of Florida, Jeanne married Glenn Macdonald whom she met during the first football game of the season her last year at Virginia Tech.

I certify that I have read this study and that in my opinion it conforms to acceptable standards of scholarly presentation and is fully adequate, in scope and quality, as a dissertation for the degree of Doctor of Philosophy.



Anthony Brennan, Chairman
Professor of Materials Science and Engineering

I certify that I have read this study and that in my opinion it conforms to acceptable standards of scholarly presentation and is fully adequate, in scope and quality, as a dissertation for the degree of Doctor of Philosophy.



Ron Baney
Professor of Materials Science and Engineering

I certify that I have read this study and that in my opinion it conforms to acceptable standards of scholarly presentation and is fully adequate, in scope and quality, as a dissertation for the degree of Doctor of Philosophy.



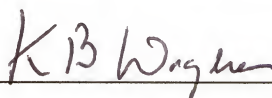
Christopher Batich
Professor of Materials Science and Engineering

I certify that I have read this study and that in my opinion it conforms to acceptable standards of scholarly presentation and is fully adequate, in scope and quality, as a dissertation for the degree of Doctor of Philosophy.



Laurie Gower
Professor of Materials Science and Engineering

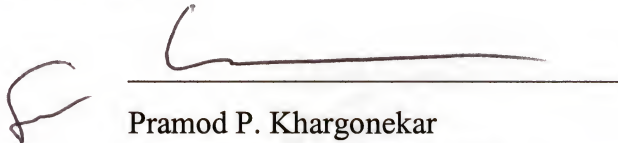
I certify that I have read this study and that in my opinion it conforms to acceptable standards of scholarly presentation and is fully adequate, in scope and quality, as a dissertation for the degree of Doctor of Philosophy.



Kenneth Wagener
Professor of Chemistry

This dissertation was submitted to the Graduate Faculty of the College of Engineering and to the Graduate School and was accepted as partial fulfillment of the requirements for the degree of Doctor of Philosophy.

December 2001

A handwritten signature in dark ink, appearing to be 'P. Khargonekar', is written over a horizontal line.

Pramod P. Khargonekar
Dean, College of Engineering

Winfred M. Phillips
Dean, Graduate School